The Past Nitrogen Cycle of the German Bight/SE North Sea: Stable Nitrogen Isotope Observations and Simulations

Dissertation
zur Erlangung des Doktorgrades
der Naturwissenschaften im Fachbereich
Geowissenschaften
der Universität Hamburg

vorgelegt von

Alexandra Serna

aus Caracas, Venezuela

Hamburg

2011

Als Dissertation angenommen
vom Fachbereich Geowissenschaften der Univeristät Hamburg
auf Grund der Gutachten von

Prof. Dr. Kay-Christian Emeis

und

Dr. Johannes Pätsch

Hamburg, den 21. Januar 2011

Prof. Dr. Jürgen Oßenbrügge

Leiter des Department Geowissenschaften

Zusammenfassung

Diese Arbeit befasst sich mit der Rekonstruktion von historischen Stickstoffisotopensignalen und -frachten in der Deutschen Bucht/SE Nordsee, indem direkt gemessene Daten von Sedimenten mit einem auf den Stickstoffkreislauf spezialisiertes numerisches Ökosystemmodel kombiniert werden. Die Abschätzung der Stickstoffeinträge aus Flüssen für den Zeitraum vor den 1970er Jahren mit dem Ziel, die flussinduzierte Eutrophierung in der deutschen Bucht zu reduzieren, ist einerseits für das Umweltmanagement und den Gesetzgebungsprozess von Bedeutung; andererseits wird gerade diese Abschätzung durch die unzureichende Datenlage erschwert. Modelle stellen daher ein wertvolles Instrument zur Identifizierung von ursprünglichen Bedingungen dar, um die Wissenslücke von historischen Stickstofffrachten der Flüsse zu schließen. Im Kern basiert diese Arbeit auf der Annahme, dass stabile Stickstoffisotopen-verhältnisse ($\delta^{15}N$) in archivierten Sedimentproben und in datierten Sedimentkernen die Nitrateinträge durch die Flüsse widerspiegeln. Modell-Simulationen von $\delta^{15}N$ bieten bei der Untersuchung von Prozessen die Möglichkeit, die $\delta^{15}N$-Werte und ihre räumliche Verteilung in Oberflächensedimenten in der Deutschen Bucht zu bestimmen. Die Simulationen wurden mit dem dreidimensionalen Ökosystemmodell ECOHAM erstellt, das um ein *N-Isotope-Tracking* Modul ergänzt wurde.

Die Arbeit gliedert sich in drei Hauptschritte:

(1) Implementierung des *N-Isotope-Tracking* Moduls in das ECOHAM Modell und Validierung der Modellergebnisse mit Hilfe von heutigen $\delta^{15}N$-Daten in Oberflächensedimenten (Kapitel 2).
Das ECOHAM Modell wurde dadurch validiert, dass die modellierte räumliche $\delta^{15}N$-Verteilung für das Jahr 1995 mit der beobachteten $\delta^{15}N$-Verteilung von Oberflächensedimenten der Jahre 1989-2009 verglichen wurde. Sensitivitätstests ergaben, dass die relevantesten Parameter zur Reproduktion der beobachteten $\delta^{15}N$-Werte in Sedimenten die Verhältnisse von $^{15}N/^{14}N$ in reaktiven Stickstoffquellen (z.B. Flüsse, Atmosphäre) sind, ebenso wie der Fraktionierungsfaktor, der mit den Umsetzungsprozessen von reaktivem Stickstoff (z.B. Nitrataufnahme durch Phytoplankton und N-Einlagerung) verbunden ist.

(2) Erfassung der ursprünglichen Isotopensignale und Stickstofffrachten in den Flüssen (Kapitel 3).
Für diesen Schritt wurde das Modell angewendet, um die räumlichen Verteilung von $\delta^{15}N$ in Oberflächensedimenten für heutige (1990-1999) und historische (1960 und 1860) Bedingungen abzuschätzen. Die Verteilung von $\delta^{15}N$ in heutigen Oberflächensedimenten in der Deutschen Bucht zeigen signifikant ansteigende Werte von den offenen Schelfgebieten hin zur inneren Bucht, hauptsächlich bedingt durch von deutschen Flüssen eingetragenen ^{15}N-angereicherten Stickstoff. Die Rekonstruktionen der historischen Bedingungen zeigen,

dass die Periode von 1950-1969 durch moderate Eutrophierung charakterisiert ist, wohingegen die Bedingungen vor 1860 als repräsentativ für Nitratgehalte in Flüssen gelten, die die Vorindustrialisierung darstellen. Die gemessenen $\delta^{15}N$-Werte aus Sedimentkernen steigen seit ca. 1860 deutlich an und weisen aufgrund ihrer veränderten Isotopenzusammensetzung auf ansteigende Nitrateinträge in Folge von menschlicher Aktivität hin.

(3) Untersuchung zu möglichen Veränderungen der Isotopenzusammensetzung von partikulärem Stickstoff während des Transports durch die Wassersäule und der Einlagerung im Sediment (Kapitel 4).
Dieses Kapitel untersucht die Rolle des Abbaus von organischem Material und dessen Einfluss auf das $\delta^{15}N$-Signal von suspendiertem Material und Sedimenten. Die Verteilung von Aminosäuren, ein Maß für den Abbaugrad des organischen Materials, zeigt, dass das rekonstruierte sedimentäre $\delta^{15}N$-Signal nicht durch Diagenese überprägt ist. Eine variable Verschiebung der $\delta^{15}N$-Werte im suspendierten partikulären Material zu den Oberflächensedimenten spiegelt das integrierte Signal der saisonalen Umsetzungsprozesse und den Beitrag des ^{15}N-angereicherten Nitrats aus den Flüssen wider.

Zusammengefasst konnte gezeigt werden, dass die modellierten und gemessene $\delta^{15}N$-Niveaus in Oberflächensedimenten der Deutschen Bucht übereinstimmen. Die sedimentären $\delta^{15}N$-Signale wurden dabei unter Annahme verschiedener Einflussmengen sowie unterschiedlicher $\delta^{15}N$-Werte von gelöstem und partikulärem Stickstoff aus den Flüssen modelliert. Der Vergleich zwischen Modellergebnissen mit Werten von $\delta^{15}N$ in datierten Sedimenten an verschiedenen Stellen in der Deutschen Bucht ermöglicht die Bestimmung historischer $\delta^{15}N$-Werte und Stickstoff-Einträge. Die modellierten $\delta^{15}N$-Werte für die Bedingungen um 1860 können als repräsentativ für die Nitrat-Signaturen aus Flüssen vor der Industrialisierung angesehen werden. Die angenommenen N-Frachten (28% der heutigen jährlichen Atmosphäreneinträge und 10% der heutigen jährlichen Flussfrachten), die für die Simulation von 1860 verwendet wurden, repräsentieren ursprüngliche (pristine) Bedingungen.

Abstract

This work reconstructs historical nitrogen isotope signals and nitrogen loads in the German Bight/SE North Sea in an approach that combines observational data from sediments and numerical ecosystem modelling focused on the nitrogen cycle. Scarce observational data of river nitrate loads prior to the 1970s complicate the assessment of target conditions for environmental management and legislation aiming to combat river-induced eutrophication in the shallow German Bight. In the absence of knowledge on historical nitrogen loads from rivers, models represent a highly useful tool to identify pristine conditions. This study is based on the assumption that stable nitrogen isotope ratios ($\delta^{15}N$) in archive sediment samples and dated sediment cores image riverine nitrate contributions. Simulations of $\delta^{15}N$ also help to investigate the processes that determine the levels of and spatial distribution of $\delta^{15}N$ in surface sediments of the German Bight. The simulations are carried out with the three-dimensional ecosystem model ECOHAM amended with an N-isotope-tracking module.

The work is done within three main steps:
(1) Implementation of the N-isotope-tracking module in the ECOHAM model and validation of the model performance using recent surface sediment data of $\delta^{15}N$ (Chapter 2).
The ECOHAM model was validated by comparing the modeled $\delta^{15}N$ spatial distribution for the year 1995 with the observed $\delta^{15}N$ distribution of surface sediments collected from 1989-2009. Sensitivity tests suggest that the most relevant parameters to reproduce the observed $\delta^{15}N$ in sediments are the $^{15}N/^{14}N$ ratios in reactive nitrogen sources (e.g. rivers, atmosphere), and the fractionation factors associated with turnover processes of reactive nitrogen (e.g. nitrate uptake by phytoplankton and N burial).

(2) Hindcast of pristine isotopic signal and N-loads from rivers (Chapter 3).
Here, the model is applied to estimate the spatial distribution of $\delta^{15}N$ in sediments for modern (1990-1999 AD) and historical (1960 AD and 1860 AD) conditions. $\delta^{15}N$ of modern surface sediments in the German Bight exhibit significantly increasing values from the open shelf sea to the inner bight, mainly attributed to ^{15}N-enriched nitrogen discharged by the German rivers into the North Sea. Reconstructions of historical conditions indicate that the period 1950-1969 is characterized by moderate eutrophication, whereas pre-1860 AD conditions can be considered representative of pre-industrial riverine nitrate levels. Markedly increasing $\delta^{15}N$ values observed in sediment cores from approximately 1860 AD onwards indicate changes in isotopic composition of riverine nitrate loads as a consequence of human activities.

(3) Study of possible alterations of the isotopic composition of particulate nitrogen during transit through the water column and burial in the sediment (Chapter 4).
This chapter investigates the role of organic matter degradation in coining $\delta^{15}N$ signals of suspended matter and sediments. Amino acid (AA) composition, a measure of the state of

degradation of organic matter, indicates that the reconstructed sedimentary $\delta^{15}N$ are not overprinted by diagenesis. A variable offset between $\delta^{15}N$ in suspended particulate matter and in surface sediments reflects an integrated signal of seasonal turnover processes and the contribution of ^{15}N-enriched riverine nitrate sources.

In summary, modeled and measured levels of $\delta^{15}N$ in surface sediments of the German Bight agree. The sedimentary $\delta^{15}N$ signals were modeled at various assumptions of magnitude of input and river $\delta^{15}N$ composition of dissolved and particulate nitrogen. Comparing the model results to levels of $\delta^{15}N$ in dated sediments at various locations in the German Bight constrains historical $\delta^{15}N$ signals and nitrogen loads. The modeled $\delta^{15}N$ values for 1860 AD conditions can be considered representative of riverine nitrate signatures before industrialization. The N-loads (28% of the modern annual atmospheric loads and 10% of the modern annual river loads) assumed for 1860 AD simulations represent pristine conditions.

Table of Contents

List of Figures

List of Tables

Chapter 1

Introduction

The following chapter provides an insight into the application of nitrogen isotopes as a proxy for past states of the nitrogen cycle in the German Bight/SE North Sea. The focus is on both modelling and direct observations of nitrogen isotopes in suspended matter, surface sediments and sediment cores. The applicability of the approach based on nitrogen isotope composition is motivated by the requirements of marine eutrophication policy to reconstruct environments differing from today and in the absence of observational data. This introduction also includes details of the study area and lays out specific objectives of the thesis.

1.1. The changing N-cycle

The global N-cycle is largely controlled by biologically mediated processes. Nitrogen compounds in nature are divided into nonreactive (N_2 gas) and reactive nitrogen (Nr), which includes inorganic reduced forms (e.g. ammonia and ammonium), inorganic oxidized forms (e.g. nitrogen oxide, nitric acid, nitrous oxide, and nitrate) and organic compounds (e.g. urea, amines, and proteins) (Galloway et al., 2003). Dissolved nitrate (NO_3^-), nitrite (NO_2^-), and ammonium (NH_4^+) dominate the biologically available forms of fixed nitrogen in aquatic and terrestrial environments (Canfield et al., 2005).

Figure 1.1 depicts some of the microbiologically mediated processes and species in the N-cycle. Starting with nitrogen fixation, prokaryotes convert atmospheric nitrogen (N_2) into ammonia (NH_3), which is a form utilizable by biota. Through ammonification, most of the organic nitrogen is again recycled into NH_4^+. Thereafter, it can be re-assimilated by microbes or plants, or it can be oxidized by prokaryotes to NO_2^- and NO_3^-. In the classical nitrogen cycle, NO_2^- and NO_3^- are either assimilated by microorganisms and plants, or in the absence of oxygen transformed by bacteria through denitrification to N_2, which is returned to the atmosphere (Canfield et al., 2005). Ammonium oxidation (anammox), which involves the anaerobic NH_4^+ oxidation with the NO_2^- reduction, may also produce N_2.

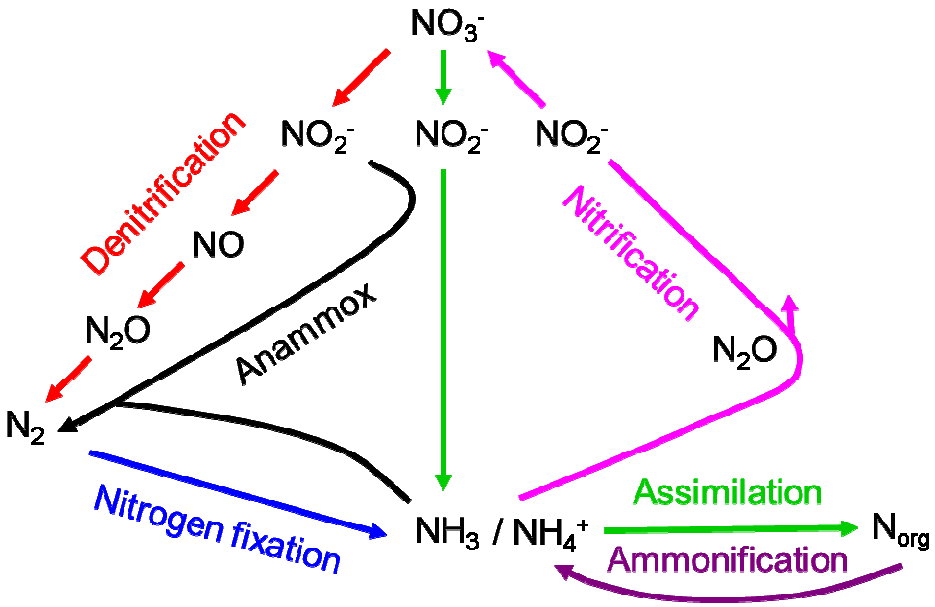

Fig. 1.1. Diagram of the marine nitrogen cycle (modified after Codispoti et al., 2001).

The global N-cycle has been significantly altered over the past century as a consequence of human activities. In the pre-human world, biological nitrogen fixation and oxidation of N_2 by lightning were the dominant processes by which Nr was created from N_2 (Galloway and Cowling, 2002). Nowadays, the amount of fixed nitrogen produced by industrial nitrogen fixation into fertilizer via the Haber-Bosch process (100 x 10^{12} g N yr^{-1}; Gruber and Galloway, 2008) is in magnitude equivalent to marine biological nitrogen fixation (~100 x 10^{12} g N y^{-1}; Gruber and Sarmiento, 1997; Canfield et al., 2005). Another source of anthropogenic Nr is extensive cultivation of legumes and rice, since it creates environments that enhance nitrogen fixation. The increase in Nr production is also caused by fossil fuel combustion, which converts both atmospheric N_2 and fossil fuel nitrogen into reactive NO_x.

In spite of intensive research, there are large uncertainties in estimates of the present-day nitrogen budget. Studies estimate that today's total oceanic denitrification exceeds total oceanic nitrogen fixation, originating a large imbalance of the marine N budget (Codispoti, 1995; Codispoti et al., 2001; Codispoti, 2007). However, it is obvious that the rate of Nr production by human activity has dramatically increased since 1960, and consequently Nr has accumulated in the environment because it exceeds the rates of Nr removal through denitrification (Galloway et al., 2003). Although in coastal ecosystems most Nr is eventually denitrified to N_2, considerable Nr inputs have led to many contemporary environmental problems, such as eutrophication (Rabalais, 2002; Galloway et al., 2003).

1.2. Stable nitrogen isotopes as recorders of the past nitrogen cycle

Nitrogen consists of two stable isotopes: the light isotope (^{14}N) and the heavy isotope (^{15}N). In atmospheric N_2, the largest N-pool on Earth, these isotopes occur in a natural abundance of 99.6337 atom% ^{14}N and 0.3663 atom% ^{15}N. The isotope composition of a sample is usually expressed as $\delta^{15}N$ in ‰ relative to a standard:

$$\delta^{15}N\ (‰) = (R_{sample} / R_{standard} - 1) \times 1000 \quad (1.1)$$

where R_{sample} and $R_{standard}$ are the $^{15}N/^{14}N$ ratios of the sample and the standard, respectively. The standard for nitrogen is atmospheric N_2, defined as $\delta^{15}N = 0‰$ (Mariotti et al., 1981).

As molecular bonds are a little stronger when ^{15}N is involved (vibrational energies are smaller), molecules containing ^{15}N are slightly less reactive than those containing ^{14}N. Therefore, organisms preferentially use molecules containing ^{14}N over molecules with ^{15}N. As a consequence of biologically mediated non-equilibrium transformation processes in the N-cycle, almost any product is depleted in ^{15}N in relation to the substrate. The isotopic enrichment/depletion of the product relative to the substrate is defined as the isotope fractionation factor ε and can be expressed in ‰:

$$\varepsilon\ (‰) = (R_{product} / R_{substrate} - 1) \times 1000 \quad (1.2)$$

where $R_{product}$ and $R_{substrate}$ are the $^{15}N/^{14}N$ ratios of the product and the substrate, respectively. A negative fractionation factor indicates discrimination against the heavy isotope. According to the so-called Rayleigh distillation model in an ideal closed system, the isotopic composition of the accumulated product of each transformation in the N-cycle should equal the isotopic composition of the original substrate when the substrate is completely consumed. Figure 1.2 exemplifies the isotopic fractionation that occurs during nitrate assimilation into particulate nitrogen (algal cells) in a closed system. The instantaneously produced N in biomass is depleted by a certain $^{15}\varepsilon$ relative to the residual nitrate; whereas the accumulated product becomes progressively enriched until the initial value of the substrate nitrate is reached at complete nitrate utilization.

The degree of isotope fractionation for each transformation process can be highly variable and depends on environmental conditions such as temperature, water chemistry, substrate availability and microorganisms involved. The fractionation that occurs during **nitrate**

assimilation and concomitant production of particulate nitrogen (PN) varies from -6 to -20‰ (Needoba et al., 2003; Granger et al., 2004). **Assimilation of ammonium** is associated with a fractionation factor $^{15}\varepsilon$ between -4 and -27‰ (Hoch et al., 1992). **Nitrogen fixation** occurs with little effective isotope discrimination; therefore, the reduced nitrogen produced by marine nitrogen fixers differs only slightly from the $\delta^{15}N$ of air (0 to -2‰; Carpenter et al., 1997). Similarly, the production of ammonium from organic nitrogen, **ammonification**, usually causes no fractionation (~0‰; Kendall, 1998). However, Möbius et al. (2010) assume a negative fractionation during ammonification. A large isotopic effect is associated with **nitrification** since it is a multi-step oxidation process: ammonium oxidation (from -14 to -38‰; Casciotti et al., 2003) followed by nitrite oxidation to nitrate, which has been shown in laboratory experiment by Casciotti (2009) to have a positive fractionation factor (+12.8‰). There are estimates of -22 to -30‰ for the isotopic effect of **water column denitrification** (Brandes et al., 1998; Altabet et al., 1999), whereas **sedimentary denitrification** is typically assumed to have a negligible isotopic effect (Brandes and Devol, 2002; Lehmann et al., 2004) due to diffusion control and complete nitrate utilization. There are no existing measurements of the isotopic impact of **anammox,** but a negative fractionation factor is likely.

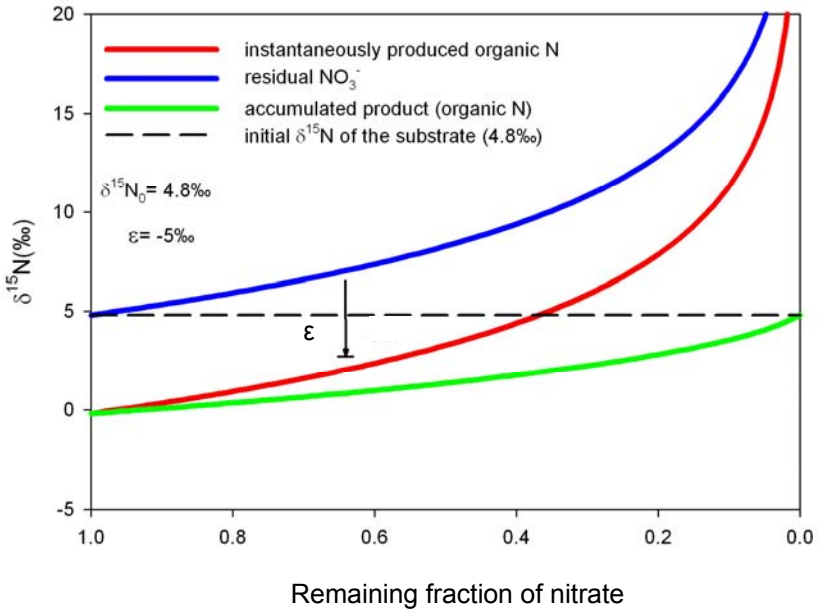

Fig. 1.2. Example of Rayleigh fractionation during nitrate assimilation in a closed system assuming initial isotopic composition of the substrate (nitrate) $\delta^{15}N_0$ = 4.8‰ and isotope fractionation factor ε = -5‰.

The various fractionation processes in the N-cycle give a distinctive isotopic signature to different nitrogen pools (Fig. 1.3). These isotopic signatures can be highly variable even for same N-species. Accordingly, the interplay of different N sources and the degree of utilization is reflected in the isotopic composition of sediments and can be used to trace changes in the

contribution of nitrogen sources, including anthropogenic nitrogen inputs. For example, the $\delta^{15}N$ values in marine near-shore sediments can provide information of the proportion of riverine nitrate assimilated by phytoplankton and the extent of nutrient utilization. Systematic relationships to other proxies are useful to decipher sources and processes involved.

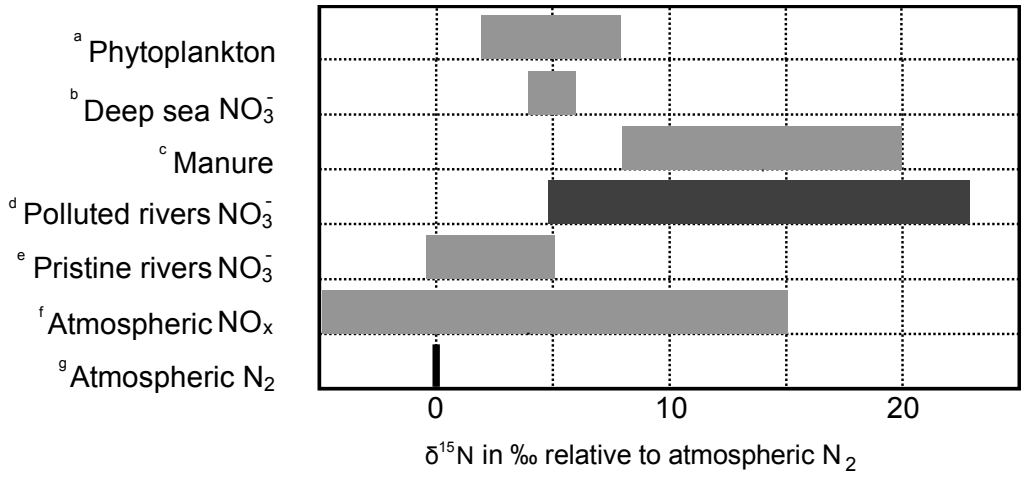

Fig. 1.3. Source specific nitrogen isotope signatures. References: [a] Mariotti et al., 1984; [b] Liu and Kaplan, 1989; Sigman et al., 2000; [c] Heaton, 1986; Bateman et al., 2005; Voß et al., 2006; [d] Voß et al., 2006; Johannsen et al., 2008; [e] Voß et al., 2006; [f] Kendall et al., 2007; [g] Mariotti et al., 1981.

The interpretation of sedimentary $\delta^{15}N$ data is generally hampered by early diagenetic overprint that can occur during sediment settling in the water column and at the sediment-water interface under oxic conditions. The systematic relationship to compositional changes of amino acids (AA), which are the main carriers of nitrogen in organic matter, represents a useful tool to interpret the data correctly (Gaye-Haake et al., 2005; Möbius et al., 2010). Amino acids spectra in water depth profiles of suspended matter (Haake et al., 1992, 1993) and downcore in sediments (Cowie and Hedges, 1992; Gupta and Kawahata, 2003) have been used to determine the degradation state of the organic matter (Dauwe and Middelburg, 1998) and have charted the effect on $\delta^{15}N$ values. Further proxies that contribute to the successful application of $\delta^{15}N$ to the question of past states of the N-cycle in the German Bight are total nitrogen (TN), total carbon (TC), organic carbon (TOC), biogenic silica (BiSi), C/N ratios, and stable carbon isotope ratios ($\delta^{13}C$). Together, the data sets in surface sediments and in dated sediment cores can help to correctly reconstruct changes in the N-cycle, the eutrophication history, and to investigate the effect of policy measures aimed to combat environmental deterioration caused by excessive Nr introduced to the coastal ocean.

1.3. The eutrophied German Bight

The term eutrophication refers to the changes induced at the ecosystem level by an increase of nutrients from external sources (Brockmann et al., 1988). For the purpose of the OSPAR Eutrophication Strategy (OSPAR Commission, 2003a), eutrophication is defined as the anthropogenic enrichment of water by nutrients causing an accelerated growth of algae and higher forms of plant life to produce an undesirable disturbance to the balance of organisms present in the water and to the quality of the water concerned.

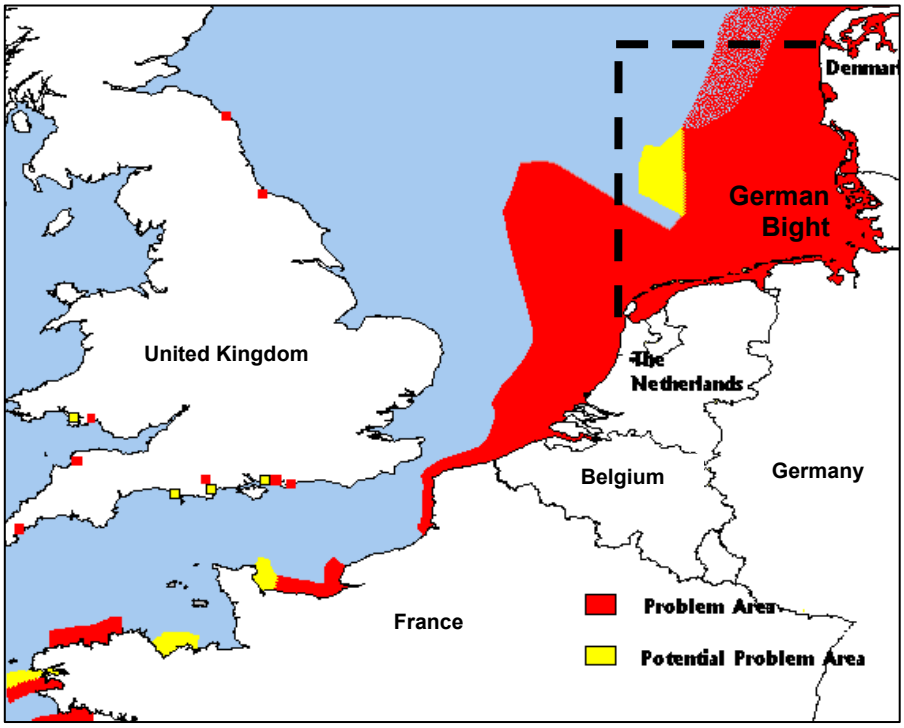

Fig.1.4. Map of areas identified as eutrophication problem areas in the southern North Sea based on the OSPAR common procedure to combat eutrophication (OSPAR Commission, 2003b). Dashed lines mark the boundary of the German Bight (53°-57°N, 4°-10°E) studied in this thesis.

According to the OSPAR Commission for the Protection of the Marine Environment of the North-East Atlantic, the North Sea is the most problematic region in the North East Atlantic in terms of eutrophication (OSPAR Commission, 2008). Reasons for this are high population densities and related high nutrient inputs, mostly by rivers. Between 1950 and 1990, N-loads of coastal waters increased by a factor of 1.62 and P-loads by 1.45 (Vermaat et al., 2008). In addition to input from land, atmospheric deposition of nitrogen contributes one third of all nitrogen inputs for the North Sea (OSPAR Commission, 2007). Furthermore, the shallow

character of the shelf sea and its hydrodynamic characteristics enhance eutrophication processes.

The shallow German Bight is a highly eutrophied area in the south eastern edge of the North Sea (Fig. 1.4). Freshwater input in the bight leads to a salinity range of 30 in the near shore German Bight to > 33 in the outer German Bight (Schott, 1966; Scheurle et al., 2005). Sources of Nr in the German Bight are (1) anthropogenic nitrogen loads, which derive from the densely populated adjacent land and reach the German Bight via atmospheric deposition or riverine input (Beddig et al. 1997; Brion et al. 2004); (2) recycling and processing of organic matter in sediments or supended matter in the German Bight itself (Hydes et al. 1999); and (3) advective fluxes of waters from the open North Sea (Pätsch et al., 2010). Direct discharges by rivers dominated by the Elbe and Weser and the Rhine outflow entering from the east mostly influence the nutrient concentration in the German Bight. The semi enclosed nature and its shelf sea character along with the counter-clockwise residual current pattern that tends to isolate riverborne substances near the coast favour the accumulation of nutrients in the German Bight (Hickel et al., 1993).

A political action rose against marine pollution at an international level after the observation of oxygen deficiency in large areas of the German Bight in 1981 (Rachor and Albrecht, 1983). To protect the marine environment and to combat eutrophication, the Second International North Sea Conference in 1987 decided to reduce nitrogen and phosphorus inputs into the North Sea to 50% of the 1985 level by 1995 (INSC, 1987). The P-loads declined after 1990 from 1.8 g m^{-2} y^{-1} to about 1.4 g m^{-2} y^{-1} in 2000, whereas N-loads declined less (Vermaat et al., 2008). Even though a slight downward trend of riverine nitrogen inputs has been reported (Carstensen et al. 2006; Radach and Paetsch 2007), attenuation mechanisms are still unclear and inputs remain far above the desired threshold of the European Union Water Framework Directive (WFD, 2000). Meanwhile, scientific activity has contributed to predict the effects of 50% nutrient reduction (Lenhart et al., 2010). Although other factors such as climatic changes play an important role in marine eutrophication, the identification of the role of anthropogenic nutrient inputs in the changes observed in the marine environment has special relevance to the policy (de Jong, 2006). This approach aims to assess the historical contribution of different sources to the Nr pool of the German Bight as compared to present-day conditions.

1.4. Modelling studies

Moll and Radach (2003) provided a comprehensive overview about three-dimensional models used to describe and to predict how the marine ecosystem of the North Sea functions. Some of these ecosystem models have been used to investigate the effects of reduced riverine nutrient loads on the North Sea ecosystem. The ecosystem model ERSEM (European Regional Seas Ecosystem Model; Baretta et al., 1995) has been applied to questions regarding eutrophication of the coastal zone caused by changing nutrient loads from river management strategies (Lenhart et al., 1997; Lenhart, 2001). Similar simulation efforts have been made by Pätsch and Radach (1997) to explore the long term consequences of anthropogenic nutrient input into the North Sea. Skogen et al. (2004) studied the environmental effects of reducing nutrient loads to the North Sea using the coupled three-dimensional physical, chemical and biological model system NORWECOM (The NORWegian ECOlogical Model system; Skogen and Søiland, 1998). Lenhart et al. (2010) give a summary of the work promoted by the OSPAR Intersessional Correspondence Group on Eutrophication Modelling on likely future eutrophication status of specific areas of the North Sea following riverine nutrient reductions via modelling. However, a recurrent problem of all these efforts was the lack of nutrient input data and concentration data to validate the models. Accurate data are not only needed to validate numerical models, but also provide an overview of spatial and temporal developments in the marine environment (de Jong, 2006). Thus, this thesis aimed at a model-data study to estimate the natural Nr levels in the North Sea in the absence of knowledge on historical nitrogen loads and to distinguish past and modern contributions from riverine and atmospheric sources to the Nr-pool of the North Sea.

For this study the model ECOHAM (Ecological North Sea Model, Hamburg) previously implemented by Pätsch and Kühn (2008) is amended by an N-isotope module (Pätsch et al., 2010; Chapter 2). The model is used here as a tool to reconstruct N-isotope composition in surface sediments in the absence of samples from past decades, and ultimately to simulate the fluxes of Nr. This approach builds on the underlying rationale that N-isotope composition in surface sediments of the coastal zone affected by river inputs integrates N-cycling in the ecosystem and records magnitude and isotopic composition of anthropogenic loads. In other words, $^{15}N/^{14}N$ ratios of spatially distributed sample sets taken in the past or time slices in dated sediment cores are set as target levels for hindcasting model runs with Nr loads that differ from those of present loads and have different isotopic composition.

The domain of the large-scale ECOHAM model area comprises the Northwest European Shelf (47° 41'-63° 53' N, 15° 5'-13° 55' E). In this thesis a nested version of the model is used (50° 53'-57° 17' N, 3° 25' W-9° 15' E). Special attention is given on the German Bight (53°-57°N, 4°-10°E). The horizontal resolution on the continental shelf was 0.2° in latitude and 1/3° in longitude, i.e. about 20 km for both directions. The model was set up with 21 vertical layers

with increasing thickness towards the bottom. The layers 0-50 m were resolved by 5 m steps (Δz = 5 m). Below 50 m the thickness of the layers increased successively.

The model consists of two components: the hydrodynamic module HAMSOM (Pohlman, 1996) and the biogeochemical part with explicit treatment of nitrogen isotopes. Two nitrogen cycles are independently treated for each stable isotope of nitrogen, and the model includes two state variables for each nitrogen compartment (phytoplankton-N, zooplankton-N, detritus-N, dissolved organic nitrogen, buried material, bacteria-N, nitrate and ammonium). The ^{15}N isotope concentration of each state variable is calculated with prescribed $\delta^{15}N$ values for the boundaries of the nest and all initial biogeochemical parameters containing nitrogen. Together with these given $\delta^{15}N$, the fractionation factors of each N-turnover process determine the $\delta^{15}N$ values of the state variables. Initial $\delta^{15}N$ values and fractionation factors are prescribed according to published data from several authors (Chapter 2). To simulate sedimentation on longer time scales, the sedimentary N-pool which is buried is fed by 1% of the detritus reaching the seafloor (de Haas et al., 2002).

The coarse model was run initially, providing the necessary boundary and initial values for the fine grid. The ECOHAM model that includes the N-isotope-tracking module was first implemented for the year 1995 (Chapter 2) using atmospheric nitrogen deposition data from the “Cooperative program for monitoring and evaluation of the long-range transmissions of air pollutants in Europe” (EMEP) and riverine nitrogen loads from Radach and Pätsch (2007). River loads, atmospheric loads and boundary conditions are supplied by observational data and/or extrapolation of data depending on the simulated case (past or present conditions, Chapter 3). The spin-up procedure used was 10 years for each run.

1.5. Objectives

The overall objective of this study is to reconstruct the N-cycle of the German Bight. Thereby, the primary interest is to reconstruct pristine riverine $\delta^{15}N$ signals and N-loads as target for environmental legislations. The modelling studies are performed using the three-dimensional ecosystem model ECOHAM (Pätsch and Kühn, 2008) amended with an N-isotope-tracking module. The study focused on the following questions:

What are the dominant factors affecting the spatial and temporal distribution of $\delta^{15}N$ in recent sediments of the German Bight?

Is it possible to reconstruct pristine N-loads in the German Bight using a $\delta^{15}N$-model-data study by means of nitrogen isotope signatures?

Is there a relationship between $\delta^{15}N$ and degradation, as expressed by AA composition?

This was a new approach and entailed several steps:

1. Implementation of a $\delta^{15}N$ module in the three-dimensional ecosystem model ECOHAM (Chapter 2).

2. Validation of the model by comparison of observed $\delta^{15}N$ in recent surface sediments and $\delta^{15}N$ values simulated for the year 1995 (Chapter 2). Accessible surface sediments are designated into two different periods, recent (1989-2009) and older (1950-1969) surface sediments.

3. Hindcast of pristine conditions of the North Sea (atmospheric and riverine N-loads not measured in the past) by comparison of observed $\delta^{15}N$ in older surface sediments and sediment cores with $\delta^{15}N$ values simulated for the years 1960 and 1860 (Chapter 3).

4. Comparison of sedimentary inventories between different zones of the German Bight to gauge the degradation state on a horizontal plane by means of variations in AA composition. Additionally, a comparison is made between the organic matter compositions in suspended matter and in the underlying surface sediments (Chapter 4).

5. Study of the relationship between $\delta^{15}N$ and degradation. The origin and digenetic history of organic matter in sediment cores is assessed by means of variations in AA composition (Chapter 4).

1.6. Thesis outline

This thesis is based on three journal publications, each of them includes a short summary, introduction, methods, results and conclusion - some recurrences may occur:

Chapter 2 describes the implementation of the $\delta^{15}N$ module in the three-dimensional ecosystem model ECOHAM as its validation with observational data. It has been published as: *Pätsch, J., Serna, A., Dähnke, K., Schlarbaum, T., Johannsen, A., Emeis, K.-C., 2010. Nitrogen cycling in the German Bight (SE North Sea) – clues from modelling stable nitrogen isotopes. Continental Shelf Research 30, 203-213*. My contribution to this publication is: a) generation of isotopic data in surface sediments of the German Bight, b) optimization of model input parameters for implementation and validation of the model, c) co-work in manuscript preparation.

Chapter 3 presents the reconstruction of the historical nitrogen loads of the German Bight in terms of isotopic composition. It has been published as: *Serna, A., Pätsch, J., Dähnke, K., Wiesner, M.G., Hass, H.C., Zeiler, M., Hebbeln, D., Emeis, K.-C., 2010. History of anthropogenic nitrogen input to the German Bight/SE North Sea as reflected by nitrogen isotopes in surface sediments, sediment cores and hindcast models. Continental Shelf Research 30, 1626-1638*. The surface sediment distributions of $\delta^{15}N$ have in part been separately published in: *Dähnke, K., Serna, A., Blanz, T., Emeis K.-C., 2008. Sub-recent nitrogen-isotope trends in sediments from Skagerrak (North Sea) and Kattegat: Changes in N-budgets and N-sources? Marine Geology 253, 92-98*. I contributed most of the sediment surface data to the publication and to the writing and the scientific discussion.

Chapter 4 investigates the influence of degradation in the isotopic composition of particulate matter and sediments. It will be submitted as: *Serna, A., Pätsch, J., Lahajnar, N., Emeis, K.-C. Stable nitrogen isotopes and amino acid composition as indicators of organic matter sources and degradation state of suspended matter, surface sediments and sediment cores of the German Bight/SE North Sea. Marine Chemistry*.

Chapter 5 contains the main conclusions of this thesis and description of future perspectives and recommendations.

Chapter 2

Nitrogen cycling in the German Bight (SE North Sea) – clues from modelling stable nitrogen isotopes

Abstract

Nitrogen isotope values ($\delta^{15}N$) of surface sediments in the German Bight of the North Sea exhibit a significant gradient from values of 5-6‰ of the open shelf sea to values above 11‰ in the German Bight. This signal has been attributed to high reactive N (Nr) loading enriched in ^{15}N from rivers and the atmosphere. To better understand the processes that determine the intensity and spatial distribution of $\delta^{15}N$ anomalies in surface sediments, and to explore their usefulness for reconstructions of pristine N-input from rivers, we modelled the cycling of the stable isotopes ^{14}N and ^{15}N in reactive nitrogen through the ecosystem of the central and southern North Sea (50.9-57.3°N, 3.4°W-9.2°E) for the year 1995. The ecosystem model ECOHAM amended with an isotope-tracking module was validated by $\delta^{15}N$ data of surface sediments within the model domain. A typical marine value ($\delta^{15}N_{nitrate}$ = 5‰) was prescribed for nitrate advected into the model domain at the seaside boundaries, whereas $\delta^{15}N_{nitrate}$ of river inputs were those measured bi-monthly over one year; $\delta^{15}N$ values of atmospheric deposition were set to 6‰ and 7‰ for NO_x and NH_y, respectively. The simulated $\delta^{15}N$ values of different nitrogen compounds in the German Bight strongly depend on the mass transfers in the ecosystem. These fluxes, summarized in a nitrogen budget for 1995, give an estimate of the impacts of hydrodynamical and hydrological boundary conditions, and internal biogeochemical transformations on the nitrogen budget of the bight.

Sensitivity tests suggest that the most relevant parameters to reproduce observed sediment $\delta^{15}N$ are the $^{15}N/^{14}N$ ratios in Nr-sources (e.g. river, atmosphere), and the fractionation factors associated with Nr turnover processes, in particular nitrate uptake by phytoplankton and N burial. In accord with observations, the modelled surface sediments of the inner German Bight are enriched in ^{15}N ($\delta^{15}N > 9.5‰$). The general gradient of decreasing $\delta^{15}N$ in sediments from the coast to the open shelf primarily reflects the amount of ^{15}N-enriched reactive nitrogen discharged by the German rivers into the North Sea. Smaller patterns are created by different conditions of the nitrogen pools in combination with corresponding isotope fractionation processes in the course of the year. These conditions can be caused by a heterogeneous topography or by varying sediment properties, most prominently porosity variations. Both simulation results and observational data show that maximum $\delta^{15}N$ values do not occur directly in front of riverine discharge areas, but along the North Frisian coast due to incomplete nitrate assimilation near the river mouths and as a consequence of the prevailing current pattern. In a scenario run with reduced nitrogen river loads, this maximum migrates towards the river mouth. This shift is a consequence of the lower nitrogen loads and a faster complete consumption of riverborne nitrogen by phytoplankton.

2.1. Introduction

A well-studied example of the effects of eutrophication on coastal marine ecosystems is the North Sea that has a watershed populated by 164 million inhabitants, who caused a ten fold increase of nitrate loads since the 1950s (Behrendt and Opitz, 1999). A particular hot-spot of environmental deterioration and ecosystem change is the German Bight in the southeastern corner of the North Sea (Beddig et al., 1997; van Beusekom et al., 1999) that receives significant river discharges from German rivers (Radach and Pätsch, 2007). Nutrient turnover in sediments of the extensive mudflat areas bordering the German Bight and estuaries may have quintupled in step with rising river loads (van Beusekom, 2005). Reacting to rising nutrient discharges and incipient environmental deterioration, countries bordering the North Sea in 1985 agreed to reduce nutrient discharges by 50% to re-establish a status approaching that of the pristine North Sea. Since then, significant nitrogen load-reduction has been achieved: Bergemann and Gaumert (2008) compared the Elbe river nitrate load of 2006 with that of 1986 (both years had similar freshwater fluxes), and found a decrease of 28% for nitrate and 93% for ammonium. Reduced river input led to a decrease in winter nitrate in the northern Wadden Sea (van Beusekom et al., 2009).

While efforts are continuing to reduce river nitrate loads, a major scientific challenge remains in setting the environmental goals for further reduction efforts: What is the desired target status, and what were pristine nutrient concentrations before the onset of serious eutrophica ion? In the absence of observational data for the pristine status, models are the tool of choice,

and have been used to estimate river loads from land-use patterns and hydrology (Behrendt et al., 2001; Seitzinger et al., 2002). In the case of the North Sea, available observational data (from 1977 onwards) and model estimates have been compiled for time series of river-runoff spanning the period from 1955-1993 by Pätsch and Radach (1997), who simulated consequences of anthropogenic nutrient (including Nr) input into the North Sea with an ecosystem model of coarse regional resolution. Similar simulating efforts have been made with several 3D-ecosystem models (Moll and Radach, 2003), but all hindcasts based on nutrient element mass fluxes prior to the onset of systematic monitoring (approximately mid 1970s) suffer from a lack of data to validate the model results.

To remedy this shortcoming, “fingerprints” of eutrophication are needed that can be detected from archives of past nutrient conditions, such as marine sediments, fossils, or biological collections. A promising tool is the use of stable nitrogen isotope ratios in sedimentary and biological archives: They have been used successfully as indicators for nitrogen input sources in several studies, because they are characteristic for different DIN sources. High $\delta^{15}N$ values in biota and sediments (in the absence of water-column denitrification) indicate sewage input (Holmes et al., 1998) and/or ^{15}N-enrichment of residual nitrate from mineral fertilisers in agricultural runoff (Costanzo et al., 2001). The signal is not only found in nitrate, but also in macrophytes that take up the riverborne nitrogen (Costanzo et al., 2001; Cole et al., 2004), in herbivores (McClelland and Valiela, 1998) and in many coastal and lacustrine sediments worldwide (Bratton et al., 2003; Church et al., 2006; Wu et al., 2007). Studies in NW Europe addressed the imprint of eutrophication in sediment records of the Baltic Sea (Voß and Struck, 1997; Struck et al., 2000; Emeis et al., 2002), the northern North Sea and Kattegat (Dähnke et al., 2008) as well as in several fjords and estuaries (Clarke et al., 2003; Clarke et al., 2006).

According to this empirical evidence, N-isotope composition of sediments carries a fingerprint of anthropogenic loads, and may be a tool to explore past ecosystem situations. To develop this tool, we present here the theoretical basis for, and first results of a new approach to estimate recent and historical Nr loads of rivers discharging into shelf seas. This approach uses $\delta^{15}N$ in sediment records as a target to inversely simulate the fluxes of Nr with an ecosystem model of a given shelf sea. This approach builds on the underlying rationale that N-isotope composition in surface sediments integrates N-inputs and N-cycling in the ecosystem. To explore the factors that determine the surface sediment $^{15}N/^{14}N$ ratios in spatially distributed samples, we added an N-isotope module to the regional ecosystem model ECOHAM for the North Sea. This approach allows us to trace ^{15}N-enriched river inputs of Nr in the model, and to compare the distribution of $^{15}N/^{14}N$ ratios in surface sediments of the coastal zone (German Bight) affected by these river inputs with model results. Used inversely, the approach helps to determine historical loads: If $^{15}N/^{14}N$ ratios in arrays of dated sediment cores (or in spatially distributed sample sets taken in the past) are available, they

set target levels and patterns for hindcasting model runs with reduced Nr loads and/or $^{15}N/^{14}N$ ratios that differ from those of present loads.

Our specific objectives here are firstly, to present the model results for the present-day German Bight and to compare these with observed patterns of $\delta^{15}N$ in sediments. With the knowledge about the model-dynamics, we are able to explore driving forces that shape the main patterns. This objective includes sensitivity tests for model parameterizations. Secondly, we show that modeled enrichment levels and spatial patterns of enriched sediment $\delta^{15}N$ in the German Bight indeed change in response to reduced river inputs by simulating a 50% reduction in river loads.

2.2. The model

The simulations were performed with a new version of the 3D-ecosystem model ECOHAM (Pätsch and Kühn, 2008) that includes the hydrodynamical model HAMSOM (Pohlmann, 1996). This new version (ECOHAM 4.4) was implemented for a region of the central and southern North Sea that includes the area of the German Bight, a hot-spot of river-induced eutrophication (Fig. 2.1). Boundary and initial values for both the hydrodynamic and the biogeochemical parameters were derived from a simulation of the biogeochemistry and hydrodynamics of the larger Northwest European Shelf domain obtained from ECOHAM 3.0 (Pätsch and Kühn, 2008), into which the smaller model domain is nested. Figure 2.1 illustrates the model domain of the large model and the nest. Parameterizations that differ from those used in Pätsch and Kühn (2008) are listed in Table 2.1.

Figure 2.2 depicts the schematic layout of N cycling implemented in ECOHAM 4.4; in this model, two N-cycles are independently run for each stable isotope of N, so that the model includes two state variables for each nitrogen compartment (phytoplankton-N, zooplankton-N, detritus-N, dissolved organic nitrogen, bacteria-N, nitrate and ammonium). To simulate sedimentation, a set of variables has been added in ECOHAM 4.4 that are fed by 1% of the detritus, simulating that portion of particulate material that sinks into the sediment and is buried (and records the integrated effects of N-isotope turnover); the value of 1% was adopted from de Hass et al. (2002). 99% of the detritus reaching the sediment is exposed to degradation. We compare the $\delta^{15}N$ value of this state variable with observations of the $\delta^{15}N$ value of surface sediment. Details on the isotope module are given in the appendix. For all boundary and initial biogeochemical parameters containing nitrogen, the $\delta^{15}N$ values had to be estimated (Table 2.2). Following several authors (Voß and Struck, 1997; Sigman et al., 2000; Guo et al., 2004; Gaye-Haake et al., 2005) and in accord with available data (Dähnke et al., 2008), we defined the $\delta^{15}N$ values for the inorganic and the organic fractions (except bacteria) advected from outside into the model domain as 5‰.

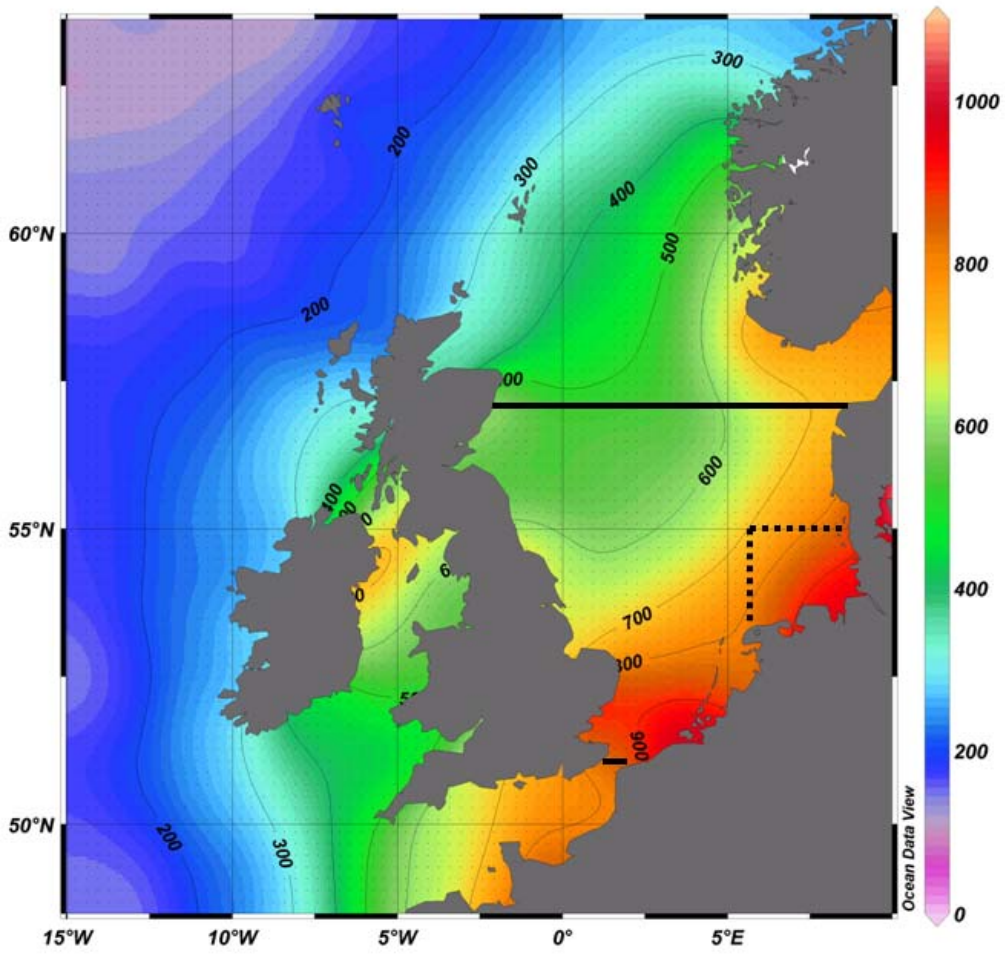

Fig. 2.1. Domain of the large-scale model ECOHAM 3.0 and the nested model ECOHAM 4.4. The latter one is indicated by the bold lines. The dashed lines mark the boundaries of the German Bight. Additionally the distribution of the annual atmospheric deposition of inorganic nitrogen (mg N m^{-2} yr^{-1}) for 1995 is shown.

Table 2.1 Parameters of the ecosystem model ECOHAM which differ from those in Pätsch and Kühn (2008).

Parameter	**Unit**	**Value**
Remineralisation rate of benthic carbon	d^{-1}	brc = 0.0222
Remineralisation rate of benthic nitrogen	d^{-1}	brn = 0.0333
Breakdown rate of slowly sinking detritus	d^{-1}	μ_4 = 0.05
Breakdown rate of fast sinking detritus	d^{-1}	μ_5 = 0.05
Velocity of slowly sinking detritus	m d^{-1}	wd_1 = 0.4
Velocity of fast sinking detritus	m d^{-1}	wd_2 = 10.0

Table 2.2 $\delta^{15}N$ values assumed for the different state variables X at the boundaries and as initial values. The $\Delta\delta^{15}N_S$ values give the deviations (ppm - parts per million) in $\delta^{15}N$ of surface sediment of the northern grid point (Fig. 2.5) when the $\delta^{15}N$ value of variable X is increased by 1‰. References: 1 - Guo et al., 2004; 2 - Gaye-Haake et al., 2005; 3 - Voß and Struck, 1997; 4 - Brandes and Devol, 2002; 5 - Yeatman et al., 2001; 6 - Johannsen et al., 2008.

State variable (compartment) X	**$\delta^{15}N_X$ (‰)**	**$\Delta\delta^{15}N_S$ (ppm)**	**References**
Phytoplankton	+5	+9	1, 2, 3
Zooplankton	+5	+8	1, 2, 3
Slowly sinking detritus	+5	+11	1, 2, 3
Fast sinking detritus	+5	+1	1, 2, 3
Labile dissolved organic matter	+5	+1	1, 2, 3
Bacteria	0	+11	
Nitrate	+5	+35	2, 4
Ammonia	+5	+12	
Detritus sediment	+5	+2	
Atmospheric nitrate (deposition)	+7	+67	5
Atmospheric ammonia (deposition)	+6	+67	5
Nitrate River Elbe	+7 - +18	+528	6

Together with the $\delta^{15}N$ values of sources and those at the boundaries, the fractionation factors ε (for a definition see Appendix) of N-turnover processes determine the $\delta^{15}N$ values of the various state variables. Phytoplankton selectively assimilates ^{15}N-depleted, and thus enriches ^{15}N of the residual dissolved Nr, creating biomass that is slightly more depleted. We chose $\varepsilon_{NO_3} = -4.5$ for nitrate uptake and $\varepsilon_{NO_3} = -6.5$ for ammonium uptake, which are in line with experimentally derived fractionation factors at low NH_4-concentrations found in the German Bight (Waser et al., 1998; York et al., 2007). Nakatsuka et al. (1992) used values $\varepsilon_{NO_3} = -6$ and $\varepsilon_{NH4} = 0$ in their model; however, they did not implement fractionating during NH_4 regeneration processes, which in our model is indirectly treated by decay of sinking particulate organic matter ($\varepsilon_{PON} = -5$), in line with the enrichment of ^{15}N in degraded material under oxic conditions (Libes and Deuser, 1988; Guo et al., 2004). Montoya and McCarthy (1995) studied isotopic fractionation of six phytoplankton species and found high variability for diatom species ($\varepsilon = -(5\text{-}20)$) and more moderate variability for flagellates. Our model includes only one bulk phytoplankton variable, for which the assumption of moderate fractionation factors is considered to be appropriate. For the degradation of particulate organic material during deposition and burial (see last section), we assume a fractionation factor $\varepsilon_{BUR} = 0.5$. Because of the lack of data all other fractionation factors of N-cycling processes were set to zero in ECOHAM. This simplistic assumption is permitted by the sensitivity analysis, which identified changes in internal fractionating factors as being less important for the $\delta^{15}N$ value of simulated surface sediment (see Table 2.3 and below).

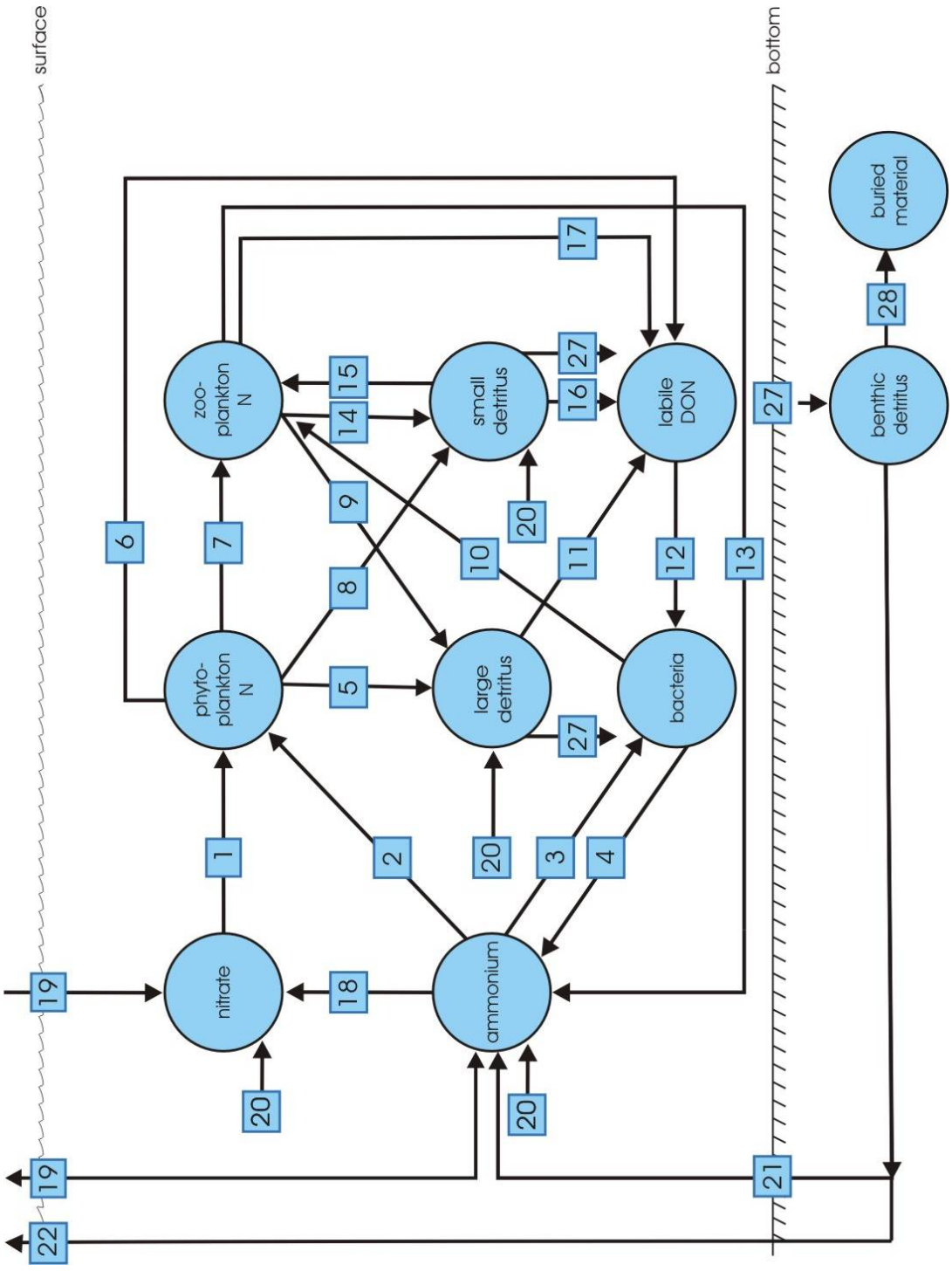

Fig. 2.2. Diagram of the nitrogen cycle of ECOHAM. The circles represent the state variables and the numbers identify the processes between the state variables: (1) uptake of nitrate; (2, 3) uptake of ammonium; (4, 13) excretion of ammonium; (5, 8) mortality; (6) exudation of labile DON; (7, 10, 15) grazing; (9, 14) fecal pellets + mortality; (11,16) decay; (12) uptake of labile DON; (17) excretion of labile DON; (18) nitrification; (19) atmospheric deposition; (20) river input; (21) benthic remineralisation; (22) denitrification; (27) sinking; (28) burial.

Table 2.3 Isotopic fractionation factors for different processes of ECOHAM 4.4. The $\Delta\delta^{15}N_S$ values give the deviations (ppm - parts per million) in $\delta^{15}N$ of surface sediment of the northern grid point (Fig. 2.5) when the fractionating factor ε is changed by $\Delta\varepsilon$. References: 7 - Nakatsuka et al., 1992; 8 - Montoya and McCarthy, 1995; 9- York et al., 2007; 10 - Libes and Deuser, 1988; 11 - Guo et al., 2004.

Process	**ε**	**$\Delta\varepsilon$**	**$\Delta\delta^{15}N_S$ (ppm)**	**References**
Nitrate uptake by phytoplankton	-4.5	-1	-144	7, 8, 9
Ammonium uptake by phytoplankton	-6.5	-1	-144	9
Decomposition of pelagic detritus	-5.0	-1	+31	10, 11
Burial	+0.5	+1	+1000	
Grazing on phytoplankton	0	+1	-31	

2.3. External data

Atmospheric nitrogen deposition as well as meteorological forcing and the loadings of carbon and nitrogen by rivers have been implemented according to Pätsch and Kühn (2008). Figure 2.1 shows the distribution of the annual deposition of dissolved inorganic nitrogen (DIN) from the atmosphere for the larger shelf area. These model data, based on observed emission data, originate from the “Cooperative program for monitoring and evaluation of the long-range transmissions of air pollutants in Europe” (EMEP). Atmospheric inputs have a pronounced gradient from the continental coast to the open North Sea, due to sources on land and water (Matthias et al., 2008). The latter ones correspond with shipping routes near the coast. From the wide spectrum of nitrogen species in the atmosphere, we only considered the oxidized components (NO_x) and the reduced components (NH_y), with $\delta^{15}N$ of 7‰ and 6‰, respectively (Yeatman et al., 2001).

For the Nr discharges of rivers Rhine, Ems, Weser and Elbe, monthly $\delta^{15}N$ values of nitrate are available that bracket a full yearly cycle in 2006/2007 (Johannsen, 2007: Johannsen et al., 2008). Although hindcasting the year 1995 with river loads of this year (Radach and Pätsch, 2007), we used these data of 2006/2007 for the $\delta^{15}N$ of river nitrate and ammonium inputs. Corresponding $\delta^{15}N$ values for the total organic N-fraction (TON) were available only for the river Elbe. This river discharged 9.1, 0.5 and 2.2 Gmol N yr^{-1} nitrate, ammonium and organic nitrogen in 1995, respectively. For all other rivers discharging into the North Sea, we estimated annually averaged $\delta^{15}N$ values of 8.2‰ for DIN and 8.0‰ for TON, corresponding to the minimum annual averages in 5 rivers (Johannsen et al., 2008), and in the Elbe, respectively. Figure 2.3 illustrates the annual cycles of the variable $\delta^{15}N$ values.

While the river Rhine exhibits only a small range in $\delta^{15}N_{nitrate}$ (7.2-10.5‰), the German rivers Ems and Elbe show a larger seasonal range of 8-18‰. The minimum occurs during the first months of the year while the maximum lies in summer. As maximum discharge occurs mostly in April and minimum discharge in summer (Radach and Pätsch, 2007), the effect of the large range of $\delta^{15}N_{nitrate}$ of the German rivers is damped to some extent. ECOHAM 4.4 simulated the year 1995 ten times successively (spinup) of which the last run is used for evaluation.

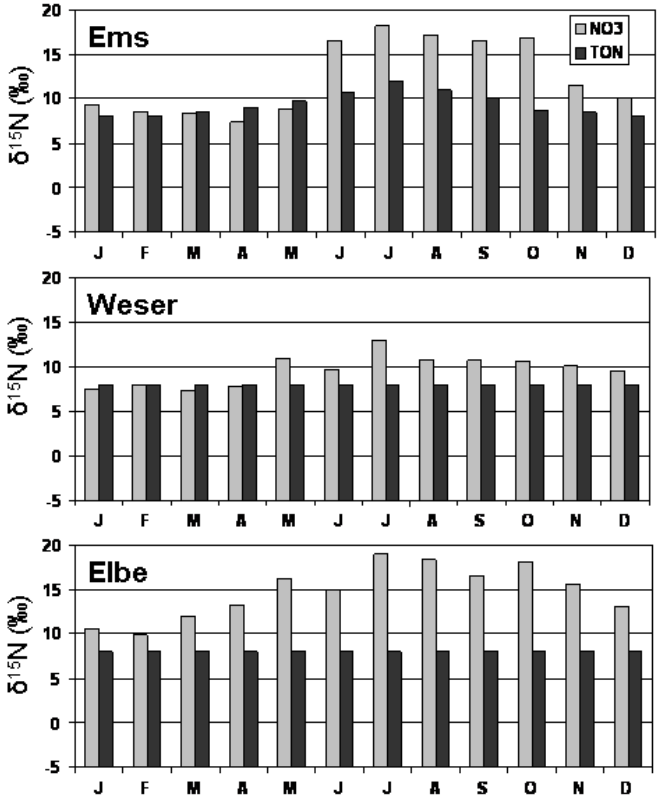

Fig. 2.3. Monthly means of $\delta^{15}N$ values of nitrate and total organic nitrogen in the rivers Ems, Weser and Elbe (Johannsen et al., 2008).

2.4. Results

2.4.1. Distribution of $\delta^{15}N$ values in surface sediments – data and model output

Observed $\delta^{15}N$ values in surface sediments ($\delta^{15}N_{obs}$) are depicted in Fig. 2.4; the samples used for determination of $^{15}N/^{14}N$ ratios of total N in sediments were collected in the period 1985-2007. For the purpose of this paper, individual data sets have not been binned according to age in order to yield an overall enrichment pattern that can be compared to the

model output for the year 1995. In our estimate, the $\delta^{15}N$ values of surface sediments in the German Bight are integrated signals over at least 2 decades due to bioturbation and trawling. In the observation data set, sediments enriched in ^{15}N ($\delta^{15}N_{obs}$ > 9‰) cover an area near the North Frisian Islands. A second local maximum in $\delta^{15}N_{obs}$ is found in the immediate vicinity of the Elbe and Weser estuaries; these northern and southern maxima are separated by a corridor of low values (< 9‰).

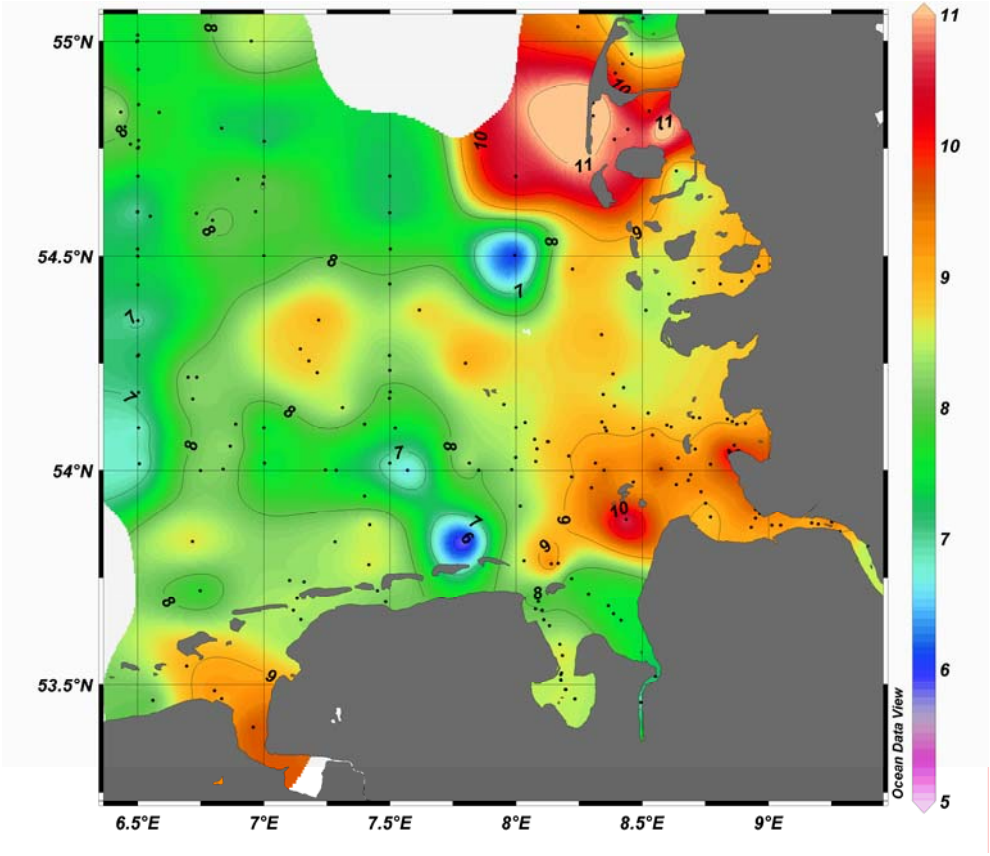

Fig. 2.4. Distribution of observed $\delta^{15}N$ values of surface sediment.

The model reproduces $\delta^{15}N$ levels of sediments ($\delta^{15}N_{mod}$) quite well, even though $\delta^{15}N_{obs}$ has considerably more structure. The model correctly depicts the overall gradient of increasing values towards the coast, and those areas affected by river discharge (Fig. 2.5). An area with $\delta^{15}N_{mod}$ higher than 8‰ extends from the Netherlands coast (53°N, 5°E) to Denmark (56.3°N, 8.2°E) and outlines the seafloor overlain by the coastal water mass of low salinity in the German Bight; this German Bight Water mass is most strongly affected by river discharges. Secondary patterns modulate the general gradient: Highest values ($\delta^{15}N_{mod}$ > 9‰) are modeled within a large area of the northern German Bight bordering the North Frisian Islands close to the Danish border (around 54.5°N, 8.2°E). Moderately high values of $\delta^{15}N_{mod}$ (> 8-9‰) mark the vicinities of estuaries of rivers Weser and Ems, whereas more enriched $\delta^{15}N_{mod}$ (> 9‰) are modeled in the mouth of river Elbe. Between the Elbe estuary and the maximum near the

North Frisian Islands, the model calculates a distinct local minimum $\delta^{15}N_{mod}$ ~ 8‰) that is also apparent in $\delta^{15}N_{obs}$. On the other hand, $\delta^{15}N_{mod}$ and $\delta^{15}N_{obs}$ diverge locally: In spite of elevated $\delta^{15}N_{nitrate}$ in river discharge (Johannsen, 2007; Johannsen et al., 2008), sediments in the estuary of river Weser have no significant enrichment $\delta^{15}N_{obs}$ < 8‰), whereas the model predicts an enrichment > 9‰. The distribution of $\delta^{15}N$ in surface sediments mirrors the prevailing anticlockwise circulation in the North Sea. For the German Bight, this current pattern causes an inflow from the west and an outflow to the north (see Fig. 2.7). Elbe water with enriched $\delta^{15}N$ values is entrained into the northward flow and affects the North Frisian coast. The southern Wadden Sea is only rarely reached by Elbe water during sporadic meteorological blocking events.

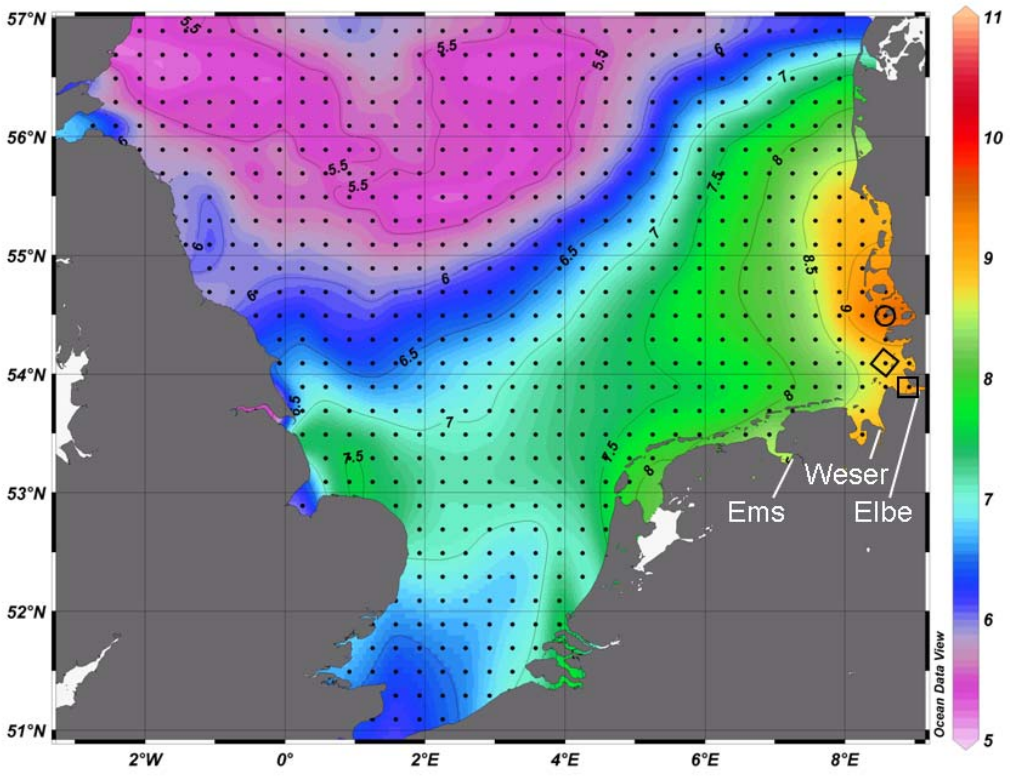

Fig. 2.5. Distribution of simulated $\delta^{15}N$ values of surface sediment.

2.4.2. A budget of reactive nitrogen for the German Bight in 1995

Because the mass fluxes on Nr are a key to the isotope budget, a budget of reactive nitrogen for the German Bight was derived for the year 1995. Figure 2.1 illustrates the boundaries of this area by the dotted line. We defined the western border at 6.1°E, and the northern border at 55°N (A = 28.415 km^2). Figure. 2.6 shows the annual cycle (1995) for total nitrogen (TN) and DIN in the pelagic system of the German Bight as monthly means. The values of TN vary between 3 and 11.4 Gmol N in September and April, respectively. The annual cycle of DIN

runs in phase with TN (1.7-10 Gmol N). The values of DIN for the model year 1995 compare very well with those calculated from observations for 1991/92 (Beddig et al., 1997), although these authors give much higher values for TN. The hydrodynamics underlying the Beddig et al. (1997) - and our budget estimate are comparable, because they are both based on the HAMSOM model (Pohlmann, 1996). We assume that the data of Beddig et al. (1997) also include a rather large amount of refractory dissolved organic nitrogen (DON), which is not included in our model.

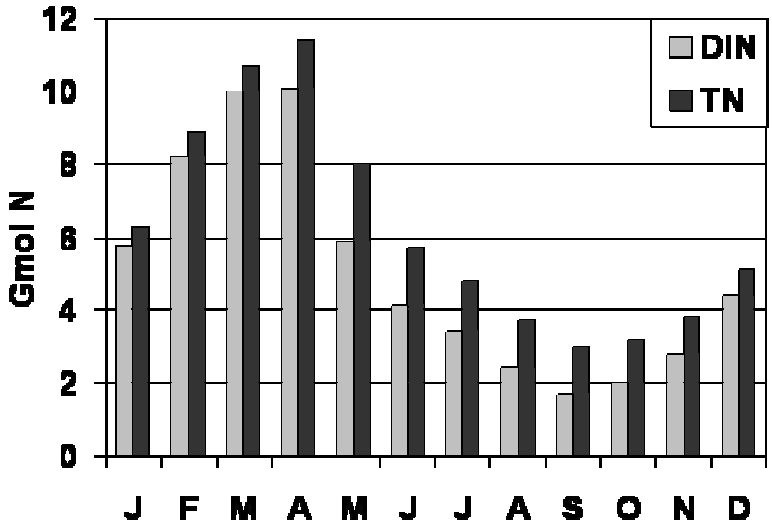

Fig. 2.6. The annual cycle (1995) for total nitrogen (TN) and DIN (mmol m^{-3}) in the pelagic system of the German Bight as monthly means.

The mass budget for nitrogen (Fig. 2.7) shows annual fluxes of TN (Gmol N yr^{-1}). The German Bight receives a net influx across the western border (Fig. 2.1) and loses by a higher net outflux across the northern border. This pattern is a consequence of the general anti-clockwise circulation pattern of the North Sea (Otto et al., 1990) and of Nr added by rivers and atmospheric input. The river loadings for the simulation (1995) and the years 1991/92 correspond to those given by Radach and Pätsch (2007). Beddig et al. (1997) estimated the atmospheric deposition as twice as high as our estimate based on EMEP. The dominant sink for nitrogen is benthic denitrification that eliminates nitrate and forms N_2. This simulated flux is much higher in our budget than that assumed by Beddig et al. (1997) based on too low measured values. These measurements were based on the acetylene blocking method which tends to underestimate denitrification rates by a factor of two to ten (van Beusekom et al., 1999). These authors estimated the annual denitrification as high as 40-80% of the combined river and atmospheric input. In our calculations the simulated denitrification amounts to 69% of the river and atmospheric fluxes. On the other hand, the Beddig et al. (1997) estimate for the benthic remineralisation is higher than simulated. In order to judge the fluxes of benthic

remineralisation and denitrification, we completed the budget (Fig. 2.7) by the modelled annual phytoplankton assimilation of ammonium and nitrate. From these numbers, an estimate for the f-ratio (nitrate uptake / (nitrate + ammonium uptake) of 0.28 is derived. 28.7% of the nitrogen uptake by phytoplankton is thus provided from remineralisation in the benthic system.

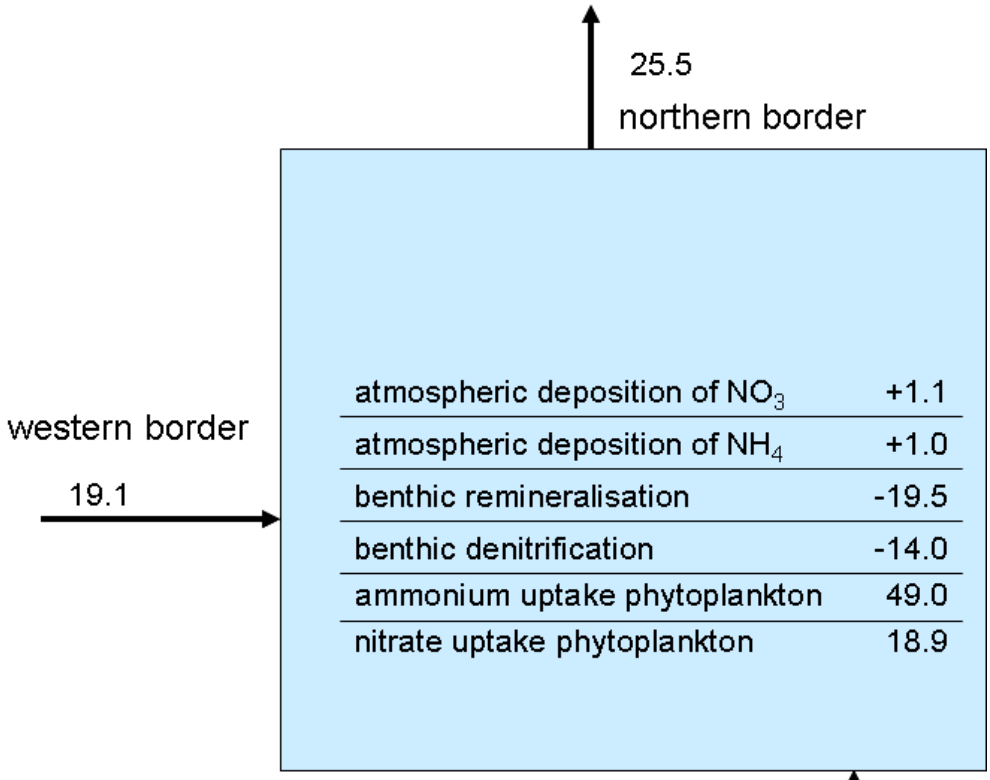

budget	
western border	19.1
river	18.3
atmosperic deposition	2.1
northern border	-25.5
benthic denitrification	-14.0
sum	0.0

Fig. 2.7. Nitrogen fluxes (Gmol N yr^{-1}) in the German Bight as simulated for 1995.

2.4.3. Sensitivity tests of assumptions in the model

The influences of the isotopic composition of Nr at the boundaries and of isotope fractionation factors on simulated $\delta^{15}N$ values in surface sediments were investigated by different sensitivity tests. Table 2.2 is a synopsis of the effects, where the $\Delta\delta^{15}N_S$ values give the deviations (ppm - parts per million) in $\delta^{15}N$ of surface sediment of the northern grid point in the German Bight (Fig. 2.5, circle) when the $\delta^{15}N$ value of variable X at the boundaries is increased by 1‰ (or 1000 ppm). If this signal would translate directly into the $\delta^{15}N$ value of surface sediment of the designated grid point, we would expect a value of 1000 ppm for $\Delta\delta^{15}N_S$. Strongest impacts are modeled for the change in $\delta^{15}N$ of marine nitrate advected into the model domain (35 ppm), while the weakest effects are noted for changes in the $\delta^{15}N$ of DON and of fast-sinking detritus (1 ppm). Corresponding changes of isotope ratios in the sources (river input and atmospheric deposition) cause much more pronounced changes in the $\delta^{15}N$ values in surface sediments: +528 ppm (River Elbe) and +67 ppm (deposition) were detected, respectively. If the $\delta^{15}N$ value of atmospheric nitrogen deposition (nitrate: 7‰ and ammonium: 6‰ as given by Yeatman et al. (2001) for aerosol nitrogen and used in this model), were changed to 1‰ (as suggested by Freyer, 1991), the modeled $\delta^{15}N_S$ value at the grid point would decrease by 0.4‰.

Whereas some changes of fractionation factors in the ECOHAM N-isotope module (Table. 2.3) have a large impact on simulated $\delta^{15}N$ values in surface sediments, other factors are of minor relevance. The fractionation factors of the internal transformations, such as grazing on phytoplankton or breakdown of detritus, show a smaller impact ($\Delta\delta^{15}N_S \approx$ +/-31 ppm) than those at the beginning (nitrate/ammonium assimilation: $\Delta\delta^{15}N_S \approx$ -144 ppm) or at the end (burial: $\Delta\delta^{15}N_S \approx$ +1000 ppm) of the ecosystem N-cycle.

2.5. Discussion

Having shown that the levels of enrichment and their spatial patterns observed in actual surface sediments are approximated well by the modeled levels and patterns, we can use the model to explore the origin of patterns, and address differences between $\delta^{15}N_{mod}$ and $\delta^{15}N_{obs}$. We can further make a first estimate of changes caused by different river loads.

2.5.1. Causes of spatial inhomogeneities

A somewhat counter-intuitive observation both in model and data is that highest $\delta^{15}N$ are not necessarily tied to sediments of estuaries. In order to shed some light on the mechanisms that

cause the simulated pattern of isotopic enrichment between the North Frisian Island and the mouth of river Elbe, we examined the course of the simulated nitrogen cycle over the year at three grid points of the model in more detail. The southern grid point is identified by a square, the northern grid point by a circle, and the central grid point by a diamond in Fig 2.4.

Figure 2.8 shows simulated annual cycles at the three grid points for a) surface water nitrate (mmol N m^{-3}), b) nitrate uptake by phytoplankton (mmol N m^{-2} d^{-1}), c) $\delta^{15}N$ of surface water nitrate (‰), d) $\delta^{15}N$ of phytoplankton (‰), e) $\delta^{15}N$ of detritus entering the sediment (‰), f) flux of detritus-N into the sediment (mmol N m^{-2} d^{-1}), and g) $\delta^{15}N$ of the accumulating surface sediment (‰). Nitrate is never entirely exhausted in surface waters at the southern grid point (black line; Fig. 2.8a). Here, the preferential ^{14}N uptake by phytoplankton continued and the $\delta^{15}N$ value of phytoplankton (and sediment) is approximately 4-5‰ lower than the corresponding Elbe nitrate value (compare Fig. 2.3). In contrast, at the northern grid point nitrate is depleted by assimilation into phytoplankton from day 134 onwards with only sporadic recharge (mainly from benthic mineralization or strong advective events) during the rest of the year. When nitrate vanished at the northern grid point from day 134 on, the simulated phytoplankton bloom collapsed, nitrate uptake becomes very small (Fig. 2.8b) and the $\delta^{15}N$ values of nitrate (Fig. 2.8c) drastically increased to almost 30‰, because the preferred ^{14}N concentrations decreased (Mariotti et al., 1981). Shortly before that time, the $\delta^{15}N$ value of phytoplankton (Fig. 2.8d) at the northern grid point increased up to 11‰, reflecting the much more dramatic increase of the $\delta^{15}N$ values of nitrate. When the substrate (nitrate) approaches depletion, the isotope fractionation during assimilation is no longer effective (modified Rayleigh process), and any ^{15}N (for example nitrate originating from river plumes) is assimilated by phytoplankton. The enrichment seen in sediments near the northern maximum of both $\delta^{15}N_{mod}$ and $\delta^{15}N_{obs}$ is thus at least partly due to the complete consumption of river-borne nitrate that arrives in the area with elevated $\delta^{15}N_{nitrate}$ values.

At the central grid point (red line in Fig. 2.8), nitrate was never exhausted, and although nitrate concentrations here ranged below the concentrations of the southern grid point, preferential uptake of $^{14}NO_3^-$ continued to produce phytoplankton that was more depleted in $\delta^{15}N$ than the nitrate pool.

The high $\delta^{15}N$ values in phytoplankton are transfered to the detritus pool: Fig. 2.8e illustrates the $\delta^{15}N$ values of the combined fast- and slow-sinking detritus as it enters the sediment. For the northern grid point, the three maxima (near days 130, 195 and 240) correspond to those of $\delta^{15}N$ of phytoplankton (Fig. 2.8d). After day 125 when nitrated is depleted, the northern grid point consistently exhibits the highest $\delta^{15}N_{mod}$ in detritus of all three positions. The isotope discrimination process together with the varying detritus fluxes to the sediment during the annual cycle (Fig. 2.8f) thus determine the $\delta^{15}N$ values of the accumulating surface sediment

(Fig. 2.8g), resulting in highest $\delta^{15}N_{mod}$ at the northern location and lowest $\delta^{15}N_{mod}$ at the central one.

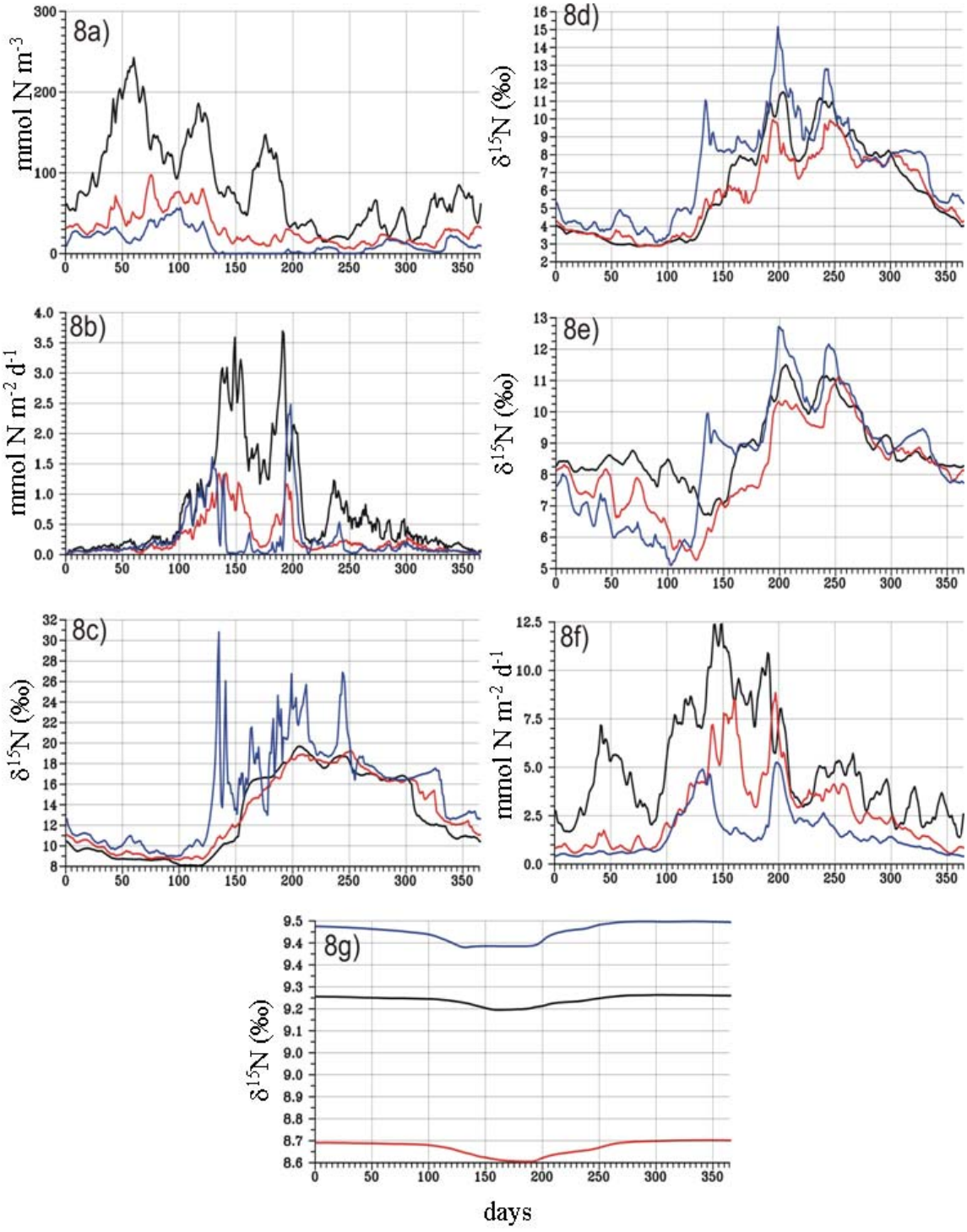

Fig. 2.8. Temporal development of different parameters at three grid points indicated in Fig. 2.5: Black line – southern grid point (square), red line – central grid point (diamond), and blue line - northern grid point (circle). The parameters are: a) pelagic surface nitrate (mmol N m^{-3}), b) nitrate uptake by phytoplankton (mmol N m^{-2} d^{-1}), c) $\delta^{15}N$ of pelagic surface nitrate (‰), d) $\delta^{15}N$ of phytoplankton (‰), e) $\delta^{15}N$ of detritus entering the sediment (‰), f) flux of detritus-N into the sediment (mmol N m^{-2} d^{-1}), and g) $\delta^{15}N$ of the accumulating surface sediment (‰).

While we found a general congruence of $\delta^{15}N_{obs}$ and $\delta^{15}N_{mod}$ distributions, some features differ. The observed low $\delta^{15}N_{obs}$ values, in particular in the estuary of the Weser River are not to be seen in model results, and are a bit of a puzzle. Although Elbe and Weser rivers have comparable Nr - concentrations and riverine $\delta^{15}N$ of nitrate, the sediments in the estuary of the Weser apparently receive particulate N that is more depleted in ^{15}N than it is the case for the other rivers. This may point to material produced at a comparatively early stage in the assimilation of nitrate and thus is comparatively ^{15}N depleted. We speculate that the reason may lie in the relatively narrow and poorly ventilated estuary, which precludes estuarine assimilation of nitrate to the same extent as in the Elbe estuary, thus producing particulate N that is less enriched. This detail (differences in adequate horizontal resolution of the estuaries) is not implemented in the model, and biases $\delta^{15}N_{mod}$.

Another deviation between $\delta^{15}N_{obs}$ and $\delta^{15}N_{mod}$ of the surface sediments is the position of the $\delta^{15}N$ maximum off the North Frisian coast. While the observed pronounced maximum is found near the island Sylt, the simulated weaker maximum is positioned about 50 km further to the south. If we assume that the observed maximum is not generated by a local source of enriched nitrogen (for example, by nitrate-rich groundwater discharge), but indeed stems from the German rivers Eider, Elbe and Weser, only a few causes for the deviation between observation and simulation are left: (1) The simulated advection of material from the inner German Bight to the northern boundary of the Bight may be too weak or too diffusive. On the other hand, model tests with passive tracers released in the river mouths simulated reasonable spreading behaviour in the southern North Sea. (2) The simulated uptake of nitrate by phytoplankton may be too fast, so that the complete incorporation of riverborne nitrogen into the food web and thus the modified Rayleigh process would cause a spatially compressed domain of the heavy nitrate in the modeled river plume. However, observed nitrogen limitations near the island Sylt (Loebl et al., 2009; van Beusekom et al., 2009) support our simulations of nitrate depletion (Fig. 2.8a). (3) The N-loads of rivers may be higher than estimated. The load calculations for the river Elbe originate from concentration and water discharge measurements near Hamburg, about 100 km above the river mouth (Pätsch and Lenhart, 2004). They estimated that additional 21% of final Elbe discharges are added along the way from Hamburg to the North Sea, possibly not balanced by nitrate loss due to estuarine denitrification (Dähnke et al., 2008). Clearly, the modeled location of the North Frisian is subject to several influences that are not tightly constrained in the model.

2.5.2. Effects of decreased river loads on levels and patterns of $\delta^{15}N_{mod}$

An overall aim of our effort is to use the model for reconstructions of past river loads and their effects on $\delta^{15}N$ levels and spatial patterns. To demonstrate that this is indeed feasible, we performed a simulation (full spinup) with 50% reduced Nr inputs via rivers. In this simulation, the monthly $\delta^{15}N$ values of river Nr loads were again those of 2006/2007 and the mass and isotopic composition of atmospheric input was also retained. We are certain that both were different in the past: River inputs of Nr certainly have been more depleted in ^{15}N in accordance with different land-use in the catchments (Mayer et al., 2002; Voß et al., 2006; Johannsen et al., 2008), and atmospheric inputs must have been less significant (Bartnicki and Fagerli, 2004) and possibly had a different isotopic composition. But even with these uncertainties, the pattern of $\delta^{15}N_{mod}$ is significantly different from that modeled for present-day inputs. Most significantly, the extent of the area with $\delta^{15}N_{mod}$ values > 8‰ - characteristic for the present-day eutrophied coastal water mass of the German Bight - decreases (compare Fig. 2.9 and Fig. 2.4). In addition, the maximum near the North Frisian Island Pellworm disappears, whereas a pronounced maximum (> 10.5‰) emerges in the outer estuary of river Elbe. This experiment demonstrates that the amount of nitrogen discharged by rivers has indeed a strong impact on the distribution of $\delta^{15}N$ values of the surface sediments.

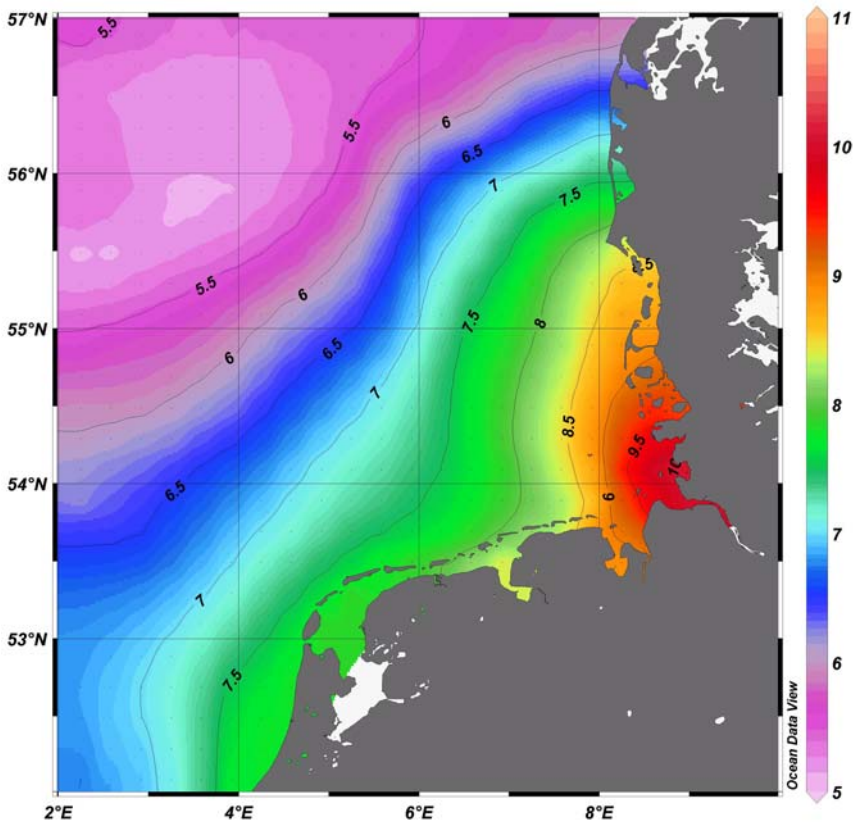

Fig. 2.9. Distribution of simulated $\delta^{15}N$ values of surface sediments with 50% of the nitrogen riverloads.

The difference between $\delta^{15}N$ values of surface sediments from the simulation with full and half river loading (Fig. 2.10) is largest in a band about 200 km off the continental coast. Towards the open North Sea the difference converges against zero, while lowest and even negative values appear near the large river inlets. The winter surface salinity patterns (Fig. 2.10, black isolines) run parallel with the continental coast. Lowest $\delta^{15}N$ differences lie in the region of low-salinity water with less than 30. In the case of River Rhine the local minimum is positioned downstream some tens of kilometers east of the river mouth, while the most obvious differences are modeled for the area just north of the mouth of River Elbe. For our overall aim (to reconstruct pristine conditions based on the evolution of levels and spatial patterns of $\delta^{15}N$ enrichment in dated sediment records through time), this is an encouraging intermediate result. What is needed now are spatially distributed and dated sediment records of $\delta^{15}N_{obs}$ for time slices before eutrophication. These time-slice records can be used as targets for model runs, together with estimates of the pristine riverine $\delta^{15}N$ of Nr from dated river sediment cores, and - much more difficult - better estimates of past atmospheric deposition and its isotope signature.

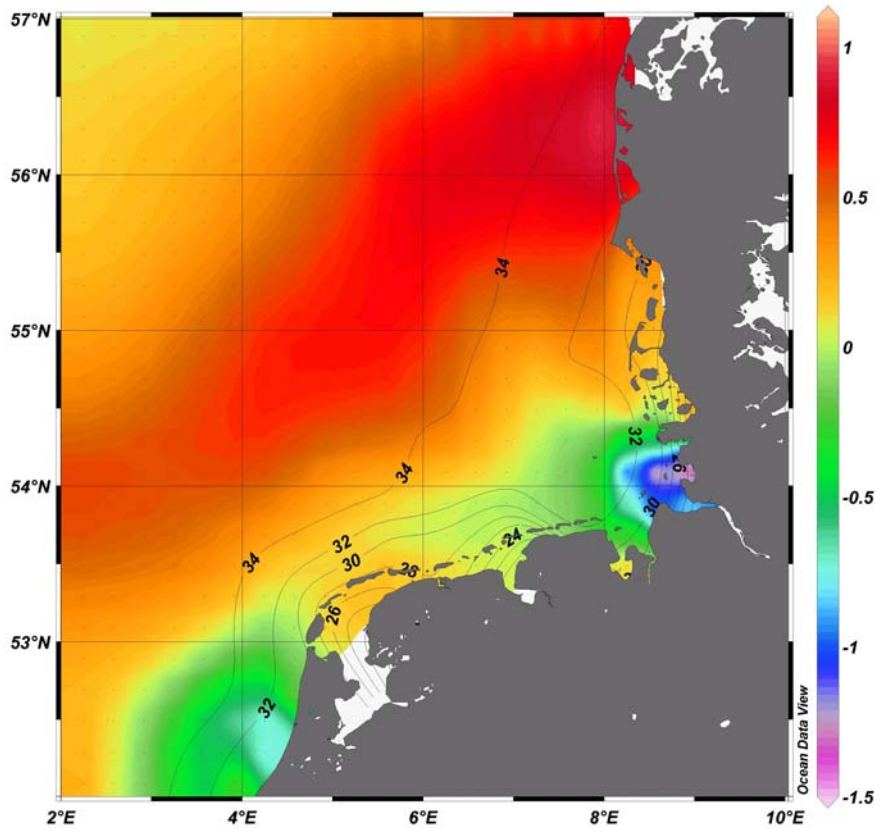

Fig. 2.10. Difference between $\delta^{15}N$ values of the surface sediments from the simulation with full and half river loading (shaded) together with surface salinity in winter (DJF) from the NOWESP database (isolines) (Radach and Gekeler, 1996).

2.6. Conclusions

We have presented data and model results that explore the feasibility for reconstructions of pristine N-cycles in shelf seas by combining ecosystem modelling and N-isotope data of sediment archives. The model results show that the amount of reactive nitrogen discharged by the Northwest-European continental rivers strongly influences the distribution of $\delta^{15}N$ values of surface sediments in the German Bight. Therefore, $\delta^{15}N$ values of dated sediment cores for pre-industrial times, in our opinion, represent a useful target to quantitatively reconstruct such river inputs by modeling N-isotopes under different riverine and atmospheric loading. The $\delta^{15}N$ values of the nitrogen loads delivered by rivers and the atmosphere become fully effective in the biological cycles and subsequently in $\delta^{15}N$ values of the surface sediments, when the nitrogen is completely taken up by phytoplankton. This was the case when river loads of Nr were low, and should be encoded in lower-than-present $\delta^{15}N$ of sediments deposited in the coastal zone of the North Sea (and other similarly impacted shelf seas). Combining data sets of such sedimentary deposits that permit precise age assignments and time-slice reconstructions of past patterns in deposited $\delta^{15}N$ with the model type proposed here will help to better constrain river loads and past states of shelf sea ecosystems.

Chapter 3

History of anthropogenic nitrogen input to the German Bight/SE North Sea as reflected by nitrogen isotopes in surface sediments, sediment cores and hindcast models

Abstract

The German Bight/SE North Sea is considered a hot-spot of river-induced eutrophication, but the scarce observational data of river nitrate loads prior to the 1970s complicate the assessment of target conditions for environmental management and legislation. Stable nitrogen isotope ratios ($\delta^{15}N$) in sediment records can be used to decipher historical river nitrate contributions. To better constrain pre-1970s conditions, we determined $\delta^{15}N$ in archive sediment samples (1950-1969) and dated cores from the Helgoland depositional area. We also modeled the $\delta^{15}N$ in past situations (1960 and 1860) using an N-isotope-tracking ecosystem model. The modeled spatial distribution of $\delta^{15}N$ in sediments for 1960 conditions and the observed spatial pattern of $\delta^{15}N$ in archive sediment samples (1950-1969) represent a period of moderate eutrophication. The modeled spatial distribution of $\delta^{15}N$ in sediments for 1860 conditions (pre-industrial) showed a moderate $\delta^{15}N$ gradient from the Elbe river mouth ($\delta^{15}N$ < 4‰) to the open sea ($\delta^{15}N$ ~ 5‰). This pattern contrasts with the $\delta^{15}N$ pattern in modern surface sediments, which exhibits a steep and inverted $\delta^{15}N$ gradient from the Elbe river mouth ($\delta^{15}N$ > 9‰) to the open sea ($\delta^{15}N$ < 7‰). Modeled $\delta^{15}N$ for 1860 conditions are consistent with $\delta^{15}N$ values observed in dated sediment cores that span the last 900 years. Value of $\delta^{15}N$ in sediment cores increased from approximately 1860 to 2000 by 2.5‰. The increasing trend reflects changes in the abundance and isotopic composition of riverine nitrate loads caused by anthropogenic activities. Sensitivity tests suggest that loads and isotopic ratios of nitrogen forms other than nitrate (ammonium and organic nitrogen) have minor impact on the modeled surface sediments, despite their higher abundance in the riverborne loads in the past. Our results suggest that eutrophication of the German Bight pre-dates the 1960 period of documented rapidly increasing river loads. Pre-industrial levels of $\delta^{15}N$ modeled with 28% of the modern annual (1990-1999) atmospheric loads and 10% of the modern annual river loads agree best with levels of $\delta^{15}N$ (~ 6 ‰) observed in sediments of the cores dated to 1860.

3.1. Introduction

Marine eutrophication caused by increased anthropogenic nutrient inputs is considered one of the major environmental problems affecting the SE North Sea. During the second half of the 20th century, the concentration of nutrients in estuaries and coastal waters of the German Bight/SE North Sea increased drastically and affected primary production rates, aggravated oxygen depletion, and adversely affected species diversity (Brockmann et al., 1988; Pätsch and Radach, 1997; van Beusekom, 2005; Pätsch and Lenhart, 2008). Rivers, together with the atmosphere and groundwater, constitute the most important source of reactive nitrogen (Nr) to coastal seas (Spokes and Jickells, 2005). During the second International North Sea Conference it was decided to reduce nitrogen and phosphorus inputs into the North Sea between 1985 and 1995 by 50% (INSC, 1987; OSPAR Commission, 2003). Attenuation efforts have already resulted in a significant reduction in phosphorus loads but nitrogen loads have declined less in response to environmental legislation (McQuatters-Gollop et al., 2007; Radach and Pätsch, 2007; Pätsch and Lenhart, 2008; Vermaat et al., 2008).

In the absence of observational data prior to the 1970's, records in sediment cores may help to identify the evolution of anthropogenic inputs throughout their deposition and may provide baseline levels as targets for reduction efforts. Dominik et al. (1978) and Hebbeln et al. (2003) have demonstrated that even shallow marine sediments of the SE North Sea provide undisturbed sedimentary records. With regard to nutrient load reconstructions, studies in coastal settings have confirmed that $^{15}N/^{14}N$ ratios, expressed as $\delta^{15}N$ (in ‰ relative to atmospheric N_2), in sediment cores are a useful tool for reconstructing historical records of nutrient availability and organic matter sources (Struck et al., 2000; Voß et al., 2000; Hu et al., 2008). The distinctive isotopic signature of different nitrogen sources can be used to trace their contribution to the sediments. Marine particles have isotopic signatures around 5‰ (Liu and Kaplan, 1989), whereas organic fertilizers, sewage and manure are characterized by $\delta^{15}N > 8$‰ (Heaton, 1986; Voß and Struck, 1997; Bateman et al., 2005; Voß et al., 2006 and references therein; Bateman and Kelly, 2007). The usefulness of $\delta^{15}N$ measurements to detect imprints of nitrate eutrophication has previously been shown from sediment records of the Baltic Sea (Voß and Struck, 1997; Struck et al., 2000; Emeis et al., 2002), the northern North Sea and Kattegat (Dähnke et al., 2008a) as well as in several estuaries in NW Europe (Clarke et al., 2003; Clarke et al., 2006).

To decipher the environmental significance of $^{15}N/^{14}N$ ratios in spatially distributed sediment records we must trace the pathways of Nr through the ecosystem from the source of nitrate in rivers to particulate nitrogen deposited in marine sediments. As a first estimate, the level of and the land to sea gradient in $\delta^{15}N$ of sediments reflects the proportion of riverine nitrate assimilated by phytoplankton and sedimented as detritus. Due to reduced river nitrate discharges in the past, the river nitrate influence may have been weaker. Therefore, we

expect both a lower absolute level of $\delta^{15}N$ in the German Bight and a gradient that differs from the present-day gradient.

A new version of the numerical ecosystem model ECOHAM (Pätsch and Kühn, 2008) that includes an N-isotope-tracking module (Pätsch et al., 2010) is used here to estimate the level of and gradient in $\delta^{15}N$ of sediments in the past with reduced river nitrate discharge. The model is calibrated to the modern patterns of $\delta^{15}N$ in surface sediments of the German Bight. These modern patterns have elevated isotopic signatures with a steep gradient over 400 km from the Elbe river mouth ($\delta^{15}N > 9‰$) to the open sea ($\delta^{15}N < 7‰$). The gradient mirrors the extent of enriched river nitrate assimilated into biomass and incorporated into sediment. For reasons discussed below, we focus our discussion on riverborne nitrate only, although the model includes other nitrogen forms.

We established coast-open North Sea gradients in $\delta^{15}N$ in recent (1989-2009) and archive (1950-1969) surface sediments samples from the German Bight, and levels of $\delta^{15}N$ for dated sediment cores from accumulation basins. We modeled the spatial distribution of $\delta^{15}N$ in sediments for modern (1990-1999) and two historical (1960 and 1860) conditions. Our specific objective is to reconstruct signatures of $\delta^{15}N$ and historical Nr loads in the German Bight.

3.2. Study area

The SE North Sea receives significant inputs of Nr from rivers draining continental Europe. High nitrate waters from rivers trapped in the German Bight/SE North Sea due to low exchange rates with open North Sea water masses bypassing the inner German Bight have caused a severe eutrophication problem (OSPAR Commission, 2003b). Besides river discharge (18 Gmol N yr^{-1}), atmospheric deposition (2 Gmol N yr^{-1}) and an import across the western border, 6.1°E, (19 Gmol N yr^{-1}) contribute to the input of total nitrogen into the German Bight (Pätsch et al., 2010). As a consequence of the counter-clockwise circulation pattern of the North Sea, a significant export towards the northern border, 55°N, occurs (25 Gmol N yr^{-1}), but 14 Gmol N yr^{-1} are retained in the German Bight, most of which is eliminated by denitrification and sedimentation (Lohse et al., 1993; Pätsch et al., 2010). Recent sedimentation of fine material is concentrated in the major depocenter of the Helgoland area, which has a mean water depth of 20 m (Eisma and Kalf, 1987; Becker, 1992). The western part of the Helgoland area consists mainly of mud, with median grain size values of < 80 µm (Wirth and Wiesner, 1988), deposited at variable sedimentation rates (average ~ 0.8 cm yr^{-1}); whereas towards the eastern part the proportion of sand increases (Hertweck, 1983). Sediments deposit in the area due to a small-scale eddy caused by the interaction of the longshore coastal current, the discharge from the Elbe and Weser rivers,

and tidal dynamics (Hertweck, 1983). Human activities (e.g. trawl fishing activities) also contribute substantially to sediment redistribution in the SE North Sea (Rijnsdorp et al., 1998; OSPAR Commission, 2000).

3.3. Materials and methods

3.3.1. Surface sediment sampling

Surface sediments from selected locations were obtained by grab sampling and coring. Sediment material includes the interval 0-1 cm or 0-2 cm; differences in $\delta^{15}N$ on both intervals for a selected set of fifteen samples were usually within the analytical precision of the method (see below). All sediments were dried at 40-50 ºC or freeze-dried over three days and treated with an ultrasonic device, prior to storage. Since we expected low contents of nitrogen in the sediments and because nitrogen compounds of the sediments occur within the finest fractions (Wiesner et al., 1990), dried samples were divided into two sub-samples. One unfractionated sub-sample was homogenized and ground to powder, while the other sub-sample was sieved through a 20 µm mesh. Only the fraction < 20 µm of the sieved sub-sample was used for $\delta^{15}N$ analysis. To determine the influence of grain size separation on $\delta^{15}N$ determinations, we complemented previous tests (Seel, 2005) with a subset of nine samples in which both unsieved and sieved samples were analyzed. Differences in $\delta^{15}N$ of the fraction < 20 µm and $\delta^{15}N$ of the unfractionated sediments was within the analytical precision of the method (see below). Surface sediment material sampled between years 1950 and 1985 were made available by the Federal Maritime and Hydrographic Agency (BSH). These samples were collected within the framework of its national mapping activities (BSH, 2007) and were dried prior to storage. We selected a subset of approximately 70 archive samples, sieved them through a 20 µm mesh and determined $\delta^{15}N$ values of the finer sub-samples. We grouped the surface sediment data into two different periods, i.e. recent (1989-2009) and older (1950-1969) surface sediments, based on reported changes in riverine nutrient inputs into North Sea coastal waters (Radach, 1998; Radach and Pätsch, 2007) and on sample availability.

3.3.2. Multicores and gravitiy cores

Three multicores (MUCs) were collected on expedition RV Heincke-267 (2007) and sliced in 1 cm intervals. Detailed information on core locations, water depths and lengths is given in Table 3.1. Gravity core (GC) HE 215/4-2 was collected from aboard the RV Heincke-215 (2004) and has been kept in a cold room since it was recovered and split (see Table 3.1 for position). Eighteen sediment samples were taken in the laboratory with sawn-off syringes pushed into the core face. For $\delta^{15}N$ analyses, samples were dried and treated the same way

as surface sediments. Details of sampling procedure for GC GeoB/4801 from the Helgoland mud area are given in Hebbeln et al. (2003).

We also analyzed sediment cores from the dredge spoil repositories Francop (53.5°N, 9.8°E) and Feldhofe (53.5°N, 10.1°E): two sites in Hamburg where material dredged from the Elbe river has been deposited. The oldest sediments are from the year 1972, when dredging and deposition of material started (A. Gröngröft, pers. comm). Additionally, we obtained two sediment cores (Table 3.1) taken in 1995 from an oxbow loop of the Elbe river (right/left bank) in the Tangermünde vicinity; Elbe 389 km from the Czech Republic/Germany border (Prange, 1997). We expect that $\delta^{15}N$ ratios in dredge materials and core sediments from the Elbe oxbows trace Nr inputs via rivers under assumed pristine loading conditions and allow us to better constrain the isotopic composition of riverine sources prior to widespread use of mineral fertilizers.

Table 3.1 Location, collection date, water depth and length of the sediment cores.

Core No.	Latitude (°N)	Longitude (°E)	Collection date	Water depth (m)	Core length (cm)
GC HE215/4-2	54.072	8.074	9/8/2004	23.0	486
GC GeoB/4801	54.102	8.034	1997	25.0	111
MUC HE267/327	54.112	8.036	5/5/2007	21.3	17
MUC HE267/329	54.099	7.521	5/5/2007	34.9	28
MUC HE267/347	54.602	6.500	5/6/2007	36.1	23
GC TK-16	52.536	11.979	11/25/1995	Unk.	291
GC TK-17	52.536	11.979	11/25/1995	Unk.	401

3.3.3. Stable isotopes

Nitrogen isotope ratios were determined using a Finnigan MAT 252 isotope ratio mass spectrometer after high-temperature flash combustion in a Carlo Erba NA-2500 elemental analyzer at 1100 ºC. The isotope ratios are reported in the conventional isotope terminology:

$$\delta^{15}N\ (‰) = (R_{sample} / R_{standard} - 1) \times 1000 \quad (3.1)$$

where R_{sample} and $R_{standard}$ are the $^{15}N/^{14}N$ ratios of the sample and the standard respectively. The standard is atmospheric N_2. The analytical precision of $\delta^{15}N$ analyses was better than 0.2‰ based on replicate measurements of six samples of varying N-content (Bahlmann et al., 2009) and repeated analyses of IAEA-N-1 and IAEA-N-2 standards.

3.3.4. Dating

The age model of core GC HE215/4-2 is based on five radiocarbon dates determined on carbonate from shell parts and benthic-foraminifera tests from five sediment samples (1 cm thick) using the Accelerator Mass Spectrometry (AMS) facility of the Leibniz Laboratory for Age Determinations and Isotope Research from the University of Kiel (Table 3.2). The age data were calibrated and converted into calendar years (given as years AD) using the MARINE04 data set in the Calib 5.0.2 software (http://calib.qub.ac.uk/calib/; Stuiver and Reimer, 1993; Hughen et al., 2004; Reimer et al., 2004). The age model for GC GeoB/4801 is based on twelve AMS ^{14}C data and ^{210}Pb dating. Analytical details are given in Hebbeln et al. (2003). Sedimentation rates for short cores were determined by the ^{210}Pb method. Because of the slight decrease in ^{210}Pb excess with depth found in the short cores, calculation of sedimentation rates is based on mean ^{210}Pb excess concentration (Table 3.3) and the average ^{210}Pb atmospheric flux over Europe (~110 Bq m^{-2} yr^{-1}; Preiss et al., 1996). Complex sedimentation processes such as lateral transport were not considered within the simple dilution model applied.

Table 3.2 Overview of the AMS ^{14}C dates in GC HE215/4-2, proposed age model in mean calendar years (AD MEAN), and sedimentation rates (SR).

Lab. number	Sample depth (cm)	Conventional age (BP)	AD- (1 sigma range)	AD+ (1 sigma range)	AD MEAN	SR (cm yr^{-1})
KIA 33646	37-38	490 ± 40	1806	1951	1879	0.52
KIA 33647	111-112	540 ± 25	1713	1811	1762	0.64
KIA 33648	214-215	735 ± 25	1531	1618	1575	0.55
KIA 33649	385-386	1255 ± 35	1099	1205	1152	0.41
KIA 33650	486-487	1340 ± 25	1026	1099	1063	1.13

Table 3.3 Measurements of ^{210}Pb activity and estimation of sedimentation rate in MUCs.

Core No.	^{210}Pb excess MEAN (Bq kg^{-1})	SR (cm yr^{-1})
MUC HE267/327	6.14	0.52
MUC HE267/329	10.43	0.96
MUC HE267/347	21.89	1.15

3.3.5. The ECOHAM model

We compare observed $\delta^{15}N$ in dated sediment cores and surface sediments with $\delta^{15}N$ patterns in surface sediments generated with the 3-dimensional ecosystem model ECOHAM (Pätsch and Kühn, 2008), amended by an isotope-module (Pätsch et al., 2010). The model was first implemented for the year 1995 (Pätsch et al., 2010) using riverine nitrogen loads from Radach and Pätsch (2007). In this study, we simulated (i) present situations based on 1990-1999 annual mean nitrogen loads, and (ii) past situations with assumed 1960 and 1860 nitrogen input conditions and isotopic compositions (Fig. 3.1). We chose the 1990-1999 annual mean nitrogen loads (14.1 Gmol N yr^{-1}; Table 3.4), instead of using nitrogen loads of 1995 only as was done in Pätsch et al. (2010), because the decadal mean integrates the loads encoded in recent sediments (1989-2009). To explore riverine N-inputs that caused the isotopic signal of archive sediments from 1950 to1969, we simulated the year 1960 as a representative year of the two decades. For a pre-industrial situation, we simulated the year 1860, because recent core data (Hastings et al., 2009) confirm the onset of anthropogenic activities in the mid 19th century.

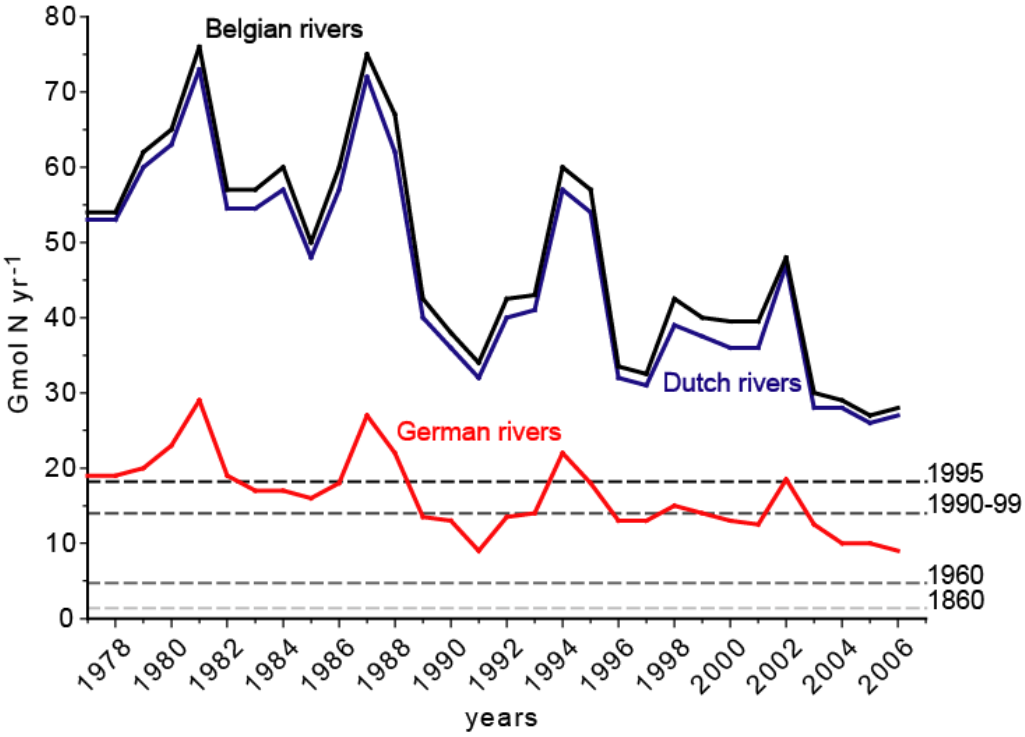

Fig. 3.1. Cumulative annual loads of total nitrogen from the North Sea continental rivers (Radach and Pätsch, 2007; Pätsch and Lenhart, 2008). Dashed lines represent the sum of total nitrogen loads of Ems, Weser and Elbe as prescribed in the model for each simulation (see Table 3.4).

The model uses atmospheric nitrogen deposition data from the "Cooperative program for monitoring and evaluation of the long-range transmissions of air pollutants in Europe" (EMEP). To simulate the recent spatial distribution of $\delta^{15}N$, we assumed the same atmospheric input as in Pätsch et al. (2010) for 1995 (Table 3.5), instead of annual mean loads because there are data available only for the years 1990, 1995 and 2000.

Table 3.4 Atmospheric and riverine loads in the German Bight used for the different simulations in comparison to those assumed in Pätsch et al. (2010) for 1995 conditions.

		1995	**1990 - 99**	**1960**	**1860**
Atmospheric load (Gmol N yr^{-1})	NO_3	1	1	0.6	0.3
	NH_4	0.8	0.8	0.4	0.2
Sum atmospheric load		*1.8*	*1.8*	*1*	*0.5*
River load – Ems, Weser,	NO_3	14.5	10.9	2.5	1.1
and Elbe (Gmol N yr^{-1})	NH_4	0.6	0.8	0.6	0.1
	TON	3.2	2.4	1.6	0.2
Sum river load		*18.3*	*14.1*	*4.7*	*1.4*
Total sum N load (Gmol N yr^{-1})		***20.1***	***15.9***	***5.7***	***1.9***

Riverborne total organic nitrogen (TON) loads, which include riverine dissolved organic nitrogen (DON), and their isotopic ratio ($\delta^{15}N_{TON}$) were used as input. Values of $\delta^{15}N_{TON}$ were available only for the Elbe river (Schlarbaum et al., 2010). For all other rivers discharging into the North Sea we used 8.0‰ based on the annual average of $\delta^{15}N_{TON}$ measured in the Elbe river. According to observational data of Schlarbaum et al. (2010) from the Elbe river estuary, DON has approximately the same isotopic composition as particulate nitrogen (PN). The authors also presented recent data of nitrite concentrations in the Elbe river showing that the present contribution of nitrite to the total NO_x pool is less than 1%. For the contribution of dissolved inorganic nitrogen (DIN) we included in the model riverborne ammonium as well as nitrate and nitrite in the proportion stated above. The same ratios of NO_2:NO_3 are used for the past conditions because we estimated that the effect on the isotopic composition of riverine sources is lower than 10%, assuming a contribution of nitrite in the past threefold the present contribution. The isotopic composition assigned for DIN is based on data of $\delta^{15}N$ of nitrate ($\delta^{15}N_{river\ nitrate}$) from the rivers Rhine, Elbe, Weser, Ems and Eider (Johannsen et al., 2008), as described in Pätsch et al. (2010), and an average of 8.2‰ for the other rivers (Forth, Tyne, Tees, Humber, Wash, Thames, Scheldt, Meuse). A typical marine value of $\delta^{15}N_{nitrate}$ = 5‰ (Liu and Kaplan, 1989; Sigman et al., 2000) was prescribed for nitrate advected into the

model domain at the seaside boundaries (Pätsch et al., 2010). In the case of riverine ammonium, we found that the isotopic composition has little impact on the simulated $\delta^{15}N$ of sediments (see sensitivity test below).

The atmospheric input for the 1960 simulations (1.0 Gmol N yr^{-1}; Table 3.4) is interpolated from Jørgensen (1987) and represents approximately 56% of the 1990-1999 annual mean atmospheric nitrate and ammonia loads. The atmospheric isotopic compositions for the 1960 simulations remained as in simulations of present situations (Yeatman et al., 2001; Pätsch et al., 2010). The riverine input (4.7 Gmol N yr^{-1}) is based on estimation from Pätsch (1997) and represents approximately 33% of the 1990-1999 annual riverine input (Table 3.4). We tested different scenarios of annual average $\delta^{15}N_{river\ nitrate}$ for the discharge of rivers Ems, Weser and Elbe: (a) low $\delta^{15}N_{river\ nitrate}$ = 3‰, (b) moderate $\delta^{15}N_{river\ nitrate}$ = 5‰ and (c) high $\delta^{15}N_{river\ nitrate}$ = 7.5‰ (Table 3.5), based on $\delta^{15}N$ observations in sediment cores from the Helgoland mud area and the Elbe vicinity. Sediments deposited in the early 1970s in the Francop and Feldhofe areas have signals in the same range ($\delta^{15}N$ = 5.1‰). For all other rivers discharging into the North Sea, the values are set to $\delta^{15}N$ = 5‰ for both DIN and TON. The Elbe river contributes nitrogen in different forms: for 1995 a molar distribution of 77% nitrate, 4% ammonium and 19% particulate and dissolved organic matter has been estimated (Radach and Pätsch, 2007), but the proportion of DON in the organic fraction remains a matter of debate. During the period 1950-1970 the nitrogen regime was different and ammonium and organic nitrogen were major components (20-40% NH_4 of TN, van Beusekom and de Jonge, 2002; 42% NH_4 of TN, Nelissen and Stefels, 1988). Sensitivity tests (see below) reveal that variations in their relative contribution to the total N-pool have no major implications for the modeled $\delta^{15}N$ in sediments.

Table 3.5 $\delta^{15}N$ ratios assumed for the different state variables X as initial values.

state variable (compartment) X	**$\delta^{15}Nx$ (‰)**					
	1990 - 99		**1960**		**1860**	
atmospheric nitrate (deposition)	+7		+7		+11	
atmospheric ammonia (deposition)	+6		+6		+10	
		low	**moderate**	**high**	**low**	**moderate**
DIN river Ems	+10 □ +19	+3	+5	+7.5	+3	+5
DIN river Weser	+7 □ +13	+3	+5	+7.5	+3	+5
DIN river Elbe	+7 □ +18	+3	+5	+7.5	+3	+5
DIN river Eider	+10 □ +13	+5	+5	+5	+5	+5
DIN river Rhine	+7 □ +11	+5	+5	+5	+5	+5

For the simulation of 1860 conditions, the atmospheric input (0.5 Gmol N yr^{-1}; Table 3.4) was set to 28% of the 1990-1999 annual mean atmospheric loads (Preunkert et al., 2003). We decided to also change the atmospheric isotopic compositions for the simulation of 1860 conditions, based on data of Hastings et al. (2009) and Freyer et al. (1996), who observed increasing $\delta^{15}N$ of atmospheric nitrate with decreasing nitrate concentrations in ice cores. Therefore, we assigned atmospheric isotopic compositions of $\delta^{15}N_{NO3}$ = 11‰ and $\delta^{15}N_{NH4}$ = 10‰ (Table 3.5). The riverine input (1.4 Gmol N yr^{-1}; Table 3.4) was set to 10% of the 1990-1999 annual mean river loads, which is comparable with estimates from Topcu et al., 2009. For the discharge of rivers Ems, Weser and Elbe, we tested two different scenarios of annual average $\delta^{15}N_{river\ nitrate}$: (a) low $\delta^{15}N_{river\ nitrate}$ = 3‰, (b) moderate $\delta^{15}N_{river\ nitrate}$ = 5‰.

The spatial distribution of $\delta^{15}N$ from observations ($\delta^{15}N_{obs}$) and $\delta^{15}N$ from simulations ($\delta^{15}N_{sim}$) were plotted using the software Ocean Data View, version 3.4.2–2008 (Schlitzer, 2002). Interpolation between data points is based on the VG Gridding algorithm, which constructs a rectangular grid with different grid-spacing along X and Y directions according to data density (Schlitzer, 2002). All estimates at grid points are within the acceptable quality limits of the method (< 3) and grid-spacing (X,Y) is set to (55,55).

3.4. Results

3.4.1. $\delta^{15}N$ observations in recent (1989-2009) surface sediments and model results for 1990-1999

The $\delta^{15}N$ distribution of recent surface sediments collected in 1989-2009 from 231 locations shows a wide range and highlight a steep gradient from $\delta^{15}N$ = 6-7‰ in the open North Sea to values $\delta^{15}N$ > 8‰ in the nearshore belt of the German Bight (Fig. 3.2). Maximum values of $\delta^{15}N$ > 11‰ are found between the northern German Islands of Sylt and Föhr and the Danish Island Rømø. A second local maximum $\delta^{15}N$ > 9‰ occurs in the inner German Bight and in the vicinity of the Elbe river mouth. At the western boundary of the German Bight, a patch of low $\delta^{15}N$ is observed with values similar to those in the open sea.

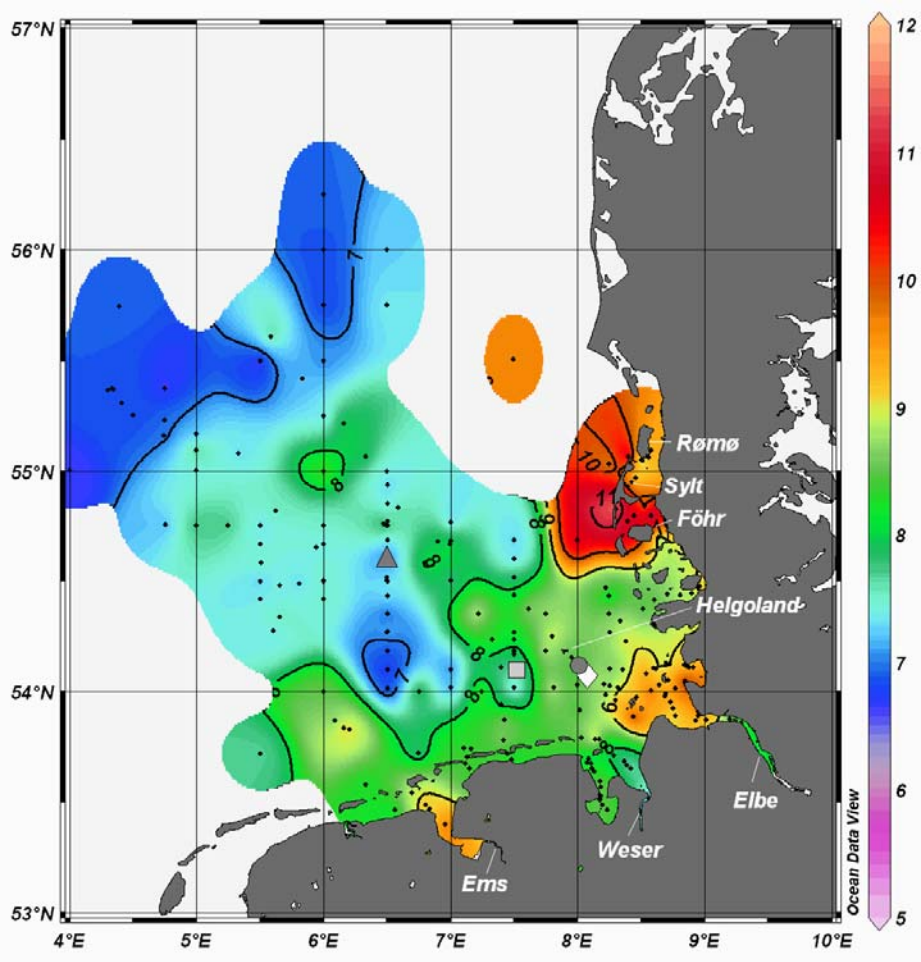

Fig. 3.2. Map of $\delta^{15}N_{obs}$ in recent (1989-2009) surface sediments in the German Bight. Dots indicate sampling locations and symbols core locations in east-west direction: GC HE215/4-2 (diamond), GC GeoB/4801 & MUC HE267/327 (circle), MUC HE267/329 (square) and MUC HE267/347 (triangle). The location of the Ems, Weser and Elbe rivers mentioned in the text are given in the map, as well as the location of the Helgoland, Föhr, Sylt and Rømø Islands.

The simulated spatial distribution for 1990-1999 conditions (Fig. 3.3) shows $\delta^{15}N$ values increasing from values $\delta^{15}N$ < 6‰ in the open North Sea to $\delta^{15}N$ > 9‰ near the Elbe river mouth, where the maximum is found. The model depicts an area of sediments enriched in ^{15}N ($\delta^{15}N$ > 9‰) extending along the coast between the Elbe estuary and off the Föhr Island. The elevated $\delta^{15}N$ values around Sylt Island seen in the observations are not replicated by the model. The section approximately 80 km wide from the Elbe estuary to the NW German Bight (map in Fig. 3.4) was defined to illustrate changes in the $\delta^{15}N$ signal from sediments in areas close to the river nitrate sources and in sediments remote from the coastal sources. The model fails to reproduce the high values ($\delta^{15}N$ = 10-12‰) near the Elbe estuary (Fig. 3.4). Otherwise, it simulates the offshore-nearshore $\delta^{15}N$ gradient observed in recent surface sediments and the relationship between $\delta^{15}N$ and distance from riverine nitrate sources quite well.

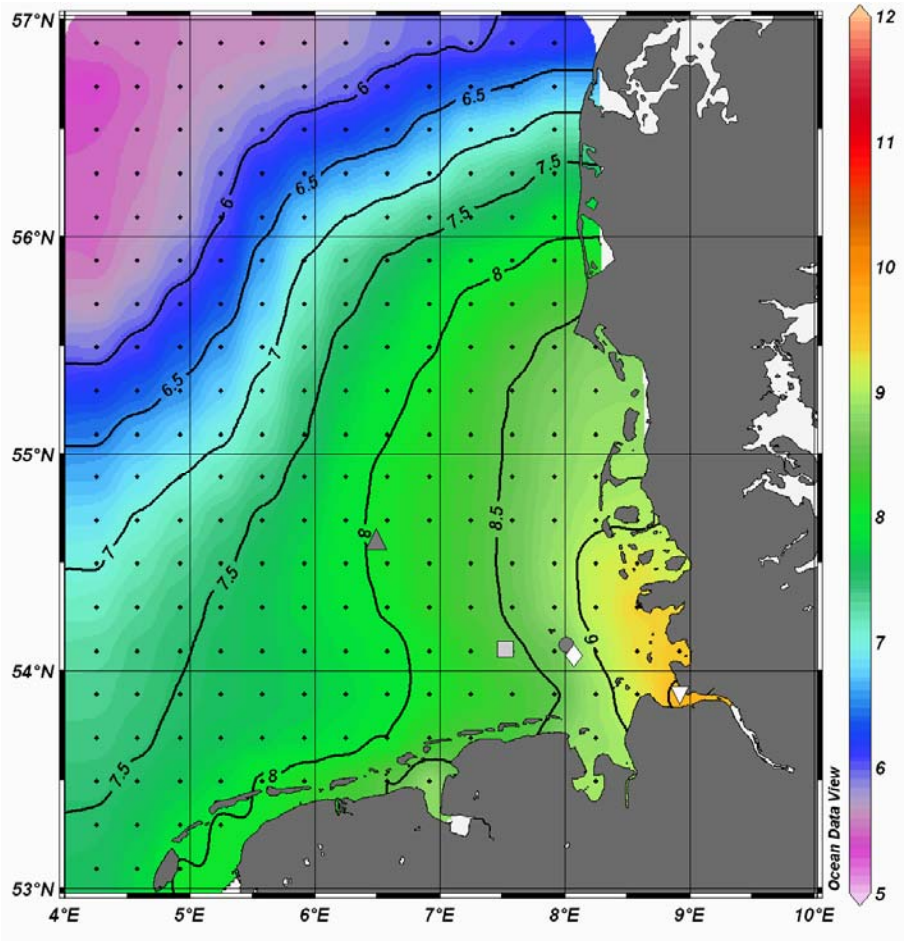

Fig. 3.3. Map of $\delta^{15}N_{sim}$ for 1990-1999 annual mean (see Table 3.4) in surface sediments of the German Bight. Dots indicate grid points of the model domain, symbols indicate core locations (see Fig. 3.2 for symbols description), and studied grid cell for sensitivity test (inverse triangle).

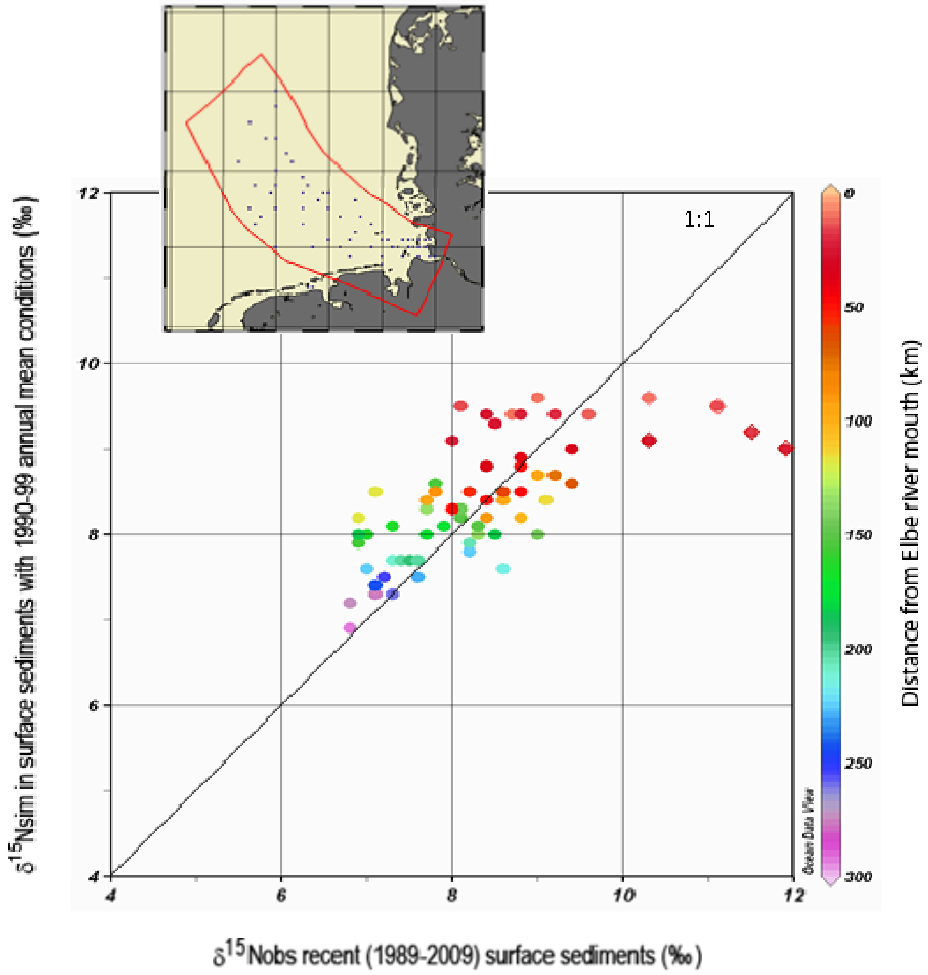

Fig. 3.4. $\delta^{15}N_{sim}$ with 1990-1999 annual mean conditions plotted against $\delta^{15}N_{obs}$ in recent (1989-2009) surface sediments in relationship to distance from riverine nitrate sources (R^2 = *0.45884, n = 67* average values from sampling locations indicated in the map). Data points marked as diamonds are from the Elbe river estuary.

3.4.2. $\delta^{15}N$ observations in older (1950-1969) surface sediments and model results for 1960

The $\delta^{15}N$ in archive surface sediments collected in 1950-1969 from 65 locations (Fig. 3.5) has a distribution similar to the one observed in recent sediments (Fig. 3.2); again the $\delta^{15}N$ values decrease in offshore direction. A maximum found off the Sylt Island with values $\delta^{15}N$ > 10‰ coincides with a maximum seen in recent sediments, and similarly a second local maximum of $\delta^{15}N$ > 9‰ is found in the vicinity of the Elbe river mouth.

In all the modeled scenarios with different annual average $\delta^{15}N_{river\ nitrate}$ (Fig. 3.6), sediments in the Ems, Weser and Elbe estuaries show notably lower $\delta^{15}N$ in simulations for 1960 than for recent conditions (Fig. 3.3). In the simulation for 1960 with low $\delta^{15}N_{river\ nitrate}$ = 3‰ and reduced atmospheric/river loads (Fig. 3.6A), the model shows $\delta^{15}N$ values increasing in

offshore direction from ~3‰ in shallow estuarine areas of the SE North Sea to higher values ~5‰ in areas of deeper waters. The modeled patterns contrast with the observed pattern in older surface sediments (1950-1969), which exhibits decreasing $\delta^{15}N$ values in offshore direction. The observed high $\delta^{15}N$ values near the Elbe estuary and Sylt Island bear little resemblance to the modeled distribution. Modeled sediment $\delta^{15}N$ in the Weser estuary are 4‰ lower than observed (Fig. 3.5).

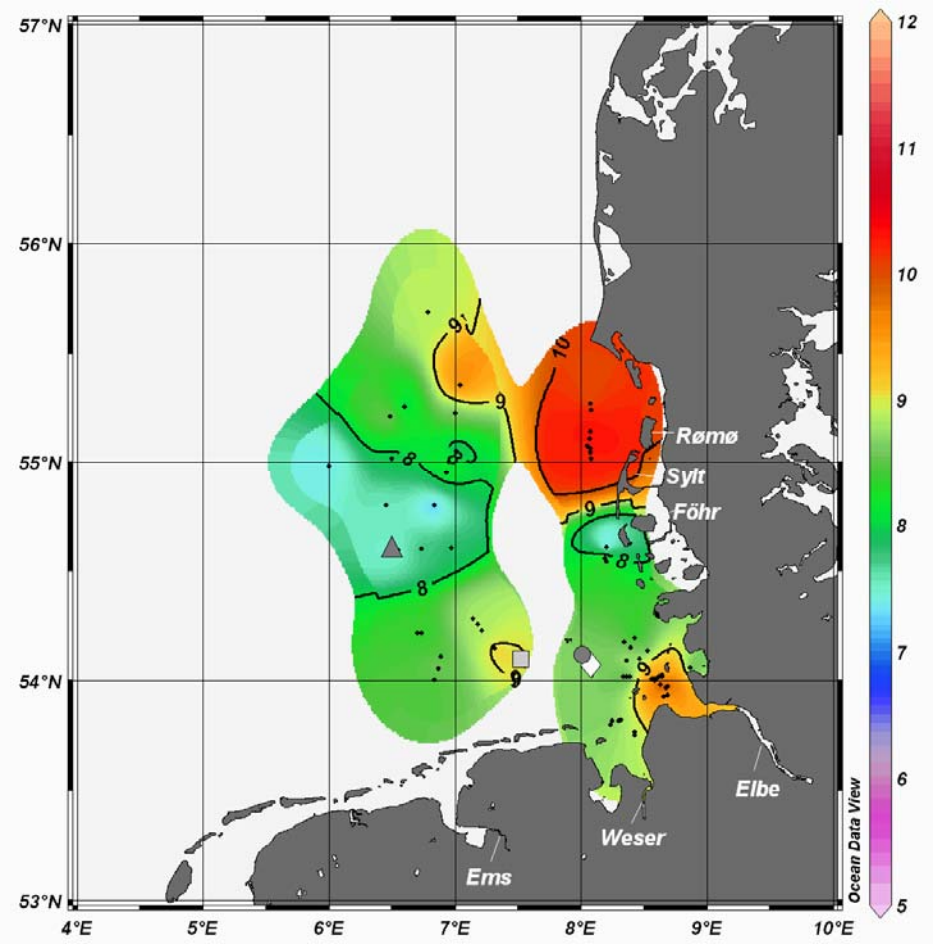

Fig. 3.5. Map of $\delta^{15}N_{obs}$ in older (1950-1969) surface sediments in the German Bight. Dots indicate sampling locations and symbols core locations (see Fig. 3.2 for symbols description).

In the simulation for 1960 with moderate $\delta^{15}N_{river\ nitrate}$ = 5‰ and reduced atmospheric/river loads, the model depicts isotopic ratios around 5‰ in the immediate vicinity of the Elbe estuary (Fig. 3.6B) and slightly higher ratios in the central German Bight. The elevated $\delta^{15}N$ values ~10‰ NW off the Sylt Island seen in the observations in older sediments (Fig. 3.5) are not replicated by the model. Instead, the model calculates $\delta^{15}N$ values in the area around 6‰. In the simulated distribution, areas of deeper water show typical marine nitrogen ratios around 5‰, whereas values in the Weser estuary are 2-3‰ lower than observed in the older sediments.

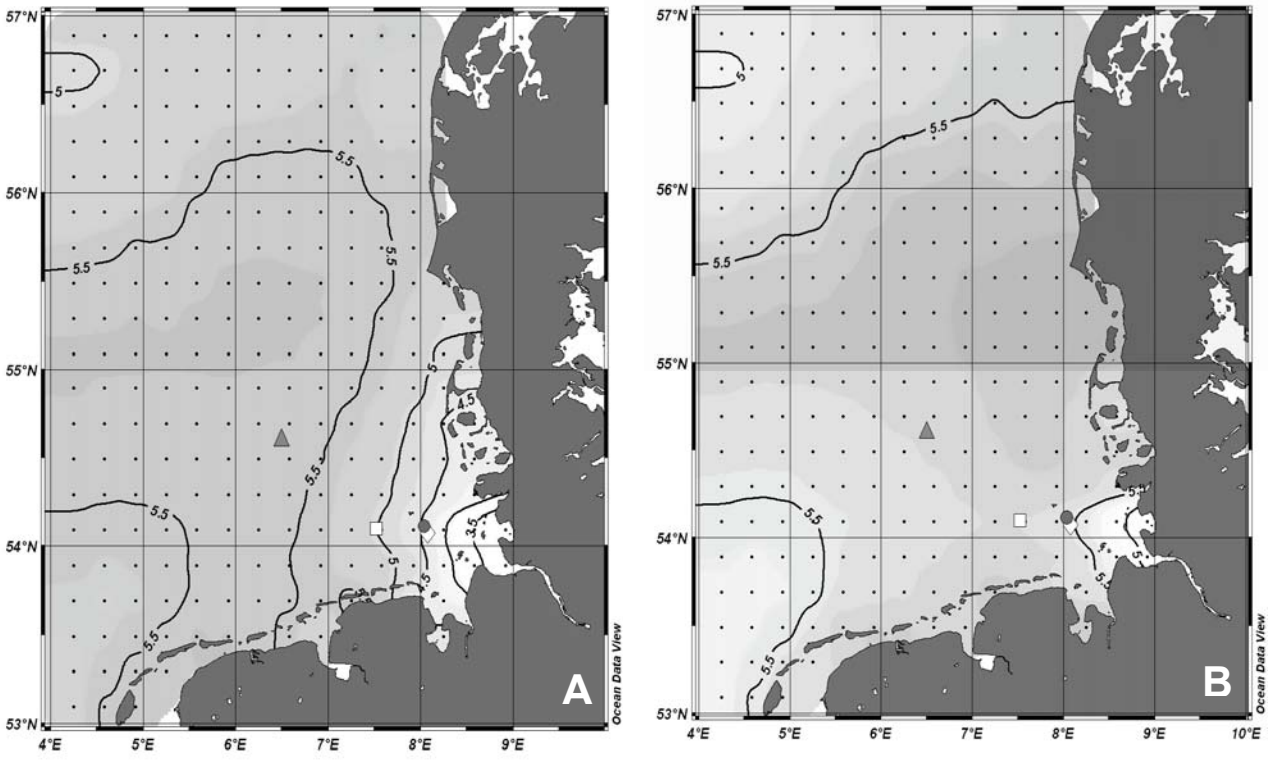

A. low $\delta^{15}N_{river\ nitrate}$ = 3‰

B. moderate $\delta^{15}N_{river\ nitrate}$ = 5‰

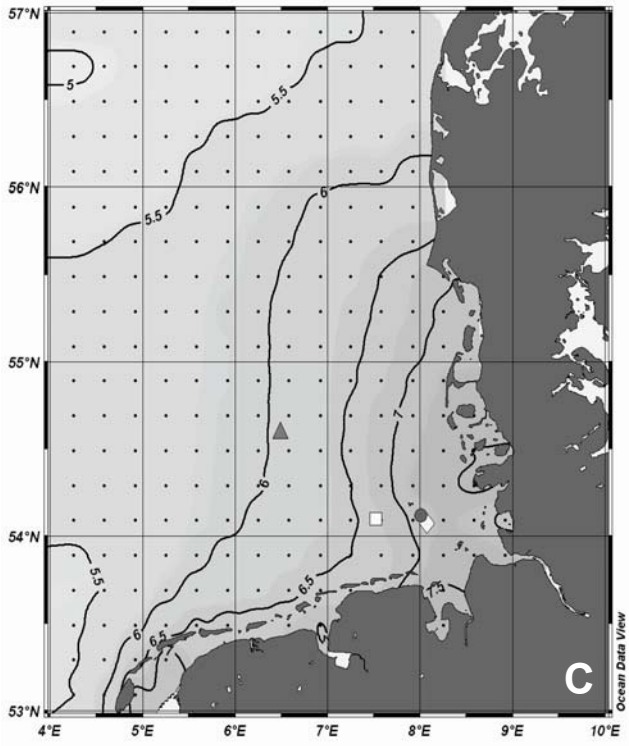

C. high $\delta^{15}N_{river\ nitrate}$ = 7.5‰

Fig. 3.6. Map of $\delta^{15}N_{sim}$ for 1960 conditions (A. low $\delta^{15}N_{river\ nitrate}$ = 3‰, B. moderate $\delta^{15}N_{river\ nitrate}$ = 5‰ and C. high $\delta^{15}N_{river\ nitrate}$ = 7.5‰ and total N-load = 5.7 Gmol N yr^{-1}, see Table 3.4) in surface sediments of the German Bight. Dots indicate grid points of the model domain and symbols indicate core locations (see Fig. 3.2 for symbols description).

In the simulation for 1960 with high $\delta^{15}N_{river\ nitrate}$ = 7.5‰ and reduced atmospheric/river loads, the model depicts an overall gradient of increasing values towards the coast (Fig. 3.6C). The highest values ($\delta^{15}N$ > 7‰) are modeled near the North Frisian Islands some tens kilometers north of the Elbe river mouth (54.3°N, 8.6°E) and in the Weser river mouth. The model shows typical marine nitrogen ratios around 5‰ in areas of deeper waters and higher values ($\delta^{15}N$ ~ 7‰) in the vicinity of the Ems and Elbe estuaries. Values in the Elbe estuary are around 2‰ lower than observed in the older sediments (Fig. 3.5).

3.4.3. Temporal evolution of $\delta^{15}N$ in dated sediment cores

Sediment cores GC HE215/4-2, GC GeoB/4801 and MUC HE267/327 (see Fig. 3.2 for position) were taken almost at the same position in the Helgoland depositional area. The longest core GC HE215/4-2 brackets pre-industrial to recent sediments from AD 2004 (year of core sampling). Sedimentation rates are high and range from 0.4 to 1.1 cm yr^{-1} with a shift from 1.1 to 0.4 cm yr^{-1} between 486 and 385 cm core depth. The age model (Table 3.2) is comparable with the results presented by Hebbeln et al. (2003) for GC GeoB/4801 from the same location. Sedimentation rates in MUC HE267/327 and the other two short MUCs taken west of the Helgoland Island suggest that sediments were deposited within the last 20-30 years and thus do not capture pre-industrial times (Table 3.3). Therefore, the exact calendar age in the recent sediments of the short MUCs is not crucial for our purpose.

In GC HE215/4-2 (Fig. 3.7A), $\delta^{15}N$ values have an average of 6.0‰ until AD 1600, where the minimum is found ($\delta^{15}N$ = 5.6‰). Thereafter, the $\delta^{15}N$ record increases and has a maximum of 8.0‰ in AD 2004. The $\delta^{15}N$ in GC GeoB/4801 are relatively stable before AD 1850 with an average of 6.2‰ and then increase up to 8.1‰ in AD 1997, which matches the $\delta^{15}N$ vertical distribution and levels of GC HE215/4-2 from the same position (Fig. 3.7B). MUC HE267/327 clearly shows an increase in $\delta^{15}N$ values over the time (Fig. 3.7C). The values range from 6.9‰ in the core bottom to 8.4‰ in the core top. The $\delta^{15}N$ values show a similar pattern and range as the upper core intervals of GC HE215/4-2 and GC GeoB/4801 from the same location. Variations in $\delta^{15}N$ values in MUC HE267/329 are more subtle than the previously analyzed cores. $\delta^{15}N$ is rather constant at the bottom sediments (mean value $\delta^{15}N_{15\text{-}27cm}$ = 7.7‰) and abruptly increase to a maximum $\delta^{15}N_{13cm}$ = 8‰ (Fig. 3.7D). Thereafter, a slight upcore decrease is observed to a minimum value of 7.2‰ at the top of the core. In MUC HE267/347, $\delta^{15}N$ values in general increase slightly over time (Fig. 3.7E), except in the top centimeters, where the values rapidly decrease from $\delta^{15}N_{3cm}$ = 7.1‰ to $\delta^{15}N_{0cm}$ = 6.0‰. Overall, the amplitude of the vertical change in $\delta^{15}N$ values of the MUCs becomes less pronounced with increasing distance from the coast.

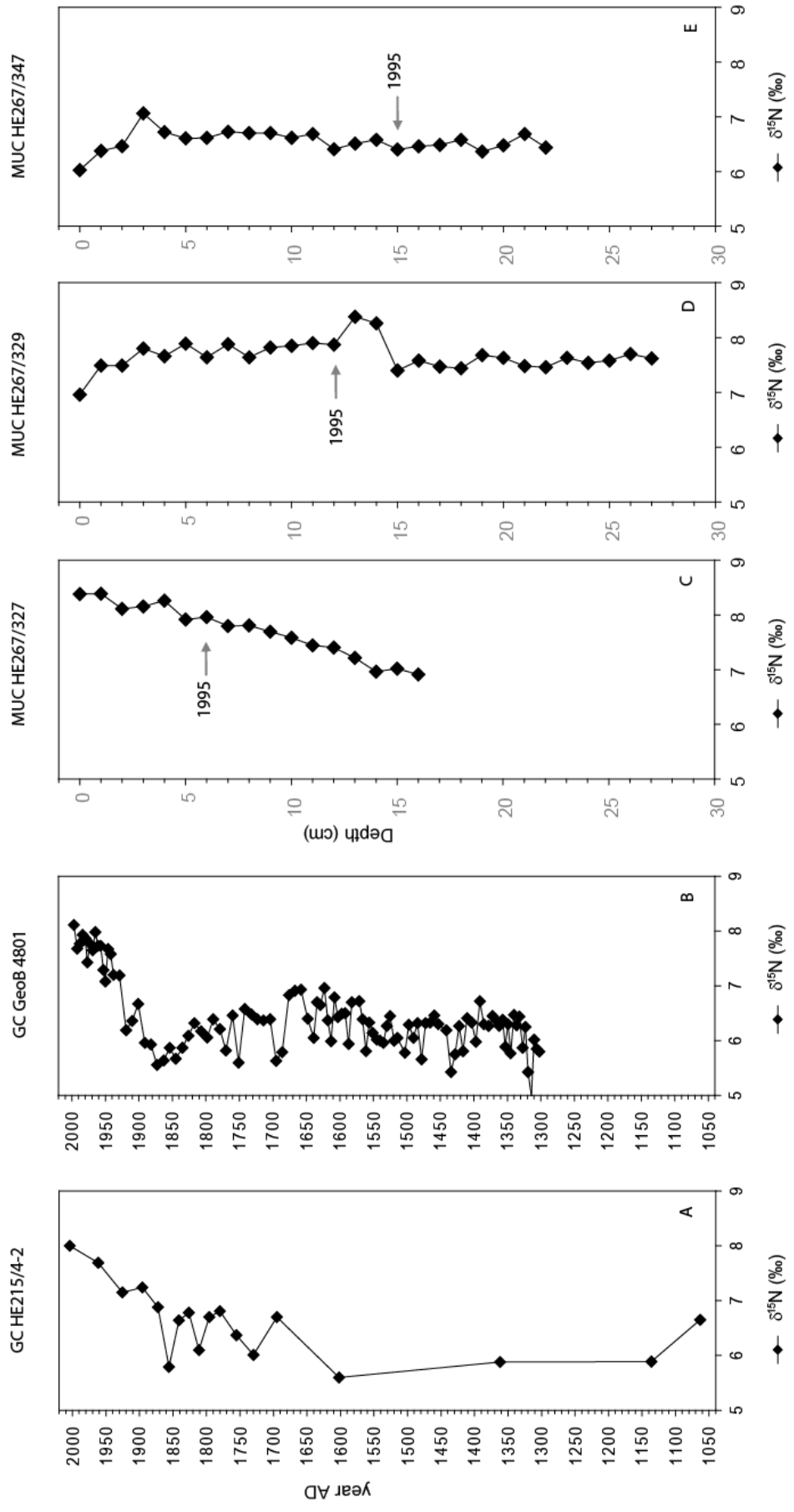

Fig. 3.7. $\delta^{15}N$ values in gravity cores and multicores, ordered in increasing distance from the Elbe river mouth. Note depth scale in MUCs. Estimated age (AD 1995) in MUCs is based on sedimentation rate from Table 3.3.

Similar to the $\delta^{15}N$ pattern observed in the three cores from the Helgoland depositional area, a general increasing trend to higher values in youngest sediments was observed in the two cores from the oxbow loop of the Elbe river (Fig. 3.8), with even more significant gradients between the top and the bottom of the cores. The $\delta^{15}N$ maxima and minima are 6.5‰ and -2.9‰ in core GC TK-16, and 7.9‰ and -1.9‰ in core GC TK-17, respectively. To a first approximation, we use the isotopic signal (~3‰ and ~5‰) of sediments at 209 cm depth in both cores to set the conditions of the ECOHAM model for past situations in terms of $\delta^{15}N_{river\ nitrate}$. We make this approximation assuming that complete assimilation of the riverine nitrate occurs and consequently the isotopic signature in rivers is mirrored in sediment $\delta^{15}N$ values (Voß et al., 2000). In the absence of chronology for these two cores, we estimate sediment ages according to dating results presented by Prange (1997) for a core from the same location of the GC TK-16 and GC TK-17 in the oxbow deposits in the Elbe river valley. These authors did not detect ^{137}Cs below 209 cm core depth, concluding that sediments below that level predate AD 1954. Prange (1997) also used heavy metal profiles together with the history of industrialization in the Elbe catchment to assign an age < AD 1936 to sediments below 220 cm core depth. The assumption of $\delta^{15}N_{river\ nitrate}$ = 3‰ coincides also with analyses of Mayer et al. (2002), Voß et al. (2006) and Johannsen et al. (2008) for the isotopic composition of pristine river nitrate.

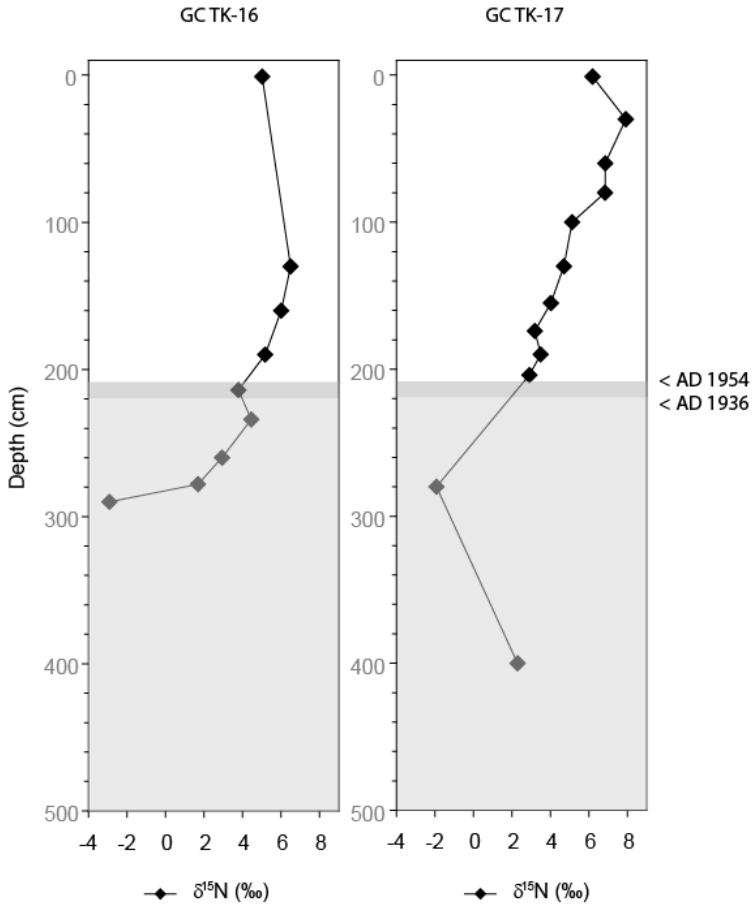

Fig. 3.8. Mean $\delta^{15}N$ values of cores GC TK-16 and GC TK-17. Gray areas indicate approximation of sediment age according to Prange (1997).

3.4.4. Distribution of modeled $\delta^{15}N$ for 1860 conditions

The assumed atmospheric isotopic compositions of $\delta^{15}N_{NO3}$ = 11‰ and $\delta^{15}N_{NH4}$ = 10‰ produce a general spatial distribution with values approximately 0.5‰ higher than with $\delta^{15}N_{NO3}$ = 7‰ and $\delta^{15}N_{NH4}$ = 6‰ assumed by Pätsch et al. (2010).

In the simulation for 1860 with low $\delta^{15}N_{river\ nitrate}$ = 3‰ and reduced atmospheric/river loads (Fig. 3.9A), the distribution in the central basin is similar to the one simulated for 1960 conditions with low $\delta^{15}N_{river\ nitrate}$ = 3‰ (Fig. 3.6A) but with higher $\delta^{15}N$ values along the coast, especially at the Weser estuary. The extent of the area with $\delta^{15}N \leq 5$‰ values - characteristic of the simulation for 1960 conditions - decreases and moves towards the Elbe river mouth ($\delta^{15}N$ > 3‰), where the minimum is found. The $\delta^{15}N_{sim}$ values near the coast are typical of pristine river nitrate loads (Mayer et al., 2002; Voß et al., 2006).

In the simulation of 1860 with moderate $\delta^{15}N_{river\ nitrate}$ = 5‰ and reduced atmospheric/river loads, the model shows typical marine nitrogen ratios around 5‰ in areas of deeper waters and isotopic ratios > 5‰ in the central German Bight (Fig. 3.9B) with a band of slightly higher values along the coast. The highest values were found NW off the Sylt Island (55°N, 8°E). Similar to the spatial distribution for 1960 conditions (Fig. 3.6B and Fig 3.6C), $\delta^{15}N$ values at the Weser estuary are elevated in comparison to the other river estuaries.

3.4.5. Sensitivity test of assumptions in the model

The influence of significant higher riverine reduced N (ammonia and DON) loads in the past on distributions of $\delta^{15}N$ in sediments was explored in a sensitivity analysis. As reference case (REF), we selected the conditions of the Elbe river for 1995 with 5% ammonium of DIN and $\delta^{15}N_{NH4}$ equal to $\delta^{15}N_{river\ nitrate}$. It was compared with the results of a test (TEST) with 42% ammonium of DIN and $\delta^{15}N_{NH4}$ equal to $\delta^{15}N_{TON}$ (Schlarbaum et al., 2010). We found almost no differences in the simulated $\delta^{15}N$ of surface sediments (< 0.1‰) between both cases. Additionally, we calculated for both cases the mixing of different nitrogen inputs in a grid cell where the Elbe river waters enter (Fig. 3.3, inverse triangle). After one year, the difference in $\delta^{15}N_{DIN}$ between REF and TEST was 0.88 ‰. The $\delta^{15}N_{DIN}$ represents an extreme simulated case where the water of the specific cell next to the Elbe estuary is not diluted with water from other adjacent cells in the German Bight. If there were water exchange with other model cells, the difference in $\delta^{15}N_{DIN}$ would become lower still.

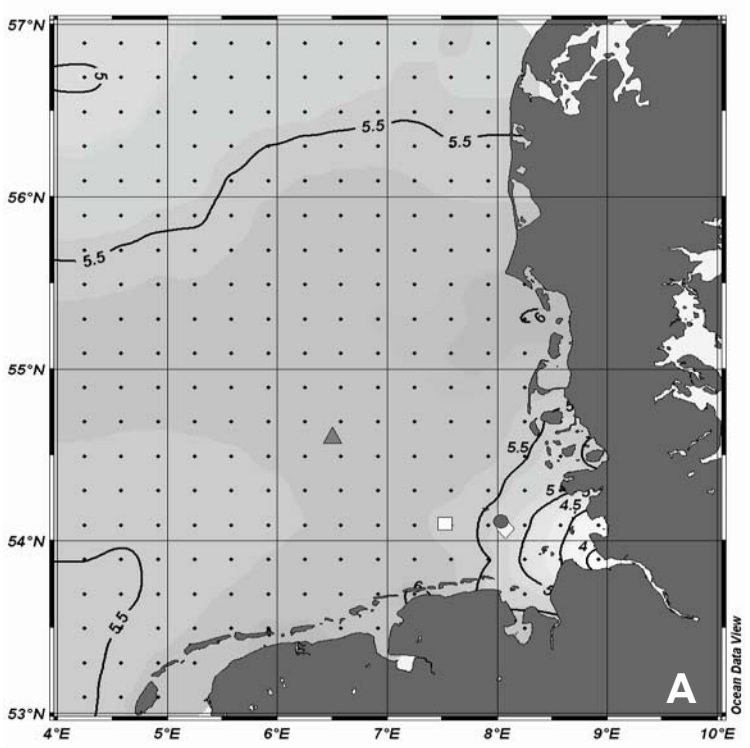

A. low $\delta^{15}N_{river\ nitrate}$ = 3‰

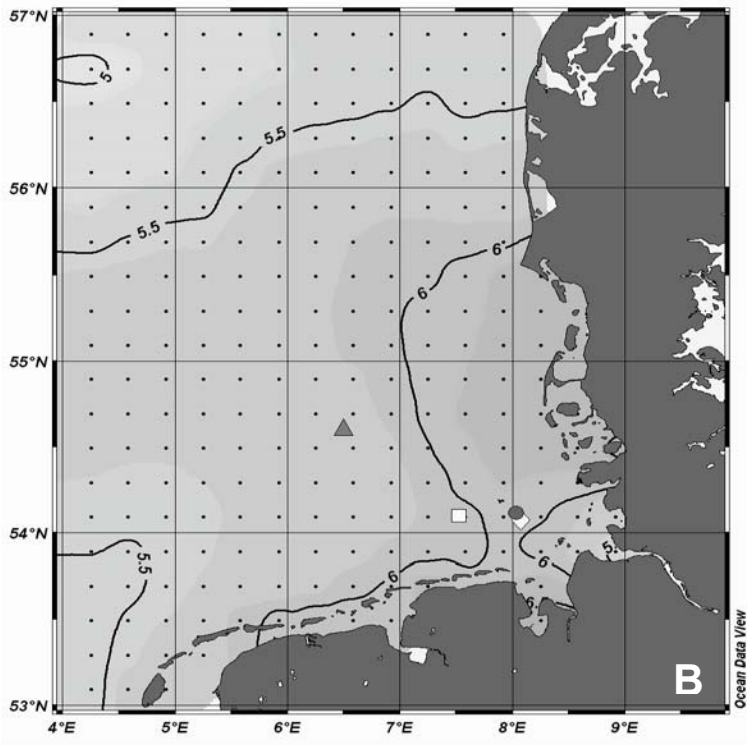

B. moderate $\delta^{15}N_{river\ nitrate}$ = 5‰

Fig. 3.9. Map of $\delta^{15}N_{sim}$ for 1860 conditions (A. low $\delta^{15}N_{river\ nitrate}$ = 3‰ and B. moderate $\delta^{15}N_{river\ nitrate}$ = 5‰ and total N-load = 1.9 Gmol N yr^{-1}, see Tab. 3.4) in surface sediments of the German Bight. Dots indicate grid points of the model domain and symbols indicate core locations (see Fig. 3.2 for symbols description).

3.5. Discussion

3.5.1. Spatial patterns in recent (1989-2009) surface sediments–data and model output

In general, the distribution of $\delta^{15}N$ in recent surface sediments signifies that the counter-clockwise circulation pattern in the North Sea affects the North Frisian coast more than the southern Wadden Sea. The low $\delta^{15}N_{obs}$ at the western boundary of the German Bight may be related to a patch with high salinity and the influence of water from the English Channel (Becker et al., 1992).

Figure 3.10 combines the overall gradient of increasing values towards the Elbe estuary in simulations of recent conditions and in observations in recent and older sediments. The simulated values show a linear decrease, whereas observations do not follow the linear pattern in the estuarine mixing area (data points encircled in Fig. 3.10) where data deviate from conservative mixing (Dähnke et al., 2008b). The discrepancy between $\delta^{15}N_{obs}$ and $\delta^{15}N_{sim}$ in the very nearshore samples is best explained by the fact that the model does not resolve estuarine productivity and mineralisation since the model-domain ends at the 5 m depth contour line defined on a 20 km grid (Pätsch and Kühn, 2008). The $\delta^{15}N$ values in the offshore area, < 300 km away from the Elbe river mouth, are slightly underestimated. The overall $\delta^{15}N$ gradient from the open sea to the Elbe river mouth is 4-5‰ in both observed (Fig. 3.2) and modeled (Fig. 3.3) spatial distributions. Figure 3.10 demonstrates that the increase in $\delta^{15}N$ towards the coastline is associated with the riverine nitrate source.

The deviation between the position of the $\delta^{15}N$ maximum in observation and simulation may be caused by underestimation of the river inputs in the simulation. Our assumed river load is approximately 20% lower than the load used by Pätsch et al. (2010) for the year 1995 (Table 3.4). It appears that the model reproduces the maximum in $\delta^{15}N$ close to Sylt only under extremely high freshwater discharges, as was the case in the years 1994 and 1995 (Radach and Pätsch, 2007). We deduce that some fractionation processes in the absence of significant riverine input may be inadequately modeled. The explanation of an underestimated advection from the outer Elbe estuary to the northern boundary of the bight is contradicted by model tests with passive tracer released in the river mouths in which reasonable spreading behavior was found in the southern North Sea. It is more likely that the amount of particulate material transported from the Elbe estuary north is underestimated in the model because it neglects processes such as the formation of transparent exopolymer particles (TEP) by self-assembly and particle coagulation (Thoms, 2006).

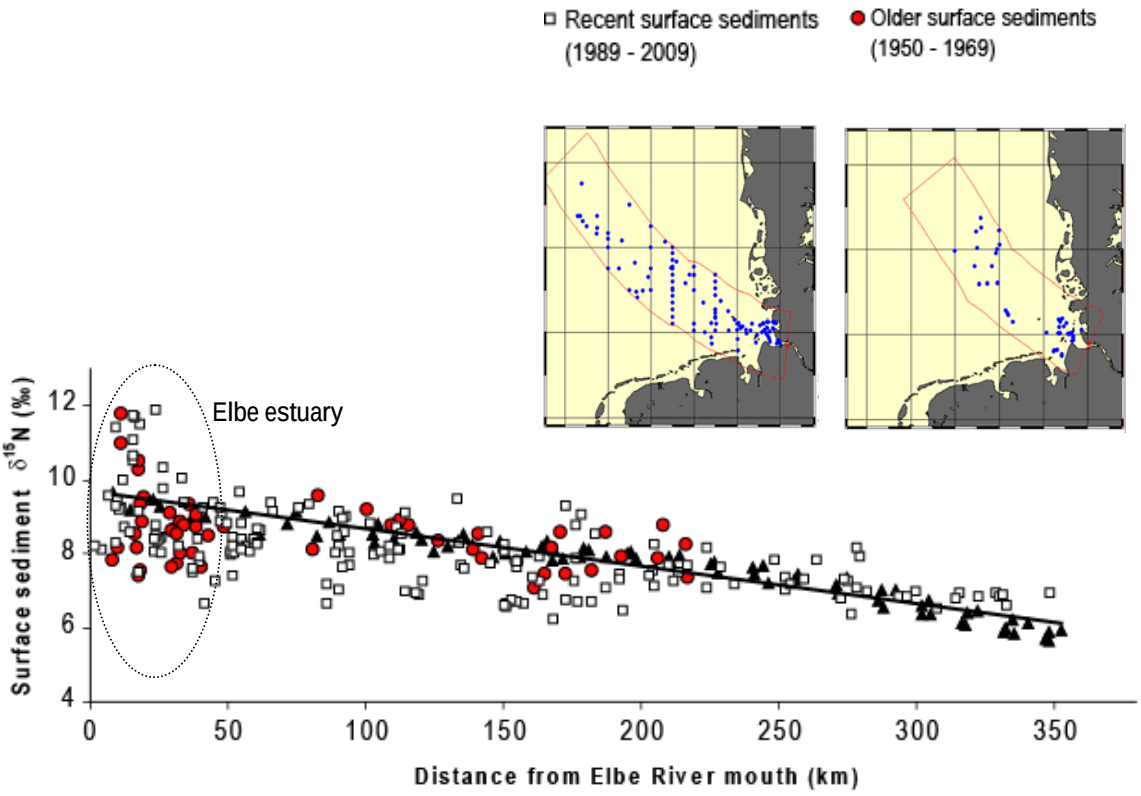

Fig. 3.10. $\delta^{15}N_{obs}$ in recent (1989-2009) -squares-, older (1950-1969) -circles- surface sediments of the German Bight and $\delta^{15}N_{sim}$ for 1990-1999 annual mean conditions -triangles- plotted against distance from Elbe river mouth. Line indicates the linear correlation of distance and $\delta^{15}N_{sim}$ for 1990-1999 annual mean conditions only (R^2=*0.9342, f(x) = -0.0101x+9.6663*).

3.5.2. Spatial patterns in older (1950-1969) surface sediments–data and model output

The modeled distribution of $\delta^{15}N$ in sediments for 1960 shows decreasing values towards the Elbe river estuary in the scenarios of low and moderate annual average $\delta^{15}N_{river\ nitrate}$ (Fig. 3.6A and Fig. 3.6B). This disagrees with the $\delta^{15}N$ pattern observed in older sediments, which exhibits increasing values towards the Elbe river estuary (Fig. 3.5) and also has a prominent $\delta^{15}N$ maximum around the island of Sylt. One simple (and likely) reason for the deviation between $\delta^{15}N_{obs}$ in older sediments and $\delta^{15}N_{sim}$ for the year 1960 may be that the river nitrogen loads for the year 1960 were higher than we assumed for the simulations. Our riverine NH_4-input for 1960 is based on constant values from Pätsch (1997) for the period 1955-1976. Nelissen and Stefels (1988) reported maximum NH_4-concentrations of the water of the Rhine river during the first half of the 1960s, but the level of NH_4-concentration assigned for 1960 was that of the 1970s. We assumed nitrate inputs for the Rhine river as 20% of input of the year 1995, whereas Nelissen and Stefels (1988) estimated nitrate concentrations in 1960 (130 µM) approximately 50% lower than in 1980 (300 µM).

The deviation between $\delta^{15}N_{obs}$ in older sediments and $\delta^{15}N_{sim}$ for the year 1960 may also be due to an erroneous assumption of $\delta^{15}N_{river\ nitrate}$ as 3‰ and 5‰ (see below section 3.5.3). Hence, our best fit for the observed pattern in older sediments with $\delta^{15}N$ values increasing towards the coast is the simulation with the highest $\delta^{15}N_{river\ nitrate}$ of 7.5‰. In any event, the similarity between the observed spatial distributions of older and recent sediments indicates that the period 1950-1969 was already characterized by increasing eutrophication in the German Bight. Opposite to the observed distribution in older sediments, the model predicts higher $\delta^{15}N$ values in the Weser estuary than in the Elbe estuary. The incongruence was already seen by Pätsch et al. (2010) in simulations of recent conditions and occurs because differences in adequate horizontal resolution of the estuaries are not implemented in the model. The $\delta^{15}N$ values of ~5.5‰ observed in the northwest sediment samples in the different simulated scenarios reflect the $\delta^{15}N_{nitrate}$ values of oceanic waters (Dähnke et al., 2010).

The $\delta^{15}N_{obs}$ maximum found off the Sylt Island in both recent and older sediments is a legacy of the dominant influence of the Elbe river water on the Wadden Sea of Sylt. By means of simulations of the nitrogen cycle over the course of the year 1995 that had elevated nitrogen loads, Pätsch et al. (2010) demonstrated that the high levels of $\delta^{15}N$ in recent sediment near the Sylt Island are partly due to the complete consumption of riverborne nitrate that arrives to the area with elevated $\delta^{15}N_{nitrate}$. When riverine nitrogen loads are reduced from 18.3 Gmol N yr^{-1} (1995) to 14.1 Gmol N yr^{-1} (1990-1999), the riverborne nitrate is consumed closer to the source, and the modeled high values close to Sylt migrate towards the Elbe estuary.

We propose two tentative explanations for the regional maximum seen in older sediments: (i) the observed costal maximum is shaped by extremes of high river discharge in the years before the sediments were sampled, similar to the 1995 situation modeled by Pätsch et al. (2010). Our model year 1960 is not one of these extreme years; (ii) the formation of transparent exopolymer particles (TEP), not simulated in the current form of the model, may significantly influence the pattern of sedimentation and particle flux from the vicinity of the Elbe estuary to the North Frisian coastal area. Hickel (1980) hypothesized that eutrophying nutrients are carried from the Elbe estuary north first in dissolved and then in particulate form and reach areas about 130 km north of the Elbe estuary. An appropriate simulation of the long-distance transport effect of material from the south-eastern bight to the northernmost basin may be critical to simulate the high levels of $\delta^{15}N$ observed in older sediments.

3.5.3. Long-term changes in cores and consistency with model results

Levels of $\delta^{15}N$ in sediments of GC HE215/4-2 and GC GeoB/4801 dated to AD 1995 (Fig. 3.7A-B) agree well with the $\delta^{15}N_{sim}$ levels for 1995 conditions presented by Pätsch et al (2010) and with our $\delta^{15}N_{sim}$ for 1990-1999 annual mean conditions (Fig. 3.3). However, $\delta^{15}N_{sim}$ are slightly higher than $\delta^{15}N_{obs}$ in cores and recent surface sediments at the location of the cores. A reason may be flawed assumptions for the atmospheric $\delta^{15}N$ (Table 3.5): In a sensitivity test we found that a change in $\delta^{15}N$ values of atmospheric nitrogen of 1‰ would lead to a 0.4‰ decrease in the $\delta^{15}N_{sim}$ values of the entire spatial distribution. The isotopic composition was set to $\delta^{15}N_{NO3}$ = 7‰ and $\delta^{15}N_{NH4}$ = 6‰ to be consistent with the control simulation of Pätsch et al. (2010) for modern conditions. Furthermore, our assumed atmospheric input corresponds to the year 1995 (Table 3.4) as in Pätsch et al. (2010), instead of annual mean loads. Another reason for the deviation between $\delta^{15}N_{sim}$ and $\delta^{15}N_{obs}$ may be the simplistic assumption of moderate fractionation factors ε, for example ε = 0 for nitrification. Pätsch et al. (2010) demonstrated that changes of the fractionation factors in the ECOHAM N-isotope model influence the $\delta^{15}N_{sim}$ in surface sediments. When setting ε = -17 for nitrification (Sigma et al., 2005) in a sensitivity test, the $\delta^{15}N_{sim}$ values from the Netherlands coast to the Denmark coast decrease by 0.2‰ and more pronounced changes are found in deeper waters (> 1‰). The assumed values are in line with the large isotope discrimination found by Sugimoto et al. (2008, 2009; ε = -15 to -25) in a eutrophic coastal environment. We see a need to quantify the isotope effect for most processes of the nitrogen cycle in order to better model $\delta^{15}N$ in surface sediments.

The model also reproduces the offshore-nearshore $\delta^{15}N$ gradient found in the $\delta^{15}N_{obs}$ spatial distribution of modern sediments. The gradient reflects the extent of the enriched river nitrate assimilated into the sediments and this may explain why the amplitude of the vertical change in $\delta^{15}N$ values of the MUCs becomes less pronounced with increasing distance from the coast (Fig. 3.7). All three cores from the Helgoland area, GC HE215/4-2, GC GeoB/4801 and MUC HE267/327, reflect a historical increase in ^{15}N, presumably from variations in the abundance and isotopic signature of riverine nitrate loads caused by anthropogenic activities such as fertilizer and manure usage in agriculture and sewage discharge, which are characterized by high $\delta^{15}N$ values (Heaton, 1986; Bateman et al., 2005; Voß et al., 2006; Bateman and Kelly, 2007; Johannsen et al., 2008). The observed increase in $\delta^{15}N$ also reflects changes in atmospheric inputs caused by anthropogenic activities such as fossil fuel burning (NO_x) and agricultural fertilization (NH_3) (Spokes and Jickells, 2005). Although the past signature of this source of Nr is considerably more difficult to estimate than that of river loads, it fortunately also has less impact on the $\delta^{15}N$ spatial distribution than river loads because it is a dispersed input.

The short cores HE267/329 and HE267/347 were sampled at more distal locations from the Elbe river mouth. Therefore, we presume that the more subtle $\delta^{15}N$ increase is due to dilution of the riverine signal from the German Bight with offshore waters. Denitrification, typical of the sediments of the area (Seitzinger and Giblin, 1996), could also explain the generally uniform $\delta^{15}N$ values. Removal of nitrate by sediment denitrification - a massive nitrate sink in shelf sediments - has no effect on the isotopic composition of residual nitrate in the water column (Lehmann et al., 2004). The slight decrease towards the younger samples of both MUCs may indicate a decrease in eutrophication over the last few years (Fig. 3.7C-E). Further complexity in the interpretation of the pattern observed in both cores arises from the fact that the uppermost sediment layer in both cores is mobile and redistributed in different intensities during storm events.

The negative $\delta^{15}N$ of pre-industrial Elbe river sediments in GC TK-16 and GC TK-17 (Fig. 3.8) are somewhat surprising, because we would have expected $\delta^{15}N$ between 2‰ and 3‰ for pristine river nitrate loads based on the analyses of Mayer et al. (2002), Voß et al. (2006), and Johannsen et al. (2008). Among the possible explanations are inputs of N from diazotrophic N_2 fixation by blue-green algae blooms in the oxbow lake, or deposition under anoxic conditions and assimilation (associated with a large fractionation factor) of ammonia. The negative values in the Elbe oxbow sediments may also suggest incomplete nitrate assimilation in past situations (Owens, 1987; Maksymowska et al., 2000). On the other hand, the dramatic increase in $\delta^{15}N$ highlights the change in $\delta^{15}N$ of riverine nitrate as a result of increasing agricultural land use in the river catchment and sewage input from urban areas and industries (Voß et al., 2006).

Neither the 1960 distribution simulated with low $\delta^{15}N_{river\ nitrate}$ (Fig. 3.6A) nor the one simulated with moderate $\delta^{15}N_{river\ nitrate}$ (Fig. 3.6B) agrees with the $\delta^{15}N_{obs}$ (~ 7.5‰) in the sediment of cores GC HE215/4-2 and GC GeoB/4801 dated to 1960. Levels of $\delta^{15}N$ in sediments of both gravity cores for the time around 1960 (Fig. 3.7A and Fig. 3.7B) agree best with the $\delta^{15}N_{sim}$ for 1960 conditions with assumed high $\delta^{15}N_{river\ nitrate}$ (Fig. 3.6C). $\delta^{15}N_{sim}$ are slightly lower than $\delta^{15}N_{obs}$ in cores, which suggests that the assumed riverine N-loads for the years 1950-1969 are flawed. As discussed above, this implies that eutrophication was already well advanced in the 1960s.

To validate the modeled distribution of $\delta^{15}N$ for the 1860 simulation, we compared it with the relatively constant values of ~ 6‰ observed in GC HE215/4-2 and GC GeoB/4801 in pre-1860 sediments (Fig. 3.7A and Fig. 3.7B). The simulated $\delta^{15}N$ levels in the Helgoland area for 1860 conditions are comparable with the average $\delta^{15}N$ values in both cores before 1860 ($\delta^{15}N$ = 6.3‰). Simulations with low $\delta^{15}N_{river\ nitrate}$ = 3‰ predicts isotopic signatures slightly lower than $\delta^{15}N$ average values in pre-1860 sediments (Fig. 3.9A), while simulations with moderate $\delta^{15}N_{river\ nitrate}$ = 5‰ shows isotopic signatures around 6‰ (Fig. 3.9B). We conclude

that $\delta^{15}N_{river\ nitrate}$ = 3‰ is unrealistically low for both of the simulations for past conditions (1960 and 1860). The assumption was based on the Elbe oxbow cores. Besides the lack of an exact chronology of the sediments, the $\delta^{15}N$ in the oxbow sediments may have been in fact lower than that of river nitrate due to incomplete nitrate utilization. The nutrient concentrations in the longitudinal profile of the Elbe river most likely were strongly influenced by phytoplankton uptake. Guhr et al. (2003) attributed the present declining concentrations of inorganic nitrogen components along the reach of the Elbe river to nitrogen incorporation into biomass (e.g., cyanophyceae and chlorophyceae) and denitrification. Assuming $\delta^{15}N_{river\ nitrate}$ = 5‰ seems to be more realistic for the riverine isotopic signature in pristine conditions, and so are higher values ($\delta^{15}N_{river\ nitrate}$ ~ 7‰) for the studied period of increasing eutrophication (1950-1969).

3.5.4. Hindcast of pristine nitrate loads

The catchment of the Elbe river and of many other northwest European rivers (Ward et al., 2009) have long been changed by human activities. Therefore, the $\delta^{15}N$ average values in pre-1860 sediments of GC HE215/4-2 and GC GeoB/4801 do not represent truly pristine $\delta^{15}N$ levels. However, the $\delta^{15}N_{sim}$ values for 1860 conditions can be considered representative of the proportion of riverine nitrate assimilated and sedimented prior to widespread use of mineral fertilizers. The abrupt increment in $\delta^{15}N$ after 1860 corresponds to increase in stable carbon isotope ($\delta^{13}C$) values and Zn content reported by Hebbeln et al. (2003), and all mirror increase in pollution in the depositional area related to accelerating industrialization. The increment is in good agreement with the observations of Freyer et al. (1996) and Hastings et al. (2009). The authors found decreasing $\delta^{15}N$ of atmospheric nitrate with increasing nitrate concentration in ice cores as early as ~ AD 1850, in association with the onset of anthropogenic NO_x emissions.

To predict natural N-loads, we used the model quasi-inversely, which means that we ran the model with different scenarios of reduced N-loads until finding an agreement with observations in sediment cores. Modeled levels of $\delta^{15}N$ for 1860 agree best with observed $\delta^{15}N$ levels in sediment cores. The nitrogen loads set as boundary conditions in the simulation for the year 1860 can be assumed to represent the natural N-loads before human impact in the German Bight (0.5 Gmol N $yr^{-1}$and 1.4 Gmol N yr^{-1} of atmospheric and riverine loads, respectively). Our values of atmospheric and riverine loads for 1860 are in accord with the pristine loads estimation in the German Bight given by Topcu et al. (2009). Our observational data show that the period 1950-1969 was characterized by increasing eutrophication. de Jonge and Postma (1974) showed a significant increase in phosphate and particulate phosphorus in the western Dutch Wadden Sea between the 1950s and 1970s. van Bennekom and Wetsteijn (1990) presented historical nutrient concentrations in the eastern

part of the Southern Bight of the North Sea showing nitrate concentration of the Rhine river increasing slowly until the 1940s and rapidly from the 1950s through the 1970s. This was confirmed by van Beusekom and de Jonge (2002) on the basis of a reconstruction of N-loads of the Rhine river for the same period. The data-model correspondence for 1860 suggests that the increase in riverine N-loads, and consequent eutrophication of the German Bight, occurred well before the first half of the 20th century.

3.6. Conclusions

We have reconstructed $\delta^{15}N$ signatures and nitrogen loads quite well: model outcome and data from surface sediments and sediment cores agree. Our measurements in sediments reflect and are mainly affected by riverine nitrogen input and by nitrate assimilation processes of the German Bight region, and to a lesser extent by atmospheric deposition of Nr. The significant difference between $\delta^{15}N$ pre-1860 values and recent ones observed in sediment cores implies that anthropogenic nitrogen has greatly influenced N-isotope signatures over time. The data of recent and archive marine sediments, in combination with the ECOHAM model results suggest that eutrophication in the German Bight predates the AD 1960 period characterized by rapidly increasing river loads. In contrast, $\delta^{15}N$ values in sediments deposited before AD 1860 ($\delta^{15}N$ ~ 6‰) agree well with $\delta^{15}N$ levels modeled with the boundary conditions of 28% of the modern annual (1990-1999) atmospheric loads and 10% of the modern annual river loads. These loads can be adopted as a suitable target for environmental legislation aiming to restore the German Bight to pristine conditions.

Chapter 4

Stable nitrogen isotopes and amino acid composition as indicators of organic matter sources and degradation state of suspended matter, surface sediments and sediment cores of the German Bight/SE North Sea

Abstract

To elucidate possible alterations of the isotopic composition of sinking nitrogen during transit through the water column and burial, we determined stable nitrogen isotope ratios ($\delta^{15}N$) and amino acid (AA) compositions, as a measure of diagenesis, in suspended matter, surface sediments, and dated short/long cores at selected sites of the German Bight/SE North Sea. The isotopic composition in particulate nitrogen reflects a signal of biological processes over the course of a seasonal cycle, whereas in surface sediments reflects an integrated annual signal. Elevated $\delta^{15}N$ values in suspended matter and in surface sediments towards the coastline are associated with anthropogenically altered riverine nitrate. Anthropogenic nitrogen inputs are recorded in sediment cores showing an upward increasing $\delta^{15}N$ pattern highly determined by changes in the abundance and isotopic composition of riverine nitrate loads over the last decades. The $\delta^{15}N$ signals before 1860 AD represent a good estimation of pre-industrial isotopic compositions with minimal diagenetic overprinting. Signals of $\delta^{15}N$ in conjunction with $\delta^{13}C$ data in cores indicate that the organic matter is of mixed marine and terrestrial origin and reveal increasing productivity most likely caused by enhanced eutrophication. The distinguishable upward decreasing C/N trend in sediments deposited the last 20-30 years and increasing C/N trend in sediment cores that span the last 900 years represent cases of very early and later stage diagenesis, respectively. Altogether, this approach reconstructs natural and human driven variations in the N-cycling of the German Bight.

4.1. Introduction

The ratios of stable nitrogen isotopes expressed as $\delta^{15}N$ in sedimentary N have recently been used to detect imprints of nitrate eutrophication in sediment records of several estuaries in NW Europe (Clarke et al., 2003; Clarke et al., 2006), in the Baltic Sea (Voß and Struck, 1997; Struck et al., 2000; Emeis et al., 2002), in the northern North Sea and Kattegat as well as in the German Bight/SE North Sea (Dähnke et al., 2008; Serna et al., 2010). Observations of $\delta^{15}N$ in dated sediment cores from the German Bight showed an increase from approximately 1860 AD to 2000 AD by 2.5‰ (Serna et al., 2010). The lower-than-present $\delta^{15}N$ of sediments were the target levels set for hindcasting pristine N-loads conditions in the area. Using a numerical ecosystem model (Pätsch et al., 2010), the $\delta^{15}N$ of surface sediments in the German Bight for pristine conditions with reduced N-loads were modeled and displayed values up to 2‰ lower than those modeled and observed for recent N load conditions (Serna et al., 2010). The increase in sedimentary $\delta^{15}N$ over time has been attributed to increased $\delta^{15}N$ of riverborne nitrate loads caused by anthropogenic activities (Johannsen et al., 2008). The approach was based on the assumption that the N-isotope composition in sediments reflects N-inputs and N-cycling in the German Bight (Pätsch et al., 2010).

However, previous studies have confirmed the sensibility of the $\delta^{15}N$ to degradation (Gaye-Haake et al., 2005), and in some cases, the isotopic composition of nitrate does not reflect exactly the isotopic values of its sources (Kendall, 1988; Johannsen et al., 2008), but is altered due to transformation processes or uptake by organisms (Wada and Hattori, 1978). Moreover, sensitivity experiments with the numerical ecosystem model suggested that a crucial step in modelling $\delta^{15}N$ patterns is to identify the isotopic fractionation effect associated with burial and degradation of detritus in the sediment (Pätsch et al., 2010). Studies in early diagenetic alteration have been performed using $\delta^{15}N$ associated with amino acid spectra, as a measure of the state of degradation of organic matter (Gaye-Haake et al., 2005; Möbius et al., 2010). Typically, the abundance of amino acids (AA) decreases with increasing depth in the water column or with the ageing of organic matter (Lee and Cronin, 1984; Cowie and Hedges, 1992).

The goal of this study is to elucidate the effect of diagenetic alteration on the isotopic composition of N in the water column and in sedimenting detritus, and its relation to the shift in $\delta^{15}N$ observed in sediment record backing the anthropogenic history of the German Bight due to ^{15}N-enriched riverborne nitrate loads. Our work aimed at the following questions: Is there a relationship between $\delta^{15}N$ and degradation, as expressed by AA composition? Do we observe a consistent offset between $\delta^{15}N$ in suspended particulate matter ($\delta^{15}N_{SM}$) and $\delta^{15}N$ in sediment ($\delta^{15}N_{SS}$)? Is the sedimentary $\delta^{15}N$ altered due to OM early diagenetic breakdown? We determined $\delta^{15}N$ and AA compositions in suspended matter and the underlying surface sediments in a transect from the Elbe estuary to the open NW North Sea and in dated cores

from the Helgoland mud area in the German Bight. To elucidate possible regional influences in the isotopic composition of N in suspended particulate matter and in sediment, we study two areas that are close to or remote from reactive nitrogen (Nr) sources: the Elbe estuary and the inner German Bight, respectively. To interpret correctly $\delta^{15}N$ signatures and to assess the origin and composition of the organic matter, the data are complemented with analytical results of total nitrogen (TN), total carbon (TC), organic carbon (TOC), C/N ratios and stable carbon isotope ratios ($\delta^{13}C$).

4.2. Study area

The shallow German Bight/SE North Sea receives nitrogen from a net influx of water masses from the west, from atmospheric deposition, and from river discharge. A significant export to the north occurs as a consequence of the counter-clockwise circulation pattern of the North Sea (Pätsch et al., 2010), and a significant amount of Nr is eliminated by denitrification in the sediments and nitrate assimilation followed by sedimentation of detritus (Lohse et al., 1993). In the water column, suspended matter concentration in the German Bight varies between 0.3 mg L^{-1}, in calm weather conditions, and 35 mg L^{-1}, during stormy weather (König et al., 1994; Puls et al., 1997). A prominent depositional area in the North Sea is the Helgoland mud area, where sediments accumulate due to a small-scale eddy driven by the interaction of the longshore coastal current, tidal dynamics, and the discharge from the Elbe and Weser rivers (Hertweck, 1983). River inputs have increased nutrient loads significantly (Howarth et al., 1996; Radach and Pätsch, 2007; Johannsen et al., 2008; Pätsch and Kühn, 2008), especially during the second half of the 20th century (Pätsch and Radach, 1997). This raised the primary production rates of the North Sea coastal waters, among other clear indications of eutrophication (Pätsch and Radach, 1997; Radach, 1998). Previous studies of sedimentary $\delta^{15}N$ in the German Bight have shown elevated signals due to increased $\delta^{15}N$ of nitrate discharged by rivers under anthropogenic influences (Johannsen et al., 2008; Serna et al., 2010) and fractionating processes occurring in the Bight during the course of the year (Pätsch et al., 2010). The Elbe river shows seasonal variations of high values of $\delta^{15}N$ in nitrate ($\delta^{15}N_{nitrate}$) with low nitrate concentrations as the result of phytoplankton nitrate assimilation during summer when high temperatures increase the phytoplankton activity (Berounsky and Nixon, 1985; van Beusekom and de Jonge, 1998; Johannsen et al., 2008).

4.3. Materials and methods

4.3.1. Surface sediments and suspended matter sampling

Surface sediments were obtained from gravity cores or van Veen grab sampler during cruises Aldebaran ALD (July, 2005) and Heincke HE267 (May, 2007) in the German Bight/SE North Sea and Valdivia VAL157 (March, 1996) on a transect from the Elbe estuary to the NW North Sea (Fig. 4.1). Sampling along the transect is aimed at illustrating changes in the $\delta^{15}N$ signal from sediments in areas close to the river nitrate sources and in sediments remote from the coastal sources. Samples were dried, sieved and homogenized for analyses of elemental, AA and isotopic composition. Procedure details are given in Serna et al. (2010). To sample suspended particles, GF/F precombusted filters were used to filtrate different volumes of water obtained with Niskin bottles. Further analyses were carried out on filters previously dried at 40-50 ºC for at least 24h.

4.3.2. Multicores and gravitiy cores

We analyzed three cores taken almost at the same position in the Helgoland depositional area (Table 4.1 and Fig. 4.1). Multicore (MUC) HE267/327 was collected on expedition Heincke HE267 (2007) and sliced in 1 cm intervals. Samples were dried and treated the same way as surface sediments. Details of sampling procedure for gravity core (GC) HE 215/4-2 and GC GeoB/4801 are given in Serna et al. (2010) and Hebbeln et al. (2003), respectively.

Table 4.1 Location, collection date, water depth and length of the sediment cores.

Core No.	Latitude (°N)	Longitude (°E)	Collection date	Water depth (m)	Core length (cm)
GC HE215/4-2	54.072	8.074	9/8/2004	23.0	486
GC GeoB/4801	54.102	8.034	1997	25.0	111
MUC HE267/327	54.112	8.036	5/5/2007	21.3	17

4.3.3. Carbon and nitrogen

Contents of TC and TN were measured by a Carlo Erba 1500 elemental analyzer. The precision of this method is 0.05% for carbon and 0.005% for nitrogen. For TOC analysis the samples were acidified with 2 N hydrochloric acid and/or 2 N phosphoric acid and then dried on a 40 ºC hot plate overnight. TOC was calculated as the difference between total carbon and carbonate carbon. Organic matter (OM) was calculated as 1.8 x TOC (Andersen and

Sarmiento, 1994; Francois et al., 2002). TOC and TN measurements were used to compute C/N ratios, given as weight ratios.

4.3.4. Stable isotopes

Values of $\delta^{13}C$ and $\delta^{15}N$ were determined using a Finnigan MAT 252 isotope ratio mass spectrometer after high-temperature flash combustion in a Carlo Erba NA-2500 elemental analyzer at 1100 ºC. Measurements of $\delta^{13}C$ were performed after the removal of carbonate by 2 N hydrochloric acid. The isotope ratios are reported in the conventional isotope terminology:

$$\delta(‰) = (R_{sample} / R_{standard} - 1) \times 1000 \quad (4.1)$$

where δ(‰) stands for $\delta^{13}C$ or $\delta^{15}N$ and R_{sample} and $R_{standard}$ are the $^{13}C/^{12}C$ or $^{15}N/^{14}N$ ratios of the sample and the standard respectively. For carbon the standard is Vienna-Pee Dee belemnite (V-PDB) and for nitrogen it is atmospheric N_2. The analytical precision of $\delta^{15}N$ analysis was better than 0.2‰ based on replicate measurements of six samples varying N-content (Bahlmann et al., 2009) and repeated analyses of IAEA-N-1 and IAEA-N-2 standards. Duplicate measurements of $\delta^{13}C$ in samples differ by less than 0.3‰.

4.3.5. Amino acids

Total hydrolysable amino acids (AA) were analyzed with a Biochrom 30 amino acid analyzer after hydrolysis of < 0.3 mg for suspended matter and 10 mg for sediments with 6 N hydrochloric acid for 22 hours at 110 ºC. Hydrochloric acid was removed from aliquots by evaporation and the residue was taken up in an acidic buffer (pH:2.2). Individual amino acids detected are following listed: cysteic acid (Cya), taurine (Tau), aspartic acid (Asp), threonine (Thr), serine (Ser), glutamic acid (Glu), glycine (Gly), alanine (Ala), valine (Val), methionine (Met), iso-leucine (Ile), leucine (Leu), tyrosine (Tyr), phenylalanine (Phe), β-alanine (β-Ala), γ-aminobuteric acid (γ-Aba), histidine (His), tryptophan (Trp), ornithine (Orn), lysine (Lys), arginine (Arg); as well as the hexosamines, glucosamine (Gluam) and galactosamine (Galam). The relative error was 4% for total AA and 5-16% for individual monomers. For Tau, Val, Met, and Orn the errors were usually below 15%. All AA molar concentrations were calculated against a standard (SIGMA AA-S-18 by adding Cya, Tau, Orn, β-Ala, γ-Aba, Gluam, and Galam; standard concentration: 1.0 nano-mole), which was analyzed after every eighth sample. Details of the method are described by Lahajnar et al. (2007).

Two indices were used to estimate the degree of organic matter degradation: reactivity index (RI) and degradation index (DI). The RI is the ratio of the aromatic amino acids Tyr and Phe to the non-protein amino acids β-Ala and γ-Aba (Jennerjahn and Ittekkot, 1997). Poorest organic matter preservation is indicated by RI values close to 0, whereas living marine plankton ranges between 4 and 6 (Jennerjahn and Ittekkot, 1997). The DI represents the cumulative deviation with respect to an assumed average molar composition of a specific number of amino acids with negative values indicating more and positive values less degradation than the average (Dauwe and Middelburg, 1998). To verify variations in the intensity of organic matter decomposition we used also the ratios of the precursors Asp and Glu to their decompositional products β-Ala and γ-Aba, respectively (Lee and Cronin, 1982; Cowie and Hedges, 1994).

4.4. Results

4.4.1. Surface sediments and suspended matter

Samples are classified according to zones within the study area (Fig. 4.1) based on salinity characteristics of water masses as: German Bight (salinity between 31 and 33.5), central North Sea (relative constant salinity ~ 34.5) and northern North Sea (salinity > 34.5; Schott, 1966; Ittekkot, 1999; Scheurle et al., 2005). Within the German Bight, we analyzed samples from two areas: the Elbe estuary and the inner German Bight.

In the samples from the Elbe estuary collected in July 2005 (Fig. 4.2), the average $\delta^{15}N$ of suspended matter ($\delta^{15}N_{SM}$ = 12‰) is higher than the average $\delta^{15}N$ of the underlying surface sediments ($\delta^{15}N_{SS}$ = 9‰). The average OM concentration decreases from 7% in suspended matter to 3% in surface sediments. Concomitantly, average TN content decreases from 0.7% in suspended matter to ~0.2% in the underlying sediments. An increase in C/N ratios from ~7 in suspended matter to 9-10 in the underlying sediments was observed. Average AA contents decrease from 22 mg g^{-1} in suspended matter to 5 mg g^{-1} in the underlying sediments, which have an AA distribution dominated by Gly (16 mol%) and Asp (13 mol%). The sum of non-protein AA (β-Ala and γ-Aba) slightly increases from 1.0 mol% in suspended matter to 1.5 mol% in the underlying sediments. We found also a decrease of DI average values from 0.5 to 0.3 between suspended matter and surface sediments.

In the samples from the inner German Bight collected in May 2007 (Fig. 4.3), the average $\delta^{15}N$ in both suspended matter and surface sediments is around $\delta^{15}N$ = 7‰. The average OM concentration is much higher (28%) than in the underlying sediments (2%). Similarly, average TN content in suspended matter is much higher (2.6%) than in the underlying sediment (~0.2%). In the case of C/N ratios, in both suspended matter and surface sediments the

average values are similar to those of the Elbe estuary, 8 and 10 respectively (Fig. 4.2). Average AA contents decrease from 131 mg g^{-1} in suspended matter to 6 mg g^{-1} in sediments, which have a distribution dominated by Gly (15 mol%) and Asp (12 mol%). The sum of non-protein AA increases from 0.3 mol% in suspended matter to 1.6 mol% in the underlying sediments. The average value of DI decrease from 1.1 to 0.5 between suspended matter and surface sediments.

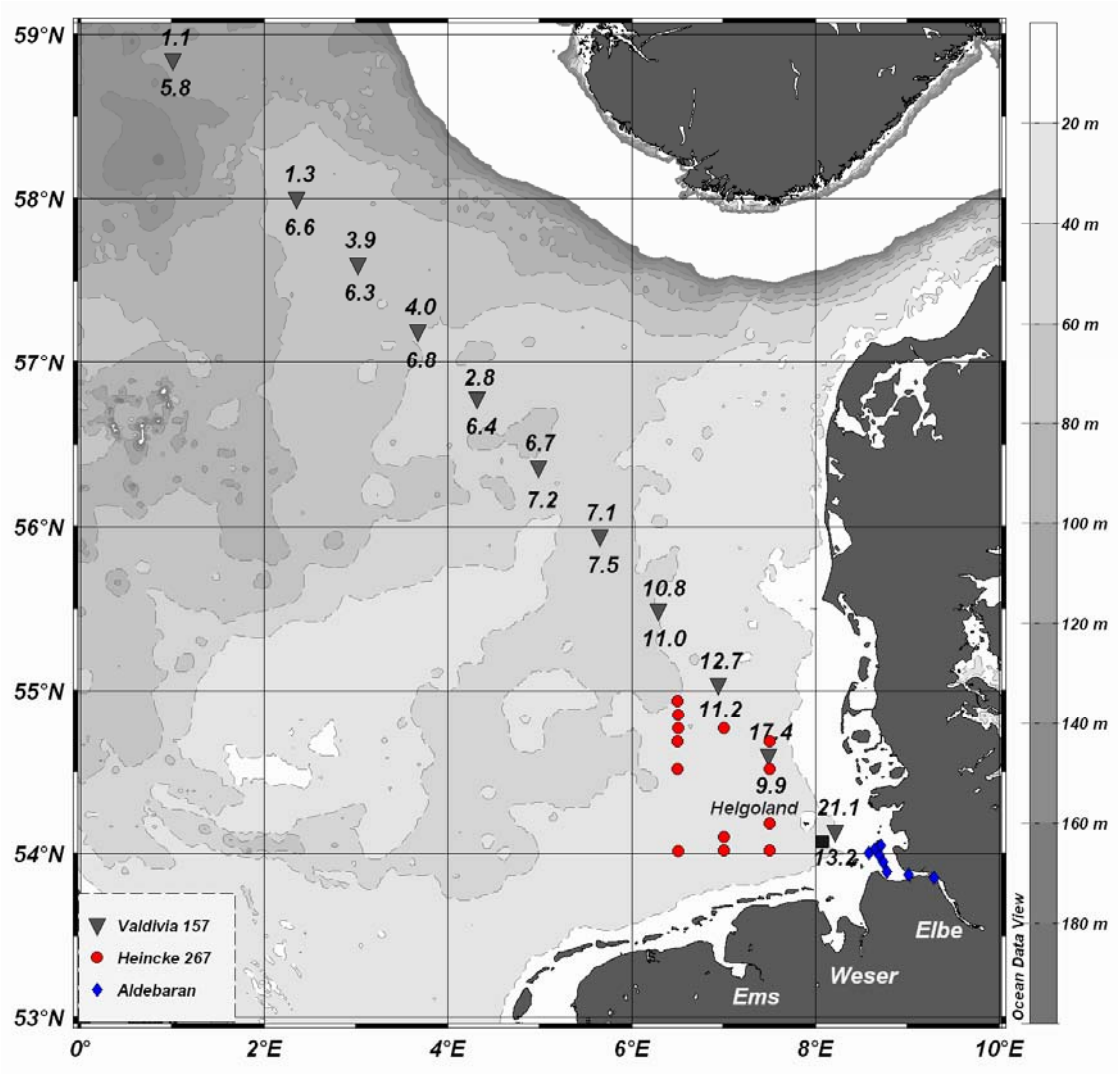

Fig. 4.1. Bathymetry of the study area and stations of the sampling campaigns: HE267 (May, 2007) - circles - , ALD (July, 2005) - diamonds -, VAL157 (March, 1996) - inverse triangles. Values above and below triangles indicate $\delta^{15}N$ (‰) in suspended matter (water depth = 3 m) and $\delta^{15}N$ in the underlying surface sediments, respectively. Square indicates location of the sediment cores GC HE215/4-2, GC GeoB/4801 & MUC HE267/327 (See Table 4.1).

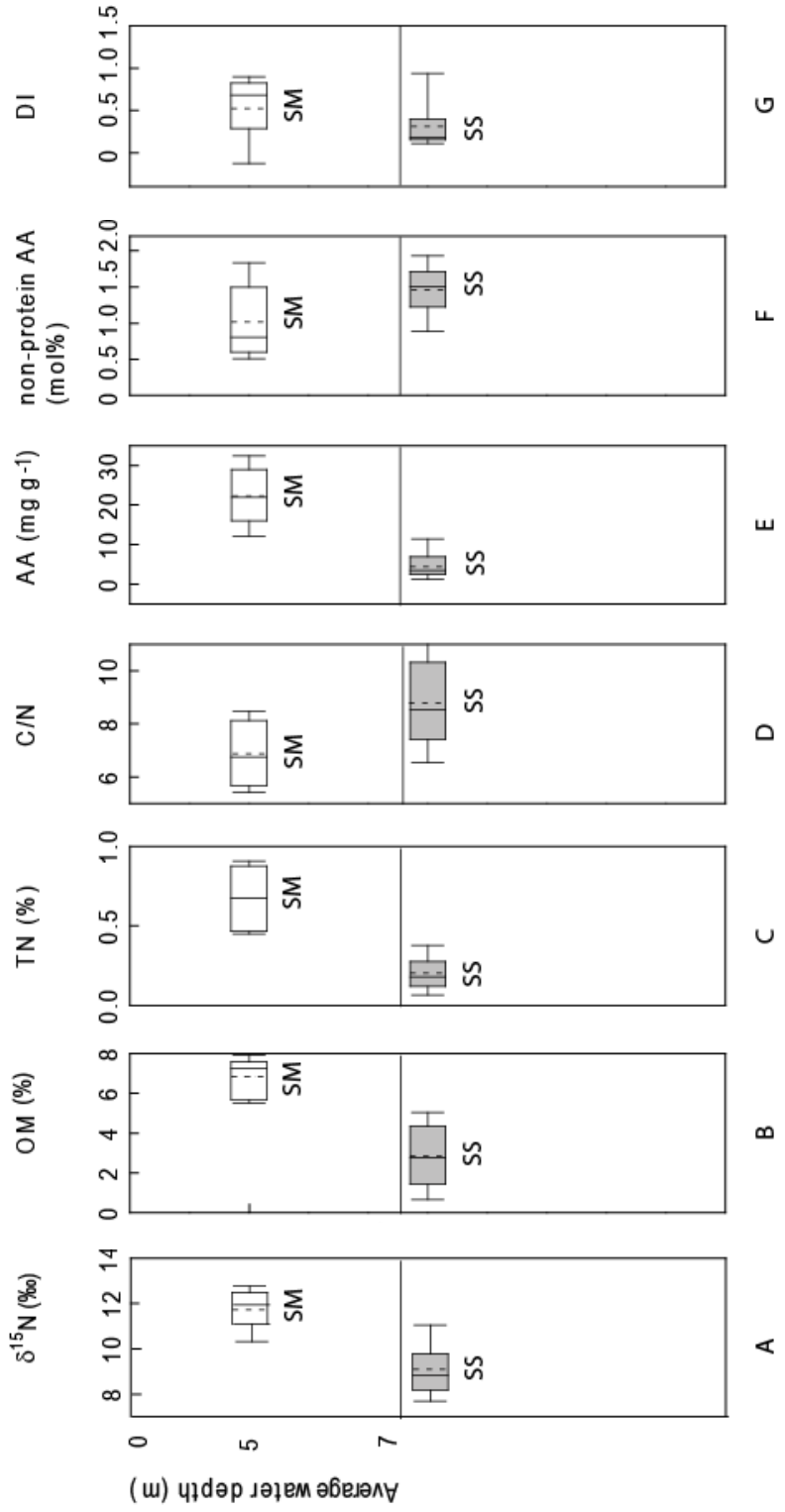

Fig. 4.2. Comparison of A) $\delta^{15}N$ (‰), B) OM content (%), C) TN content (%), D) C/N ratios, E) AA content (mg g^{-1}), F) non-protein AA content (mol%), and G) DI in suspended matter (SM) at water depth = 5 m and underlying surface sediments (SS) from the Elbe estuary (average water depth = 7 m) collected during expedition ALB (July, 2005). Box plots summarize the data of 8 samples from the Elbe estuary area. The left hand boundary of the box indicates the 25th percentile, the straight line marks the median (50th percentile), the dash line marks the mean and the right hand boundary of the box indicates the 75th percentile. In addition, error bars left and right the box indicate the 10th and 90th percentiles.

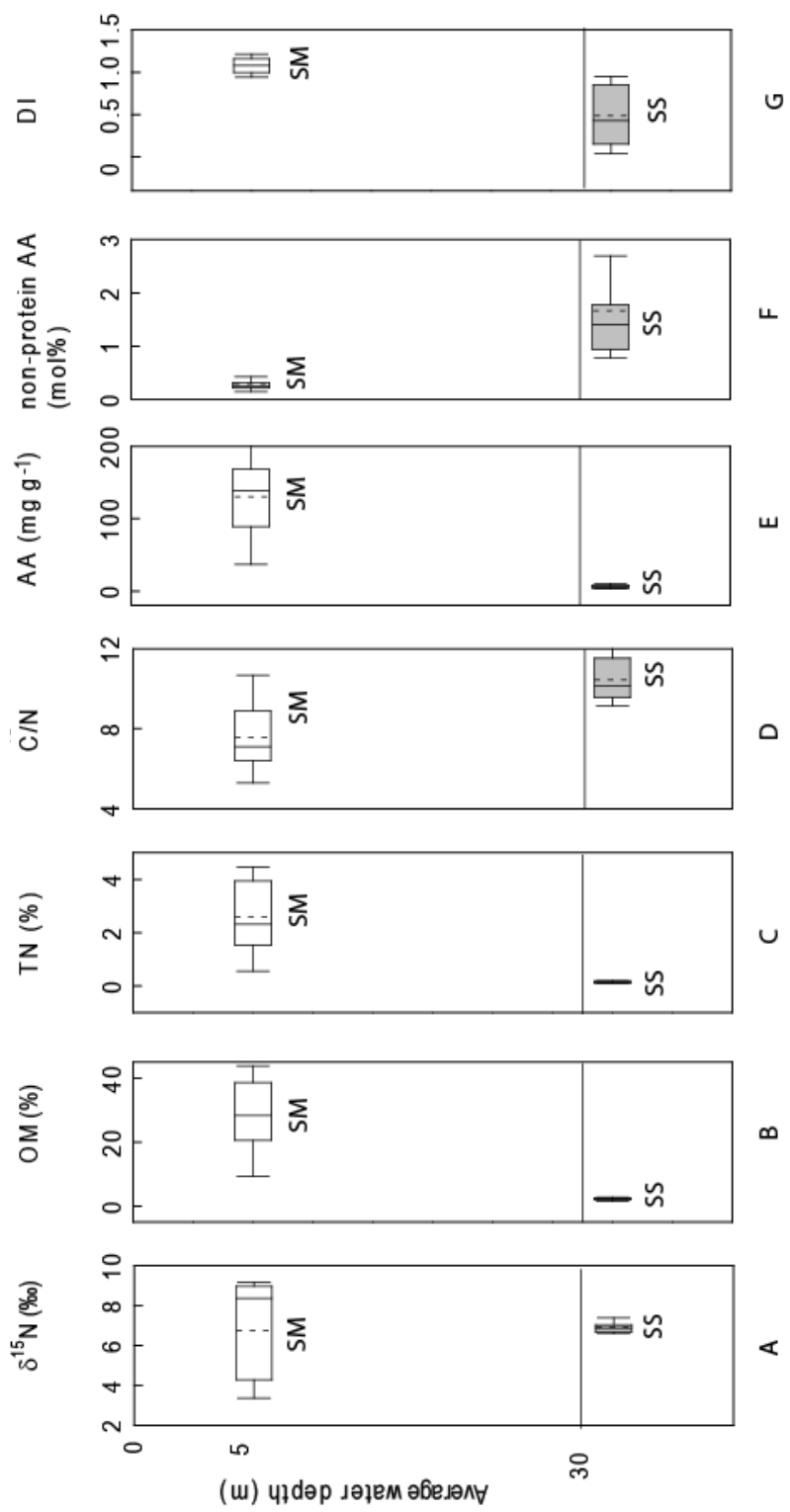

Fig. 4.3. Comparison of A) $\delta^{15}N$ (‰), B) OM content (%), C) TN content (%), D) C/N ratios, E) AA content (mg g^{-1}), F) non-protein AA content (mol%), and G) DI in suspended matter (SM) at water depth = 5 m and underlying surface sediments (SS) from the inner German Bight (average water depth = 30 m) collected during expedition HE267 (May, 2007). Box plots summarize the data of 13 samples from the inner German Bight (see Fig. 4.2 for explanation).

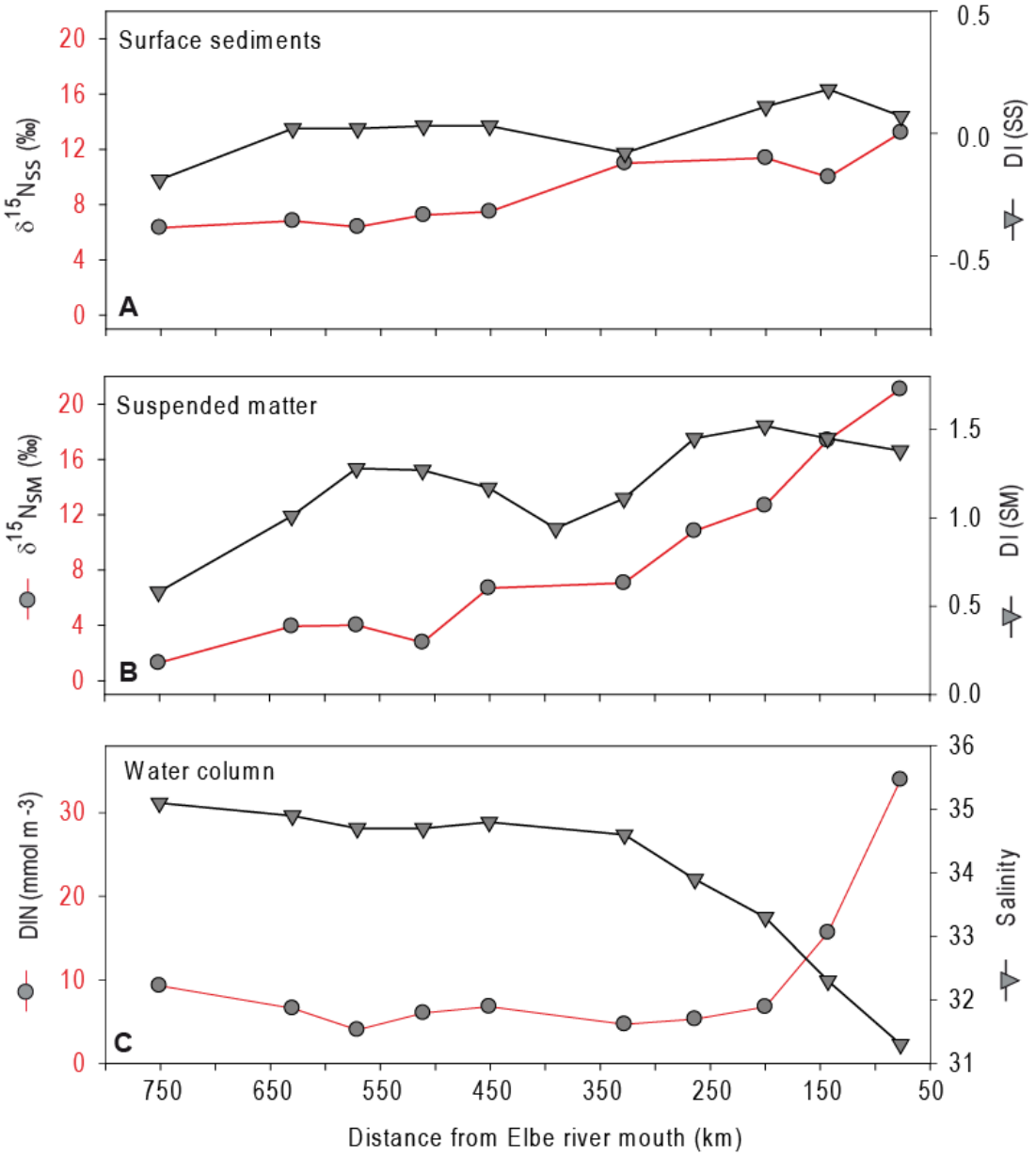

Fig. 4.4. Longitudinal section from the Elbe estuary to the NW North Sea. A) dissolved inorganic nitrogen (DIN) and salinity in the water column at 3 m depth, B) $\delta^{15}N$ and degradation index (DI) in suspended matter (SM) at water depth = 3 m, and C) $\delta^{15}N$ and DI in underlying surface sediments (SS).

In addition to the samples taken in the German Bight we analyzed isotopic and amino acid composition in samples along the transect from the Elbe estuary to the NW North Sea (Fig. 4.1). The $\delta^{15}N$ pattern in surface sediments (Fig. 4.4A) exhibits a steep $\delta^{15}N$ gradient from the Elbe river mouth ($\delta^{15}N_{SS}$ > 10‰) to the northern North Sea ($\delta^{15}N_{SS}$ ~ 6‰). The isotopic composition of suspended matter (Fig. 4.4B) also shows a decreasing trend with even more marked gradients between the German Bight ($\delta^{15}N_{SM}$ > 20‰) and the open sea ($\delta^{15}N_{SM}$ ~ 1‰). A local $\delta^{15}N_{SM}$ minimum is found in the northwestern part of the central North

Sea; thereafter the values follow the overall decreasing pattern. Values of DI in both suspended matter and surface sediments decrease in offshore direction.

Archival data of water samples along the transect from the Elbe estuary to the NW North Sea were available from Ittekkot (1999). Salinity was obtained from CTD data and nitrate, nitrite and ammonium concentrations were determined with an auto-analyzer II (Technicon, Bad Vilbel) and used to estimate contents of dissolved inorganic nitrogen (DIN). Values of DIN in the surface water decrease in offshore direction (Fig. 4.4C) from ~34 µmol m^{-3} in the German Bight to 7-9 µmol m^{-3} in the open North Sea. Salinity and DIN are anticorrelated. In a rough estimation assessing the mixing pattern of $\delta^{15}N$ across salinity gradients, we found a conservative mixing path.

4.4.2. Elemental, isotopic and amino acid composition in sediment cores

The three cores analyzed, GC HE215/4-2, GC GeoB/4801 and MUC HE267-327, were taken almost at the same position in the Helgoland depositional area (Table 4.1). The dated gravity cores GC HE215/4-2 and GC GeoB/4801 span the last 900 years, whereas MUC HE267-327 sediments were deposited within the last 20-30 years. Details of the cores chronology are given in Serna et al. (2010). In the longest core GC HE215/4-2, TOC and TN values (Table 4.2) show no clear trend with core depth (Fig. 4.5A). The C/N ratios show a decreasing trend towards the bottom sediments (Fig. 4.5B). In GC HE215/4-2, $\delta^{15}N$ values have an average of 6.0‰ until AD 1600. Thereafter, the $\delta^{15}N$ record increases and has a maximum of 8.0‰ in AD 2004 (Fig. 4.5C). The $\delta^{13}C$ values are constant in pre-1570 AD sediments and increase towards the top of the core with small oscillations and an abrupt increase after AD 1880.

The short core MUC HE267-327 recovered the topmost sediment interval that may be missed by the gravity cores GC HE215/4-2 and GC GeoB/4801. Contents of TOC and TN (Fig. 4.6A) and C/N ratios (Fig. 4.6B) increase with core depth (Table 4.2). Values of $\delta^{15}N$ increase over the time with values ranging from 6.9‰ in the core bottom to 8.4‰ in the core top (Fig. 4.6C). The same is observed in the vertical distribution of $\delta^{13}C$, which rises from -23.6‰ in the core bottom to -22.6‰ in the core top. The $\delta^{15}N$ pattern is similar to the upper core intervals of GC HE215/4-2 and GC GeoB/4801 from the same location. In GC GeoB/4801 (Fig. 4.7A), the $\delta^{15}N$ are relatively stable before AD 1850 with an average of 6.2‰ and then increase up to 8.1‰ in AD 1997. A similar pattern is observed in the vertical distribution of $\delta^{13}C$ in sediments from the same core. Values of $\delta^{13}C$ and $\delta^{15}N$ of all three cores (Table 4.2) correlate significantly (Fig. 4.7B).

Table 4.2 Elemental and isotopic composition in sediment cores

Core No.	TOC (%)		TN (%)		C/N		$\delta^{15}N$ (‰)		$\delta^{13}C$ (‰)	
	min	max	min	max	min	max	min	max	min	max
GC HE215/4-2	0.48	2.28	0.05	0.25	9.8	12.3	5.6	8.0	-24.9	-23.2
GC GeoB/4801	-	-	-	-	-	-	5.4	8.0	-24.9	-22.7
MUC HE267/327	0.46	1.07	0.06	0.10	8.9	12.1	6.9	8.4	-23.6	-22.6

The total AA pool in GC HE215/4-2 sediments is dominated by Gly (mean 19 mol%) followed by Asp (mean 13 mol%) and Ala (mean 10 mol%). The mole content of Ser and Thr (12.7 to 17.5 mol%) and Asp/Gly ratio (0.6 to 0.8) were used to differentiate diatomaceous from calcareous organic matter. The two non-protein AA, β-Ala and γ-Aba (not shown), which are degradation products of Asp and Glu, occur in minor concentration along the core (mean ~1 mol%) but tend to accumulate in older sediments of GC HE215/4-2. Consequently, Glu/γ-Aba and Asp/β-Ala ratios decrease towards the bottom sediments. There is a significant negative correlation between $\delta^{15}N$ and the amount of non-protein AA in GC HE215/4-2 (R^2*=0.5751; f(x)=-1.3385x+9.9839*) and MUC HE267/327 (R^2*=0.785; f(x)=-0.7185x+9.5667*). We calculated the RI (Fig. 4.5B and 4.6B) and found a positive correlation with $\delta^{15}N$ in sediments of GC HE215/4-2 (R^2*=0.607; f(x)=1.4139x+3.7041*) and of MUC HE267/327 (R^2*=0.6838; f(x)=0.7653x+6.2252*).

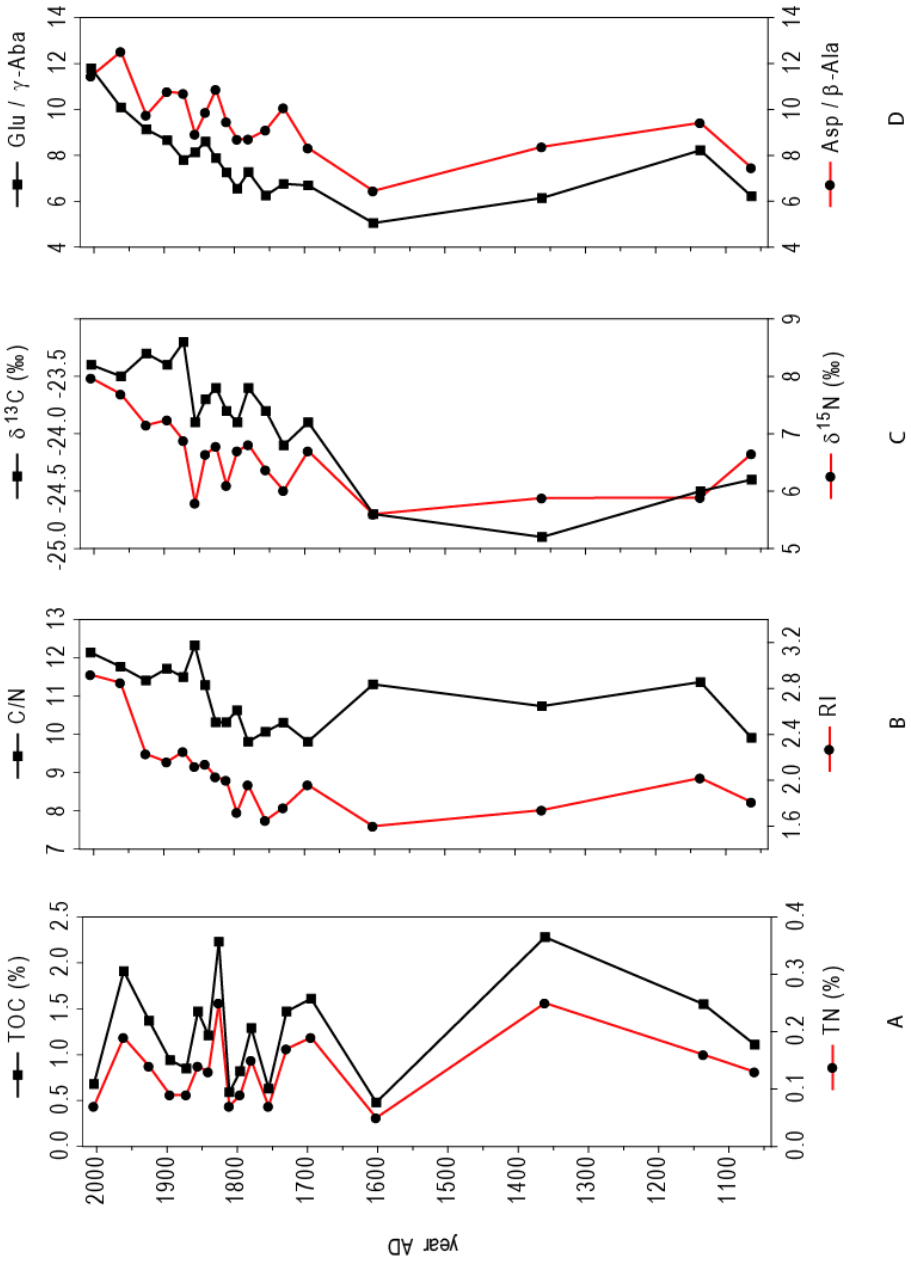

Fig. 4.5. Vertical variations in GC HE215/4-2 of A) TOC (%) and TN (%), B) C/N ratios and RI, C) $\delta^{13}C$ (‰) and $\delta^{15}N$ (‰) and D) Glu/γ-Aba and Asp/β-Ala molar ratios. The y-axis provides the age model in years AD.

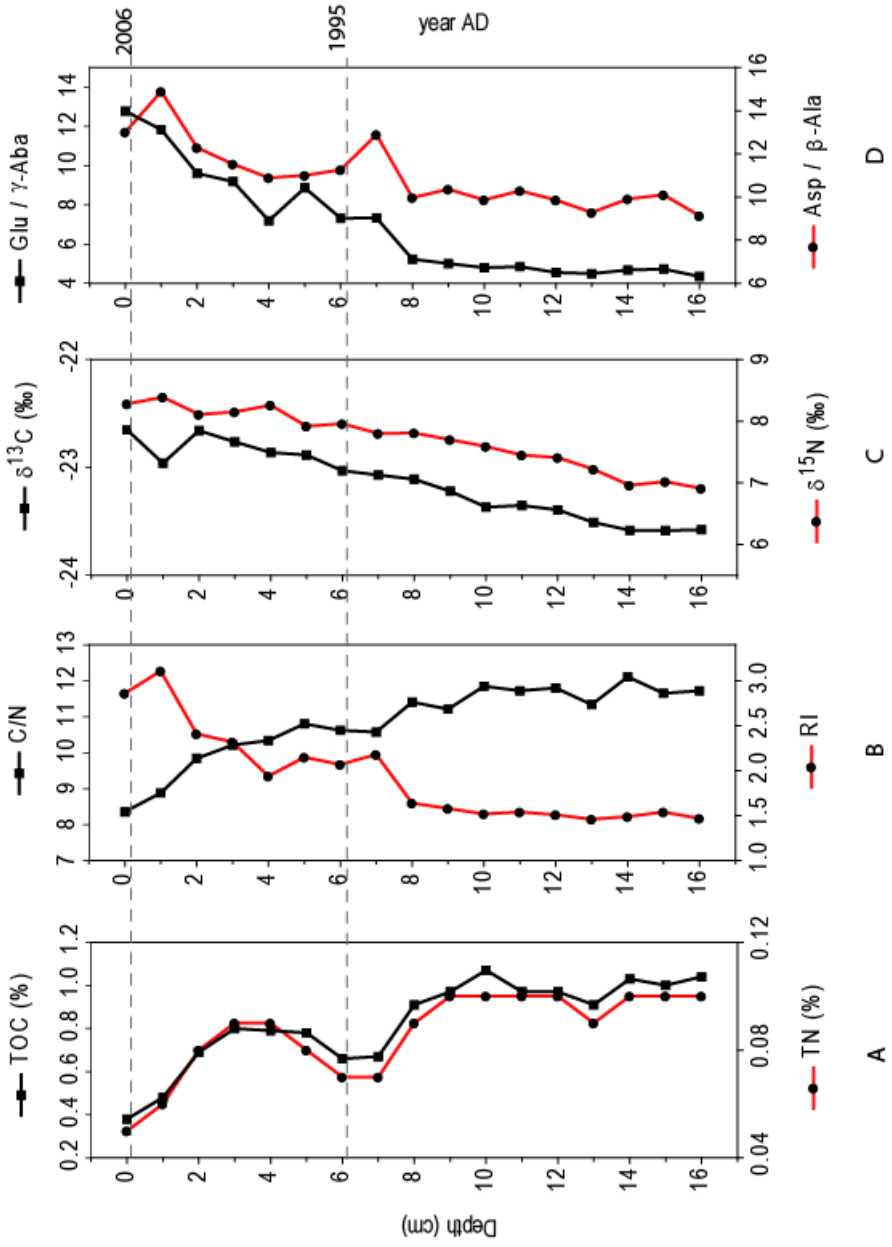

Fig. 4.6. Vertical variations in MUC HE267/327 of A) TOC (%) and TN (%), B) C/N ratios and RI, C) $\delta^{13}C$ (‰) and $\delta^{15}N$ (‰) and D) Glu/γ-Aba and Asp/β-Ala molar ratios. The right hand y-axis provides an approximated age model in years AD.

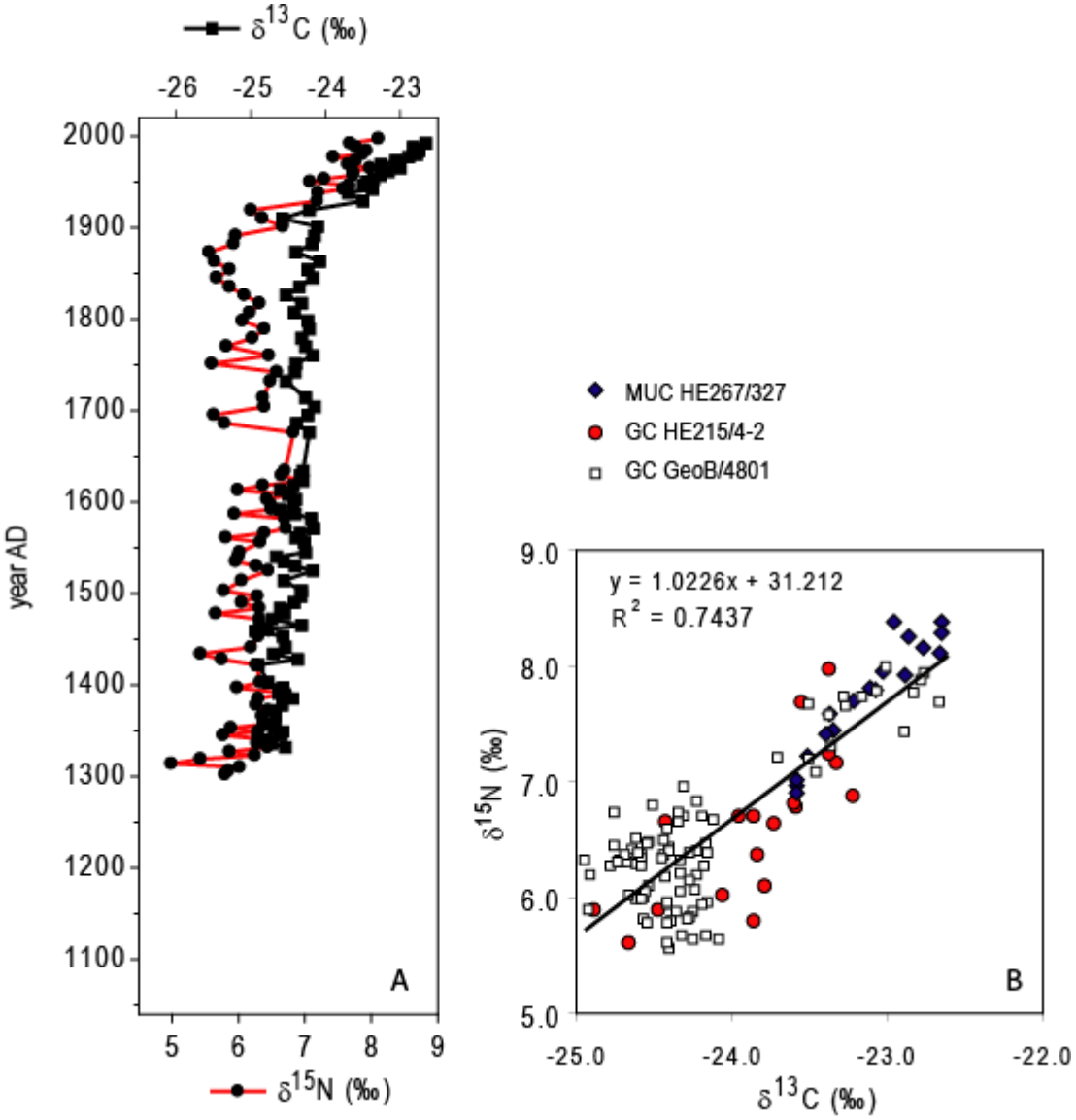

Fig. 4.7. A) Vertical variations in GC Geo/4801 of $\delta^{15}N$ and $\delta^{13}C$. The y-axis provides the age model in years AD. B) Correlation among $\delta^{15}N$ and $\delta^{13}C$ in the sediments of the three cores analyzed.

4.5. Discussion

4.5.1. $\delta^{15}N$ spatial patterns in suspended matter and surface sediments

Differences were found between $\delta^{15}N$ signals in suspended matter and in surface sediments. The isotopic signals reflect: (1) isotopic discrimination processes occurring over the course of a seasonal cycle in the German Bight and (2) local inputs of ^{15}N-enriched nitrate.

Previous studies demonstrate variations of high values of $\delta^{15}N$ in nitrate associated with fractionating processes occurring in the Bight during the course of the year (Berounsky and Nixon, 1985; Johannsen et al. 2008; Dähnke et al., 2010; Pätsch et al., 2010). Sampling in the inner German Bight and in Elbe estuary occurred during different seasons. The inner German Bight samples collected in early May 2007 when primary production was high, show average $\delta^{15}N$ in suspended matter around 7‰ (Fig. 4.3). The value corresponds to the average value found by Mariotti et al. (1984) in suspended matter collected in the Scheldt estuary during the spring bloom, when phytoplankton is the main constituent of suspended matter. The $\delta^{15}N$ values in suspended matter may reflect the isotopic composition of plankton during the bloom. Our values are also within the range of those of marine phytoplankton reported by Miyake and Wada (1967). In the Elbe estuary, the average $\delta^{15}N$ value in suspended matter is elevated over the values found in the inner German Bight (Fig. 4.2). Petersen et al. (2008) reported an intensive bloom in the German Bight off the Elbe estuary in May 2005 disappearing in mid June 2005. Therefore, the Elbe river mouth samples collected in early July 2005 must represent a post-bloom period. The composition of suspended matter during the post-bloom may be different than during the bloom phase and presumably dominated by other phytoplankton species. Contrasting, the sampling campaign in late March 1996 (Fig. 4.1) may have occurred during a pre-bloom situation, based on conditions of elevated nutrient concentrations and low biological activity (low chlorophyll-a concentrations) reported by Mieding et al. (1996).

The observed sedimentary $\delta^{15}N$ values represent an integrated annual signal, but also evidence regional gradients due to different local sources and horizontal transport (Brockmann and Kattner, 1997). The $\delta^{15}N$ values in areas closer to the riverine sources are very high, especially in the samples collected in 1996. It seems to be a relationship between the isotopic composition and the distance from riverine nitrate sources. Pätsch et al. (2010) demonstrated in simulations of the annual cycle of surface water nitrate, that it is never entirely exhausted in the Elbe mouth and preferential ^{14}N uptake by phytoplankton is continuously effective. Fractionation during nitrate assimilation may be indirectly responsible for the high $\delta^{15}N_{nitrate}$ and ^{15}N-enriched residual nitrate of the coastal waters is regularly transferred as particulate nitrogen to sediments.

The $\delta^{15}N$ values shown in Fig. 4.1 and 4.4 across salinity gradients reflect on one side the influence of the Atlantic water masses with low $\delta^{15}N_{nitrate}$ and on the other the riverine nitrate discharge in the German Bight with elevated $\delta^{15}N_{nitrate}$ (Johannsen et al., 2008). The landward increasing DIN trend (Fig. 4.4) shows that the German Bight is highly affected by the nutrient rich freshwater discharge of the Elbe river (Rick, 1999) altered by manure and fertilizer use to agricultural soils. Such application has changed both the nitrate concentration and its isotopic composition in the river (Johannsen et al., 2008). Other important nitrate sources include the Weser river, which shows also high nitrate isotopic compositions (Johannsen et al., 2008),

and coastal water advected by the Rhine river (Brockmann et al., 1999). Altogether, the $\delta^{15}N_{SM}$ reflects a seasonal signal of sources and nutrient utilization whereas $\delta^{15}N_{SS}$ reflects an integrated annual signal of different bloom phases in the German Bight.

4.5.2. Effect of diagenesis on $\delta^{15}N$ values in surface sediments and suspended matter

There are several indications of decomposition during transport through the water column. First, we examined the trend of OM contents. We observed higher C/N ratios in surface sediment than in suspended matter presumably due to preferential loss of nitrogen relative to organic carbon during decomposition through the water column (Fig. 4.2 and Fig. 4.3). Remineralization in the water column is evidenced by the decrease of TN between the suspended matter and the sediments (Libes and Deuser, 1988). Second, we study the abundance of AAs, which is lower in surface sediments compared to suspended matter. The AA spectra in sediments of both regions the Elbe estuary and the inner German Bight, show a similar composition typical of coastal environments dominated by Gly (Dauwe and Middelburg, 1998). The two non-protein AA, β-Ala and γ-Aba, which are degradation products of Asp and Glu respectively, occur in minor concentration in the suspended matter but tend to accumulate in the surface sediments.

Another indication of degradation is that the calculated values of DI in suspended matter are higher than in the underlying sediments. Higher DI values indicate better preservation than lower values. Likewise, calculated RI values (not shown) are higher in suspended matter than in the underlying surface sediments. In the samples from the offshore-nearshore transect (Fig. 4.1), the decreasing DI trend in offshore direction found along the transect (Fig. 4.4) indicates that suspended matter in the open sea is mainly constituted by more degraded material, whereas in the Elbe estuary the suspended particulate matter mainly consists of fresh non-degraded material, typical of coastal environments. We were expecting that the $\delta^{15}N$ values become ^{15}N enriched with increasing degradation due to preferential loss of the lighter isotope (Gaye-Haake et al., 2005). However, $\delta^{15}N$ values decrease with increasing degradation in offshore direction (Fig. 4.4), as reflected by the decreasing trend of DI in offshore direction. The spatial gradient with increasing $\delta^{15}N$ values onshore direction is largely controlled by Nr sources. The elevated isotopic signal originates from the assimilation of isotopic heavy nitrogen from the Elbe river and enriched particulate nitrogen deriving from river suspended loads. The ^{15}N-enriched nitrate in the water column is transferred as particulate nitrogen to the sediments of the coastal area.

We can conclude that the sedimentary $\delta^{15}N$ signals reflect the signature of mixing inputs: processes that consume or transform nitrate, riverine sources (Dähnke et al., 2010) and at a

lesser degree the effect of early diagenesis. Therefore, the demonstrated relationship between diagenetic unaltered isotopic composition in surface sediments and N sources enriched in ^{15}N shows that surface sediments can obviously be used as a reliable tracer of anthropogenic N sources in the German Bight.

4.5.3. Origin and long term changes of organic matter in cores

Carbon and nitrogen ratios have been widely used to distinguish between marine and terrestrial organic matter (C/N ~ 4-10 and C/N > 20, respectively). The differences among C/N ratios of algae and land-plant are due to the absence of cellulose in algae and its abundance in vascular plants (Meyers, 1997). The overall C/N ratios (9 to 12) in the two cores GC HE215/4-2 and MUC HE267/327 indicate that algal sources dominate the organic matter input of the sediments. C/N ratio of sedimentary organic matter usually increases upon early diagenesis due to preferential loss of nitrogen relative to organic carbon during decomposition (Hedges et al., 1997; Meyers, 1997), which explains the increasing C/N ratios with depth in MUC HE267/327 (Fig. 4.6). Conversely, the decreasing C/N ratios with depth in GC HE215/4-2 (Fig. 4.5) may be due to preservation of organic nitrogen compounds probably caused by sorption to clay minerals protecting them against bacterial attack during diagenesis (Müller, 1977). The organic carbon is converted to CO_2 which diffuses out the sediments, while the organic nitrogen converted to NH_4^+ is absorbed by clays (Meyers, 1997). While sediments of MUC HE267/327 span only the last 20-30 years, GC HE215/4-2 brackets pre-industrial to recent sediments (last 900 years). The contrasting C/N trends between MUC HE267/327 and GC HE215/4-2 represent cases of very early and later stage diagenesis, respectively. The trend in GC HE215/4-2 may also represent an enhanced proportion of terrestrial organic matter relative to marine organic matter (Hu et al., 2006).

Though C/N ratios indicate a dominance of algal input, $\delta^{13}C$ and $\delta^{15}N$ compositions (Fig. 4.7A) and the linear correlation between them (Fig. 4.7B), indicate that there are several sources in the organic matter of the sediments. Our $\delta^{13}C$ (-25 to -22‰) are between the limits of organic matter derived from terrestrial C_3 plants (-28 to -26‰) and marine organic matter (-22 to -19‰), therefore the organic matter is considered to be a mixture (Gearing, 1988). In the case of $\delta^{15}N$, though it is known that terrestrial plants have a $\delta^{15}N$ range of -5‰ to 18‰ (with average around 3‰; Müller and Voss, 1999) and marine organisms of 7‰ to 10‰ (with average around 6‰; Peters et al., 1978; Müller and Voss, 1999), the interpretation of our $\delta^{15}N$ values (5.4 to 8.4‰) in terms of marine and terrestrial sources is more complex. The $\delta^{15}N$ upward increasing trend observed in the cores reproduces changes in isotopic composition due to human activities and/or natural processes.

As riverine nitrate is reflected in the isotopic composition of surface sediments along the offshore-nearshore transect, the Helgoland depositional centre were the sediment cores were collected was viewed as an ideal site to study changes in the riverine loads and their isotopic composition in the past. There is a clear difference between $\delta^{15}N$ of sediments deposited before 1860 (average value $\delta^{15}N$ ~ 6‰) and recent sediments ($\delta^{15}N$ ~ 8‰) reflecting changes in the abundance and isotopic composition of riverine nitrate loads caused by anthropogenic activities. Isotopically enriched anthropogenic nitrogen was found also in two sediment cores from the Kattegat area, a depositional center in the North Sea close to eutrophication sources on land (Dähnke et al., 2008). In the two cores from the Kattegat basin, the increase in $\delta^{15}N$ values over pre-industrial sediments amounts to 1.3 ‰. Nitrate entering the German Bight via rivers (Rhine, Elbe, Weser, Ems, and Eider) has an elevated isotope signals ranging from 8 to 12‰ (Johannsen et al., 2008) originally derived from anthropogenic input, e.g. sewage and/or manure ($\delta^{15}N$ > 10‰; Heaton, 1986) as well as organic fertilizers utilization ($\delta^{15}N$ ~ 8.6‰; Bateman and Kelly, 2007). The increase of $\delta^{15}N$ values in GC HE215/4-2 and GC GeoB/4801 after ~1850 AD coincides with significant reduced salinity after 1870 AD and pronounced freshwater inflow from the Elbe river reconstructed by Scheurle et al. (2005) using stable oxygen isotopes ($\delta^{18}O$).

Schmiedl et al. (in prep.) found that the relationship between increasing $\delta^{15}N$ in GC HE215/4-2 and abundance of benthic foraminifera opportunistic species typically found in unpredictable environments (e.g. *Elphidium excavatum* with particular tolerance to contamination) may be a reaction to eutrophication. In GC HE215/4-2, foraminifera decreased in absolute abundance (number of foraminifera per gram of sediment) and diversity through the 1800s, due to a more stressed environmental situation caused by pollution in the area. Eutrophication is evidenced by the onset of increasing abnormal foraminiferal test abundance dated to the 1800s (Schmiedl et al., in prep.). The faunal changes coincide with an increase in $\delta^{13}C$ values and Zn contents in the sediments of GC GeoB/4801 from the same location at ~1880 AD, related to increasing environmental pollution in the course of the industrialization, as well as an increase in coarse fraction percentages most likely related to human activities (Hebbeln et al., 2003). $\delta^{13}C$ values become more positive resulting from CO_2 limitation in the C-pool caused by high productivity in response to eutrophication. Phytoplankton tends to discriminate against ^{13}C, causing heavier isotopic compositions in the dissolved inorganic carbon (DIC) pool. As supplies of CO_2 in the C-pool are depleted and enriched in ^{13}C by increased productivity, phytoplankton will discriminate less against ^{13}C (Teranes and Bernasconi, 2005). In sediment records of the Baltic Sea, increases of $\delta^{13}C$ and TOC were observed in response to elevated eutrophication (Struck et al., 2000). Unlike, no clear trend of increasing TOC was observed in GC HE215/4-2. We presume that the variation of TOC values may be instead related to a sediment grain-size effect along the cores (Wiesner et al., 1990).

The AA composition in sediments of GC HE215/4-2 and MUC HE267/327 dominated by Gly is in good agreement with the one observed by Dauwe and Middelburg (1998) in coastal sediments from the German Bight with high planktonic inputs. The range of non-protein AA in the sediments of the cores fits also into the range generally seen in coastal sediments (0.2 to 3.5 mol%; Dauwe and Middelburg, 1998). The Asp/Gly ratios (0.6 to 0.8) and mole contents of Ser and Thr (12.7 to 17.5 mol%) in sediments of GC HE215/4-2 suggest a dominance of diatomaceous organic matter (Hecky et al., 1973; Carter and Mitterer, 1978). However, the BiSi trends (not shown) observed in both cores track the TOC and TN contents and indicate that other type of algae different than diatoms may have dominated the phytoplankton community in more recent times. Such recognition may be relevant since the isotopic composition of the phytoplankton largely determines the isotopic composition of the sedimentary organic matter.

4.5.4. Effect of diagenesis on $\delta^{15}N$ values in sediment cores

There are some indications of diagenetic changes in GC HE215/4-2 and MUC HE267/327. The non-protein AA, β-Ala and γ-Aba, are both decompositional products of the precursors Asp and Glu, respectively. Therefore, the tendency of the non-protein AA to accumulate in the older sediments reflects natural downcore degradation of the organic matter. The high percentages of non-protein AA point to degradation due to bacterial breakdown of particulate organic matter (Lee and Cronin, 1982; Wakeham et al., 1993). The diagenetic origin of non-protein AA has been demonstrated by the reverse downcore behavior in amounts with respect to the precursors AA (Cowie and Hedges, 1994). Thus, the observed upward increasing trend of Asp/β-Ala and Glu/γ-Aba ratios (Fig. 4.5D and Fig. 4.6D) is also expected and indicates degradation.

Moreover, we found that $\delta^{15}N$ is negative correlated to the total amount of non-protein AA and positive correlated to the RI (Fig. 4.5B and Fig. 4.6B). Both patterns indicate that the oldest and most degraded sediments correspond with the lower isotopic signals. However, $\delta^{15}N$ values generally tend to become ^{15}N enriched with increasing degradation of organic matter resulting from preferential releases of the lighter isotope (Gaye-Haake et al., 2005; Möbius et al., 2010). As the preferential loss of ^{15}N depleted compounds should increase the $\delta^{15}N$, the explanation for the lower values of $\delta^{15}N$ in the bottom sediments and higher in the top sediments may be nitrate inputs to the German Bight with elevated isotopic signatures (Johannsen et al., 2008). Previous studies have shown a negative correlation of $\delta^{15}N$ with DI as the results of amino acid degradation (Gaye-Haake et al., 2005; Gaye et al., 2009). We selected the RI to study the relationship between organic matter preservation and the $\delta^{15}N$ based on an evaluation of degradation indices presented by Möbius et al. (under review). The authors evaluated the two preservation indices derived from AA composition, RI and DI, and

concluded that the RI is more suitable than the DI in estimating the state of organic matter in older sediments. The concurrence of increasing RI values with increasing $\delta^{15}N$ values in sediments indicates that inputs of anthropogenically derived nitrogen with elevated isotopic signatures play a major role, whereas diagenesis has only a small effect on values in the sediments. The same positive relationship between $\delta^{15}N$ and RI in core records from the Arabian Sea was attributed to changes in source nitrate composition rather than degradation (Möbius et al., under review). Heavy nitrogen inputs swamp the small diagenetic effects and presumably preservation becomes enhanced as a consequence of higher primary production and oxygen limitation. As the $\delta^{15}N$ are relatively stable before 1860 and we discard major diagenetic overprints, the average $\delta^{15}N$ levels (~6‰) represent a good approximation of the pristine isotopic composition of riverine nitrate sources in the German Bight.

4.6. Conclusions

We found a variable offset between the isotopic composition of suspended particulate matter and the underlying surface sediments due to seasonal variations and spatial distribution of nitrate sources. Elevated $\delta^{15}N$ values in surface sediments and sediment cores reflect the influence of riverine sources on the N-pool of the North Sea and its influence on the spatial and temporal distribution of nitrogen in the German Bight. Amino acid composition was used to determine the origin and degradation state of the organic matter and the effect on $\delta^{15}N$ values. The significant difference between pre-industrial $\delta^{15}N$ values and recent ones suggests that instead of diagenesis in sediments, it is the anthropogenic nitrogen what has greatly influenced N-isotope signatures over time. The sediment records evidence that the onset of eutrophication in the German Bight corresponds to the 1800s. We demonstrated that the diagenetic non altered $\delta^{15}N$ levels (~6‰) in pre-industrial intervals of cores before AD 1860 can be confidently used to hindcast pristine conditions of riverine nitrate sources in the German Bight.

Chapter 5

Concluding remarks and outlook

5.1. Conclusions

I have described in this thesis the implementation, validation and use of an ecosystem model with a $\delta^{15}N$ module. The relevance of the approach bears on its applicability to reconstruct historical N-loads conditions for policy making in German coastal areas under serious eutrophication problems.

The reconstruction of the pristine conditions of the German Bight in terms of N-loads was successful achieved by the following steps: (1) Implementation and validation of the three-dimensional ecosystem model ECOHAM with an $\delta^{15}N$ module; (2) Hindcast of atmospheric and riverine historical N-loads of the North Sea by comparison of observed $\delta^{15}N$ in older surface sediments and sediment cores with $\delta^{15}N$ values simulated for the years 1960 and 1860; (3) Study of the relationship between $\delta^{15}N$ and degradation by means of variations in amino acid composition.

The model reproduces well recent $\delta^{15}N$ levels in surface sediments, albeit with some local differences, and is used to hindcast pristine $\delta^{15}N$ levels and N-loads conditions differing from today. The combination of $\delta^{15}N$ data of sediment archives and model results presented in this thesis confirms the feasibility to reconstruct pristine N-cycles in shelf seas. The approach also contributed to the understanding of the processes involved in the determination of the spatial and temporal distribution of $\delta^{15}N$ in sediments of the German Bight. The model results showed that the amount of Nr discharged by the Northwest-European continental rivers strongly influences the distribution of $\delta^{15}N$ values of surface sediments in the German Bight. I have additionally presented measurements of amino acids as an indicator of degradation in suspended particulate matter and sediments. Paired data of $\delta^{15}N$ and amino acid-based parameters indicate that the isotopic composition in sediments is not significantly altered by degradation.

The study focused on the following questions:

What are the dominant factors affecting the spatial and temporal distribution of $\delta^{15}N$ in recent sediments?

Nitrogen isotopic signatures were successfully applied in the German Bight showing characteristic values along the region and corresponding distinctive nitrogen sources. Data from sediments and model outcome are mainly affected by riverine nitrogen input and by nitrate assimilation processes of the German Bight region, and to a lesser extent by atmospheric deposition of Nr. Not only spatial but also temporal changes were found in the sedimentary $\delta^{15}N$ signal. The significant difference between $\delta^{15}N$ pre-industrial values and recent ones in dated sediment cores suggests that anthropogenic nitrogen has greatly influenced N-isotope signatures over time.

Is it possible to reconstruct pristine conditions in term of nitrogen in the German Bight by means of nitrogen isotope signatures?

The similitude between model outcome and data from surface sediments and sediment cores confirms that $\delta^{15}N$ signals and N-loads have been reconstructed quite well. Sedimentary records clearly show that isotopic composition can be used to trace anthropogenic inputs. The large time span represented by the sediment cores together with the shift in the $\delta^{15}N$ signatures help to reconstruct past pristine situations and to constrain the input of Nr via rivers to natural conditions. To predict natural N-loads, the model was run with different scenarios of reduced N-loads until finding an agreement with observations in sediment cores. The observational data show that the period 1950-1969 was characterized by increasing eutrophication, whereas 1860 conditions correspond to unaltered levels of $\delta^{15}N$. It indicates that the estimated 1860 loads represent a suitable target for environmental legislation aiming to restore the German Bight to pristine conditions.

Is there a relationship between $\delta^{15}N$ and degradation, as expressed by AA composition?

Amino acids spectra in sediments were used to determine the degradation state of the organic matter. It has been shown that N-isotope signatures in sediment cores reflect changes in the isotopic composition of riverine sources without diagenetic alteration. A decreasing trend of $\delta^{15}N$ from the Elbe estuary to the coastal ocean represents mix signals determined not only by the contribution of riverine N sources but also fractionation processes in the N-cycle of the German Bight. Analyses of the isotopic composition in suspended matter and the underlying surface sediments indicate differences due to seasonal variations and spatial distribution of nitrate sources.

5.2. Outlook

The results in this study also bring into question possible future research and modifications in the model. There is a need for improvement of the spatial resolution of the model, which is currently set up at grid dimensions of 0.2° x 1/3°. Although the model reproduces well the $\delta^{15}N$ levels of sediments, observations of $\delta^{15}N$ in some areas still have considerable more structure that is not imaged in the modeled distributions.

Although we found that differences in $\delta^{15}N$ of the individual size fraction < 20 µm and $\delta^{15}N$ of the unfractionated sediments was within the analytical precision of the experimental method (in a test with a subset of nine samples), it would be very interesting to include the sediment distribution (sedimentary processes) in the biogeochemical model to explore in depth its effect on the modeled $\delta^{15}N$ pattern.

In the case of nitrate, which contains not only the stable isotope pair $^{15}N/^{14}N$ but also $^{18}O/^{16}O$, and based on the fact that the dual isotopic signature is source specific, the implementation of a $\delta^{18}O$ module in the ECOHAM model would significantly improve the understanding of the N-cycling in the German Bight. Combination of results with calculated patterns of $\delta^{15}N$ patterns would better assess the contribution of riverine nitrate sources to the total Nr pool of the North Sea.

Seasonality in river discharges and in biological activity should be more intensively considered in the model. The rivers Rhine, Elbe, Weser and Ems show similar seasonal patterns of increasing $\delta^{15}N_{river\ nitrate}$ values with decreasing nitrate concentrations during summer. Therefore, it is necessary to have information about actual isotopic signals over seasonal cycles to better assess the effects of variable masses and isotopic compositions of the riverine nitrate loads. Although such data are in preparation for the modern situation (A. Johannsen and T. Schlarbaum, pers. comm., 2010), it is highly unlikely that this goal can be accomplished for past situations, because not suitably preserved water samples are available for determinations of historical nitrate isotope composition.

References

Altabet, M.A., Pilskaln, C., Thunell, R., Pride, C., Sigman, D., Chavez, F. and Francois, R., 1999. The nitrogen isotope biogeochemistry of sinking particles from the margin of the Eastern North Pacific. Deep Sea Research I 46, 655-679.

Bahlmann, E., Bernasconi, S.M., Bouillon, S., Houtekamer, M., Korntheuer, M., Langenberg, F., Mayr, C., Metzke, M., Middelburg, J.J., Nagel, B., Struck, U., Voss, M., Emeis, K.-C., 2009. Performance evaluation of nitrogen isotope ratio determination in marine sediments: An inter-laboratory intercomparison. Organic Geochemistry 41, 3-12.

Baretta, J.W., Ebenhöh, W., Ruardij, P., 1995.The European Regional Seas Ecosystem Model, a complex marine ecosystem model. Netherlands Journal of Sea Research 33, 233-246.

Bartnicki, J., Fagerli, H., 2004. Atmospheric Nitrogen in the OSPAR Convention Area in the period 1990-2001, Summary Report for the German Environmental Agency (Umweltbundesamt UBA). EMEP Technical Report MSC-W 4/2004. Norwegian Meteorological Institute. Oslo, Norway.

Bateman, A.S., Kelly, S.D., Jickells, T.D., 2005. Nitrogen Isotope Relationships between Crops and Fertilizer: Implications for Using Nitrogen Isotope Analysis as an Indicator of Agricultural Regime. Journal of Agricultural and Food Chemistry 53, 5760-5765.

Bateman, A.S., Kelly, S.D., 2007. Fertilizer nitrogen isotope signatures. Isotopes in Environmental and Health Studies 43, 237-247.

Becker, G.A., Dick, S., Dippner, J.W., 1992. Hydrography of the German Bight. Marine Ecology Progress Series 91, 9-18.

Beddig, S., Brockmann, U.H., Dannecker, W., Körner, D., Pohlmann, T., Puls, W., Radach, G., Rebers, A., Rick, H.-J., Schatzmann, M., Schlünzen, H. und Schulz, M., 1997. Nitrogen fluxes in the German Bight. Marine Pollution Bulletin 34 (6), 382-394.

Behrendt, H., Kornmilch, M., Opitz, D., Schmoll, O., Scholz, G., 2002. Estimation of the nutrient inputs into river systems - experiences from German rivers. Regional Environmental Change V3 (1), 107-117.

Behrendt, H., Opitz, D., 1999. Retention of nutrients in river systems: Dependence on specific runoff and hydraulic load. Hydrobiologia 410, 111-122.

Bergemann, M., Gaumert, T., 2008. Gewässergütebericht der Elbe 2006. ARGE Elbe, (http://www.arge-elbe.de/wge/Download/Berichte/06Guetebericht.pdf), 99 pp.

Berounsky, V.M., Nixon, S.W., 1985. Eutrophication and the rate of net nitrification in a coastal marine ecosystem. Estuarine, Coastal and Shelf Science 20, 773-781.

Brandes, J.A., Devol, A.H., Yoshinari, T., Jayakumar, D.A., Naqvi, S.W.A., 1998. Isotopic Composition of Nitrate in the Central Arabian Sea and Eastern Tropical North Pacific: A Tracer for Mixing and Nitrogen Cycles. Limnology and Oceanography 43, 1680-1689.

Brandes, J.A., Devol, A.H., 2002. A global marine-fixed nitrogen isotopic budget: Implications for Holocene nitrogen cycling. Global Biogeochemical Cycles 16, doi:10.1029/2001GB001856.

Bratton, J.F., Colman, S.M., Seal II, R.R., 2003. Eutrophication and carbon sources in Chesapeake Bay over the last 2700 yr: Human impacts in context. Geochimica et Cosmochimica Acta 67 (18), 3385-3402.

Brion, N., Baeyens, W., De Galan, S., Elskens, M., Laane, R., 2004. The North Sea: source or sink for nitrogen and phosphorus to the Atlantic Ocean? Biogeochemistry 68, 277-296.

Brockmann, U., Billen, G., Gieskes, W.W.C., 1988. North Sea nutrients and eutrophication, in: Salomons, W., Bayne, B.L., Duursma, E.K., Foerstner, U. (Eds.), Pollution of the North Sea, an Assessment. Springer, Berlin, pp. 348-389.

Brockmann, U.H., Kattner, G., 1997. Winter-to-summer changes of nutrients, dissolved and particulate organic material in the North Sea. Deutsche Hydrographische Zeitschrift 49, 229-242.

Brockmann, U. et al., 1999. Seasonal budgets of the nutrient elements N and P at the surface of the German Bight during winter 1996, spring 1995, and summer 1994. Ocean Dynamics 51, 267-291.

BSH, 2007. BSH marine Data, MUDAB Data base, <http://www.bsh.de/en/Marine_ data/Environmental_protection/ MUDAB_database/ index.jsp>.

Canfield, D.E., Thamdrup, B., Kristensen, E., 2005. The nitrogen cycle, in: Southward, A.J., Tyler, P.A., Young, C.M., Fuiman, L.A. (Eds.), Aquatic Geomicrobiology. Advancess in Marine Biology. Elsevier Academic Press, Amsterdam, Boston, Heidelberg, London, New York, Oxford, Paris, San Diego, San Francisco, Singapore, Sydney, Tokyo, pp. 205-267.

Carpenter, E.J., Harvey, H. R., Fry, B., Capone, D.G., 1997. Biogeochemical tracers of the marine cyanobacterium Trichodesmium. Deep Sea Research I 44, 27-38.

Carter, P., Mitterer, R., 1978. Amino acid composition of organic matter associated with carbonate and non-carbonate sediments. Geochimica et Cosmochimica Acta 42, 1231-1238.

Carstensen, J., Conley, D.J., Andersen, J.H., Aertebjerg, G., 2006. Coastal eutrophication and trend reversal: A Danish case study. Limnology and Oceanography 51, 398-408.

Casciotti, K.L., Sigman, D.M., Ward, B.B., 2003. Linking Diversity and Stable Isotope Fractionation in Ammonia-Oxidizing Bacteria. Geomicrobiology Journal 20, 335-353.

Casciotti, K.L., 2009. Inverse kinetic isotope fractionation during bacterial nitrite oxidation. Geochimica et Cosmochimica Acta 73, 2061-2076.

Church, T.M., Sommerfield, C.K., Velinsky, D.J., Point, D., Benoit, C., Amouroux, D., Plaa, D., Donard, O.F.X., 2006. Marsh sediments as records of sedimentation, eutrophication and metal pollution in the urban Delaware Estuary. Marine Chemistry 102, 72-95.

Clarke, A., Juggins, S., Conley, D., 2003. A 150-year reconstruction of the history of coastal eutrophication in Roskilde Fjord, Denmark. Marine Pollution Bulletin 46, 1615-1629.

Clarke, A.L., Weckström, K., Conley, D., Andersson, N.J., Adser, F., Andrén, E., de Jonge, V.N., Ellegaard, M., Juggins, S., Kauppila, P., Korhola, A., Reuss, N., Telford, R.J., Vaalgamaa, S., 2006. Long-term trends in eutrophication and nutrients in the coastal zone. Limnology and Oceanography 51 (1/2), 385-397.

Codispoti, L. A., 1995. Is the ocean losing nitrate? Nature 376, 724.

Codispoti, L.A., Brandes, J.A., Christensen, J.P., Devol, A.H., Naqvi, S.W.A., Paerl, H.W., Yoshinari, T., 2001. The oceanic fixed nitrogen and nitrous oxide budgets: Moving targets as we enter the anthropocene? Scientia Marina 65, 85-105.

Codispoti, L. A., 2007. An oceanic fixed nitrogen sink exceeding 400 Tg N a^{-1} vs the concept of homeostasis in the fixed-nitrogen inventory. Biogeosciences 4 (2), 233-253.

Cole, M.L., Valiela, I., Kroeger, K.D., Tomasky, G.L., Cebrian, J., Wigand, C., McKinney, R.A., Grady, S.P., Carvalho da Silva, M.H., 2004. Assessment of a $\delta^{15}N$ isotopic method to indicate anthropogenic eutrophication in aquatic ecosystems. Journal of Environmental Quality 33, 124-132.

Costanzo, S.D., O'Donohue, M.J., Dennison, W.C., Loneragan, N.R., Thomas, M., 2001. A new approach for detecting and mapping sewage impacts. Marine Pollution Bulletin 42, 149-156.

Cowie, G.L., Hedges, J.I., 1992. Sources and reactivities of amino acids in a coastal marine environment. Limnology and Oceanography 4, 703-724.

Cowie, G.L., Hedges, J.I., 1994. Biochemical indicators of diagenetic alteration in natural organic matter mixtures. Nature 369, 304-307.

Dähnke, K., Serna, A., Blanz, T., Emeis, K-C., 2008a. Sub-recent nitrogen-isotope trends in sediments from Skagerrak (North Sea) and Kattegat: Changes in N-budgets and N-sources? Marine Geology 253, 92-98.

Dähnke, K., Bahlmann, E., Emeis, K., 2008b. A nitrate sink in estuaries? An assessment by means of stable nitrate isotopes in the Elbe estuary. Limnology and Oceanography 53, 1504-1511.

Dähnke, K., Emeis, K-C., Johannsen, A., Nagel, B., 2010. Stable isotope composition and turnover of nitrate in the German Bight. Marine Ecology Progress Series 408, 7-18.

Dauwe, B., Middelburg, J.J., 1998. Amino acids and hexosamines as indicators of organic matter degradation state in North Sea sediments. Limnology and Oceanography 43, 782-798.

Dominik, J., Foerstner, U., Mangini, A., Reineck, H-E., 1978. ^{210}Pb and ^{137}Cs chronology of heavy metal pollution in a sediment core from the German Bight (North Sea). Senckenbergiana Maritima 10, 213-227.

de Haas, H., van Weering, T.C.E., de Stigter, H., 2002. Organic carbon in shelf seas: sinks or sources, processes and products. Continental Shelf Research 22 (5), 691-717.

de Jong, F., 2006. Marine eutrophication in perspective: on the relevance of ecology for environmental policy. Springer, Berlin, Heidelberg, New York, pp. 348.

de Jonge, V.N., Postma, H., 1974. Phosphorus compounds in the Dutch Wadden Sea. Netherland Journal of Sea Research 8, 139-153.

Eisma, D., Kalf, J., 1987. Dispersal, concentration and deposition of suspended matter in the North Sea. Journal of the Geological Society of London 144, 161-178.

Emeis, K.-C., Christiansen, C., Edelvang, K., Jähmlich, S., Kozuch, J., Laima, M., Leipe, T., Löffler, A., Lund-Hansen, L.L., Miltner, A., Pazdro, K., Pempkowiak, J., Shimmield, G.B., Shimmield, T., Smith, J., Voß, M., Witt, G., 2002. Material transport from the near shore to the basinal environment in the Southern Baltic Sea, II: origin and properties of material. Journal of Marine Systems 35 (3-4), 151-168.

Francois, R., Honjo, S., Krishfield, R., Manganini, S., 2002. Factors controlling the flux of organic carbon to the bathypelagic zone of the ocean. Global Biogeochemical Cycles, 16(4), 1087, doi:10.1029/2001GB001722.

Freyer, H.D., 1991. Seasonal variation of 15N/14N ratios in atmospheric nitrate species. Tellus 43B, 30-44.

Freyer, H.D., Kobel, K., Delmas, R.J., Kley, D., Legrand, M.R., 1996. First results of $^{15}N/^{14}N$ ratios in nitrate from alpine and polar ice cores. Tellus 48B, 93-105.

Galloway, J.N., Aber, J.D., Erisman, J.W., Seitzinger, S.P., Howarth, R.W., Cowling, E.B., Cosby, B.J., 2003. The nitrogen cascade. Bioscience 53, 341-356.

Galloway, J.N., Cowling, E.B., 2002. Reactive nitrogen and the World: 200 years of change. Ambio 31, 64-71.

Gaye-Haake, B., Lahajnar, N., Emeis, K.-Ch., Unger, D., Rixen, T., Suthhof, A., Ramaswamy, V., Schulz, H., Paropkari, A.L., Guptha, M.V.S., Ittekkot, V., 2005. Stable nitrogen isotopic ratios of sinking particles and sediments from the northern Indian Ocean. Marine Chemistry 96, 243-255.

Gaye, B., Wiesner, M.G., Lahajnar, N., 2009. Nitrogen sources in the South China Sea, as discerned from stable nitrogen isotopic ratios in rivers, sinking particles, and sediments. Marine Chemistry 114, 72-85.

Gearing, J.N.,1988 The use of stable isotope ratios for tracing the nearshore-offshore exchange of organic matter, in: Jansson, B.-O. (Ed.), Lecture notes on coastal and estuarine studies 22. Springer, Berlin, pp. 69-101.

Granger, J., Sigman, D.M., Needoba, J.A., Harrison, P.J., 2004. Coupled nitrogen and oxygen isotope fractionation of nitrate during assimilation by cultures of marine phytoplankton. Limnology and Oceanography 49, 1763-1773.

Gruber, N., Sarmiento, J., 1997. Global patterns of marine nitrogen fixation and denitrification. Global Biogeochemical Cycles 11, 235-266.

Gruber, N., Galloway, J.N., 2008. An Earth-system perspective of the global nitrogen cycle. Nature 45, 293-296.

Guhr, H., Spott, D., Bormki, G., Martina Baborowski, M., Karrasch, B., 2003. The effects of nutrient concentrations in the River Elbe. Acta Hydrochimica et Hydrobiologica 31, 282-296.

Guo, L., Tanaka, T., Wang, D., Tanaka, N., Murata, A., 2004. Distributions, speciation and stable isotope composition of organic matter in the southeastern Bering Sea. Marine Chemistry 91, 211-226.

Hastings, M.G, Jarvis, J.C., Steig, E.J., 2009. Anthropogenic impacts on nitrogen isotopes of ice-core nitrate. Science 324, 1288.

Heaton, T.H.E., 1986. Isotopic studies of nitrogen pollution in the hydrosphere and atmosphere: A review. Chemical Geology: Isotope Geoscience Section 59, 87-102.

Hebbeln, D., Scheurle, C., Lamy, F., 2003. Depositional history of the Helgoland mud area, German Bight, North Sea. Geo-Marine Letters 23, 81-90.

Hecky, R.E., Mopper, K., Kilham, P., Degens, E.T., 1973. The amino acid and sugar composition of diatom cell-walls. Marine Biology 19, 323-331.

Hedges, J. I., R. Keil, R., Benner, R., 1997. What happens to terrestrial organic matter in the ocean? Organic Geochemistry 27, 195-212.

Hertweck, G., 1983. Das Schlickgebiet in der inneren Deutschen Bucht. Aufnahme mit dem Sedimentechographen. Senckenbergiana Maritima 15, 219-249.

Hickel, W., 1980. The influence of Elbe river water on the Wadden Sea of Sylt (German Bight, North Sea). Ocean Dynamics 33, 43-52.

Hoch, M.P., Fogel, M.L., Kirchman, D.L., 1992. Isotope fractionation associated with ammonium uptake by a marine bacterium. Limnology and Oceanography 37, 1447-1459.

Holmes, R.M., McClelland, J.W., Sigman, D.M., Fry, B., Peterson, B.J., 1998. Measuring N-15-NH4+ in marine, estuarine and fresh waters: An adaptation of the ammonia diffusion method for samples with low ammonium concentrations. Marine Chemistry 60 (3-4), 235-243.

Howarth, R.W., Billen, G., Swaney, D., Townsend, A., Jarowski, N., Lajtha,K., Downing, J.A., Elmgren, R., Caracao, N., Jordan, T., Berendse, F., Freney, J., Kudeyarov, V., Murdoch, P., Zhao-Ling, Z., 1996. Regional nitrogen budgets and riverine N&P fluxes for the drainages to the North Atlantic Ocean: natural and human influences. Biogeochemistry 35, 75-139.

Hu, J., Peng, P., Jia, G., Mai, B., Zhang, G., 2006. Distribution and sources of organic carbon, nitrogen and their isotopes in sediments of the subtropical Pearl River estuary and adjacent shelf, Southern China. Marine Chemistry 98, 274-285.

Hu, J., Zhang, G., Li, K., Peng, P., Chivas, A., 2008. Increased eutrophication offshore Hong Kong, China during the past 75 years: Evidence from high-resolution sedimentary records. Marine Chemistry 110, 7-17.

Hughen, K.A. et al., 2004. Marine04 marine radiocarbon age calibration, 0–26 Cal Kyr BP. Radiocarbon 46, 1059-1086.

INSC, 1987. Ministerial Declaration. Second International Conference on the Protection of the North Sea, London.

Ittekkot, V., 1999. VALDIVIA Fahrt Nr. 157. Horizontale Gradienten del Planktonentwicklung, in: Berichte über die Fharten dees Hamburger Forschungsschiffes VALDIVIA 1995 und 1996. Universität Hamburg, 119 pp.

Jennerjahn, T.C, Ittekkot, V., 1997. Organic matter in sediments in the mangrove areas and adjacent continental margins of Brazil: I. Amino acids and hexosamines. Oceanologica Acta 20, 359-369.

Johannsen, A., 2007. N-isotope composition of of riverine nitrate loads of four German rivers discharging into the North Sea. Diploma Thesis, University of Lueneburg, Lueneburg, 56 pp.

Johannsen, A., Dähnke, K., Emeis, K., 2008. N-isotope composition of riverine nitrogen loads of four German rivers discharging into the North Sea. Organic Geochemistry 39, 1678-1689.

Jørgensen, H.M., 1987. Eutrophication–some Danish comments. Contribution to the North Sea Minister's Conference, London, November 1987.

Kendall, C., 1998. Tracing nitrogen sources and cycling in catchments, in: Kendall, C., McDonell, J.J. (Eds.), Isotope tracers in catchment hydrology. Elsevier, Amsterdam, pp. 521-576.

Kendall, C. Elliot, E.M., Wankel, S.D., 2007. Tracing anthropogenic inputs of nitrogen to ecosystems, in: Lajtha, K., Michener, R.H. (Eds.), Stable isotopes in ecology and environmental science. Blackwell Scientific Publications, Oxford, pp. 375-449.

König, P., Frohse, A., Klein, H., 1994. Measurements of suspended matter dynamics in the German Bight. In: Sündermann, J., (Ed.), Circulation and Contaminant Fluxes in the North Sea, Springer, pp. 250-270.

Lahajnar, N. Wiesner, M.G., Gaye, B., 2007. Fluxes of amino acids and hexosamines to the deep South China Sea. Deep Sea Research Part I: Oceanographic Research Papers 54, 2120-2144.

Lee, C., Cronin, C., 1982. The vertical flux of particulate organic nitrogen in the sea: decomposition of amino acids in the Peru upwelling area and the equatorial Atlantic. Journal of Marine Research 40, 227-251.

Lee, C., Cronin, C., 1984. Particulate amino acids in the sea: Effects of primary productivity and biological decomposition. Journal of Marine Research 42, 1075-1097.

Lehmann, M.F., Sigman, D.M., Berelson, W.M., 2004. Coupling the $^{15}N/^{14}N$ and $^{18}O/^{16}O$ of nitrate as a constraint on benthic nitrogen cycling. Marine Chemistry 88, 1-20.

Lenhart, H.J., 2001. Effects of River Nutrient Load Reduction on the Eutrophication of the North Sea, Simulated with the Ecosystem Model ERSEM, in: Kröncke, I., Türkay, M., Sündermann, J. (Eds.), Burning issues of North Sea ecology, Proceedings of the 14th international Senckenberg Conference North Sea 2000, Senckenbergiana maritima 31 (2), 299-311.

Lenhart, H.J. et al., 2010. Predicting the consequences of nutrient reduction on the eutrophication status of the North Sea. Journal of Marine Systems 81, 148-170.

Lenhart, H.J., Radach, G., Ruardij, P., 1997. The effects of river input on the ecosystem dynamics in the continental coastal zone of the North Sea using ERSEM. Journal of Sea Research 38, 249-274.

Libes, S.M., Deuser, W.G., 1988. The isotope geochemistry of particulate nitrogen in the Peru Upwelling Area and the Gulf of Maine. Deep Sea Research 35/4, 517-533.

Libes, S.M., 1992. An introduction to marine biogeochemistry. John Wiley & Sons, Inc., New York, Chichester, Brisbane, Toronto, Singapore, 734 pp.

Liu, K.-K., Kaplan, I.R., 1989. The eastern tropical Pacific as a source of ^{15}N-enriched nitrate in seawater off southern California. Limnology and Oceanography 34, 820-830.

Loebl, M., Colijn, F., van Beusekom, J. E. E., Baretta-Bekker, J.G., Lancelot, C. Philippart, C.J.M., Rousseau, V., Wiltshire, K.H., 2009. Recent patterns in potential phytoplankton limitation along the Northwest European continental coast. Journal of Sea Research 61, 34-43.

Lohse, L., Malschaert, J.F.P., Slomp, C.P., Helder, W., van Raaphorst, W., 1993. Nitrogen cycling in North Sea sediments: interaction of denitrification and nitrification in offshore and coastal areas. Marine Ecology Progress Series 101, 283-296.

Mariotti, A., Germon, J., Hubert, P., Kaiser, P., Letolle, R., Tardieux, A., Tardieux, P., 1981. Experimental determination of nitrogen kinetic isotope fractionation: Some principles; illustration for the denitrification and nitrification processes. Plant and Soil 62, 413-430.

Mariotti, A., Lancelot, C., Billen, G., 1984. Natural isotopic composition of nitrogen as a tracer of origin for suspended organic matter in the Scheldt estuary. Geochimica et Cosmochimica Acta 48, 549-555.

Matthias, V., Aulinger, A., Quante, M., 2008. Adapting CMAQ to investigate air pollution in North Sea coastal regions. Environmental Modelling and Software 23, 356-368.

Maksymowska, D., Richard, P., Piekarek-Jankowska, H., Riera, P., 2000. Chemical and isotopic composition of the organic matter sources in the Gulf of Gdansk (Southern Baltic Sea). Estuarine, Coastal and Shelf Science 51, 585-598.

Mayer, B., Boyer, E.W., Goodale, C., Jaworski, N.A., van Breemen, N., Howarth, R.W., Seitzinger, S., Billen, G., Lajtha, K., Nadelhoffer, K., Van Dam, D., Hetling, L.J., Nosal, M., Paustian, K., 2002. Sources of nitrate in rivers draining sixteen watersheds in the northeastern U.S.: Isotopic constraints. Biogeochemistry 57-58 (0), 171-197.

Meyers, P., 1997. Organic geochemical proxies of paleoceanographic, paleolimnologic, and paleoclimatic processes. Organic Geochemistry 27, 213-250.

McClelland, J.W., Valiela, I., 1998. Linking nitrogen in estuarine producers to land-derived sources. Limnology and Oceanography 43, 577-585.

McQuatters-Gollop, A., Raitsos, D.E, Edwards, M., Pradhan, Y., Mee, L.D., Lavender, S.J, Attril, M.J., 2007. A long-term chlorophyll dataset reveals regime shift in North Sea phytoplankton biomass unconnected to increasing nutrient levels. Limnology and Oceanography 52, 635-648.

Mieding, B. Heyden, B., Ittekkot, V., Raabe, T., Fengler, G., Brockmann, U., 1996. International Symposium New Challenges for North Sea Research - 20 years after FLEX 76 -Berichte aus dem ZMK Reihe Z: Interdisziplinare Zentrumsberichte, Extended abstracts.

Miyake, Y., Wada, E., 1967. The abundance ratio of $^{15}N/^{14}N$ in marine environments. Records of oceanographic works in Japan 9, 37-53.

Möbius, J., Gaye, B., Lahajnar, N., Bahlmann, E., Emeis, K.-C., under review. Influence of diagenesis on sedimentary $\delta^{15}N$ in the Arabian Sea over the last 130 kyr. Marine Geology.

Möbius, J., Lahajnar, N., Emeis, K.-C., 2010. Diagenetic control of nitrogen isotope ratios in Holocene sapropels and recent sediments from the Eastern Mediterranean Sea. Biogeosciences Discussions 7, 1131-1165, doi:10.5194/bgd-7-1131-2010.

Moll, A., Radach, G., 2003. Review of three-dimensional ecological modelling related to the North Sea shelf system - Part 1: Models and their results. Progress in Oceanography 57 (2), 175-217.

Montoya, J.P., McCarthy, J.J., 1995. Isotopic fractionation during nitrate uptake by phytoplankton grown in continuous culture. Journal of Plankton Research, 17/3, 439-464.

Morin, S., Savarino, J., Frey, M.M., Domine, F., Jacobi, H.-W., Kaleschke, L., Martins, J.M.F., Comprehensive isotopic composition of atmospheric nitrate in the Atlantic Ocean boundary layer from 65 °S to 79 °N. Journal of Geophysical Research, accepted.

Müller, P., 1977. C/N ratios in Pacific deep-sea sediments: Effect of inorganic ammonium and organic nitrogen compounds sorbed by clays. Geochimica et Cosmochimica Acta 41, 765-776.

Müller, A., Voss, M., 1999. The palaeoenvironments of coastal lagoons in the southern Baltic Sea, II. $\delta^{13}C$ and $\delta^{15}N$ ratios of organic matter - sources and sediments. Palaeogeography, Palaeoclimatology, Palaeoecology 145, 17-32.

Nakatsuka, T., Handa, N., Wada, E., Wong, C.S., 1992. The dynamic changes of stable isotopic ratios of carbon and nitrogen in suspended and sedimented particulate organic matter during a phytoplankton bloom. Journal of Marine Research 50, 267-296.

Needoba, J.A., Waser, N.A., Harrison, P.J., Calvert S. E., 2003. Nitrogen isotope fractionation in 12 species of marine phytoplankton during growth on nitrate. Marine Ecology Progress Series 255, 81-91.

Nelissen, P.H., Stefels, J., 1988. Eutrophication in the North Sea. NIOZ Renoit 4. Netherlands Institute of Sea Research, Den Burg, 100 pp.

OSPAR Commission, 2000. Quality status report 2000. Region II-Greater North Sea, OSPAR Commission, London. 136 pp.

OSPAR Commission, 2003a. Strategies of the OSPAR Commission for the Protection of the Marine Environment of the North-East Atlantic. Agreement 2003-21. OSPAR Commission, London. 22 pp.

OSPAR Commission, 2003b. OSPAR integrated report 2003 on the eutrophication status of the OSPAR maritime area based upon the first application of the comprehensive procedure, OSPAR Commission, London. 59 pp.

OSPAR Commission, 2007. Atmospheric Nitrogen in the OSPAR Convention Area in 1990-2004 (update 2007). OSPAR Commission, OSPAR Publication Number 344/2007. 55 pp.

OSPAR Commission, 2008. Second OSPAR Integrated Report on the Eutrophication Status of the OSPAR Maritime Area. OSPAR Commission, OSPAR Publication Number 372/2008. 107 pp.

Otto, L., Zimmerman, J. T. F., Furnes, G. K., Mork, M., Saetre, R., Becker, G. A., 1990. Review of the physical oceanography of the North Sea. Netherlands Journal of Sea Research 2621(2-4), 161-238.

Owens, N.J.P., 1987. Natural Variations in ^{15}N in the Marine Environment. Advances in Marine Biology 24, 389-451.

Pätsch, J., 1997. Auswirkungen anhaltender Eutrophierung der Nordsee: Langzeituntersuchung mit dem Ökosystemmodell ERSEM. Berichte aus dem Zentrum für Meeres- und Klimaforschung Reihe B: Ozeanographie 26. Institut für Meereskunde, Hamburg, 177 pp.

Pätsch, J., Kühn, W., 2008. Nitrogen and carbon cycling in the North Sea and exchange with the North Atlantic-a model study, Part I. Nitrogen budget and fluxes. Continental Shelf Research 28, 767-787.

Pätsch, J., Lenhart, H.J. 2004. Daily loads of nutrients, total alkalinity, dissolved inorganic carbon and dissolved organic carbon of the European continental rivers for the years 1977-2002. Berichte aus dem Zentrum für Meeres- und Klimaforschung Reihe B: Ozeanographie 48. Institut für Meereskunde, Hamburg, 159 pp.

Pätsch, J., Lenhart, H.J., 2008. Daily loads of nutrients, total alkalinity, dissolved inorganic carbon and dissolved organic carbon of the European continental rivers for the years 1977-2006. Institut für Meereskunde, Hamburg, 159 pp.

Pätsch, J., Radach, G., 1997. Long-term simulation of the eutrophication of the North Sea: temporal development of nutrients, chlorophyll and primary production in comparison to observations. Journal Sea Research 38, 275-310.

Pätsch, J., Serna, A., Dähnke, K., Schlarbaum, T., Johannsen, A., Emeis, K.-C., 2010. Nitrogen cycling in the German Bight (SE North Sea) – Clues from modelling stable nitrogen isotopes. Continental Shelf Research 30, 203-213.

Peters, K.E., Sweeney, R. E., Kaplan, I.R., 1978. Correlation of carbon and nitrogen stable isotopes in sedimentary organic matter. Limnology and Oceanography 23, 598-604.

Petersen, W., Wehde, H., Krasemann, H., Colijn, F., Schroeder, F., 2008. FerryBox and MERIS - Assessment of coastal and shelf sea ecosystems by combining in situ and remotely sensed data. Estuarine, Coastal and Shelf Science 77, 296-307.

Pohlmann, T., 1996. Predicting the thermocline in a circulation model of the North Sea. Part I: Model description, calibration, and verification. Continental Shelf Research 7, 131-146.

Prange, A., 1997. Erfassung und Beurteilung der Belastung der Elbe mit Schadstoffen, TP2: Schwermetalle-Schwermetallspezies. Geogene Hintergrundwerte und zeitliche Belastungsentwicklung (BMBF 02-WT 9355/4), Band 3/3. GKSS Forschungszentrum Internal Report. 218 pp.

Preiss, N., Mélières, M-A., Pourchet, M., 1996. A compilation of data on lead 210 concentration in surface air and fluxes at the air-surface and water-sediment interfaces. Journal of Geophysical Research 101, 28847-28862.

Preunkert, S., Wagenbach, D., Legrand, M., 2003. A seasonally resolved alpine ice core record of nitrate: Comparison with anthropogenic inventories and estimation of preindustrial emissions of NO in Europe. Journal of Geophysical Research 108, 4681.

Puls, W., Heinrich, H., Mayer, B., 1997. Suspended particulate matter budget for the German Bight. Marine Pollution Bulletin 34, 398-409.

Rabalais, N., 2002. Nitrogen in aquatic ecosystems. Ambio 31, 102-112.

Rachor, E., Albrecht, H., 1983. Sauerstoff-Mangel im Bodenwasser der Deutschen Bucht. Veröffentlichungen des Instituts für Meeresforschung in Bremerhaven 19, 209-227.

Radach, G., 1998. Quantification of long-term changes in the German Bight using an ecological development index. ICES Journal of Marine Science 55, 587-599.

Radach, G., Gekeler, J., 1996. Annual cycles of horizontal distributions of temperature and salinity, and of concentrations of nutrients, suspended particulate matter and chlorophyll on the northwest European shelf. Deutsche Hydrographische Zeitschrift 48 (3/4), 261-297.

Radach, G., Pätsch, J., 2007.Variability of continental riverine freshwater and nutrient inputs into the North Sea for the years 1977-2000 and its consequences for the assessment of eutrophication. Estuaries and Coasts 30, 66-81.

Reimer, P.J. et al., 2004. IntCal04 terrestrial radiocarbon age calibration, 0–26 Cal Kyr BP. Radiocarbon 46, 1029-1058.

Rick, S., 1999. The spring bloom in the German Bight: Effects of high inorganic N:P ratios on the phytoplankton development. Berichte aus dem Institut für Meereskunde 305, 1-142.

Rijnsdorp, A.D., Buys, A.M., Storbeck, F., Visser, E.G., 1998. Micro-scale distribution of beam trawl effort in the southern North Sea between 1993 and 1996 in relation to the trawling frequency of the sea bed and the impact on benthic organisms. ICES Journal of Marine Science 55, 403-419.

Scheurle, C., Hebbeln, D., Jones, P., 2005. An 800-year reconstruction of Elbe River discharge and German Bight sea-surface salinity. The Holocene 15 (3), 429-434.

Schlarbaum, T., Dähnke, K., Emeis, K., 2010. Turnover of combined dissolved organic nitrogen and ammonium in the Elbe estuary/NW Europe: results of nitrogen isotope investigations. Marine Chemistry 110, 91-107.

Schlitzer, R., 2002. Interactive analysis and visualization of geoscience data with Ocean Data View. Computers and Geosciences 28, 1211-1218.

Schmiedl, G., Anniken B. Rotstigen, A.B., in prep. Benthic foraminifera as a proxy for natural versus anthropogenic environmental change in the German Bight, North Sea.

Schott, F., 1966. Der Oberflächensalzgehalt in der Nordsee. Ergänzungsheft zur Deutschen Hydrologischen Zeitschrift, Reihe A (8) Nr. 9, Deutsches Hydrograsphisches Institut, Hamburg, 58 pp.

Seel, A., 2005. Isotopenverhältnisse ($\delta^{15}N$) in Oberflächensedimenten und Makrophyten aus der südöstlichen Nordsee. M.Sc. Thesis, Geosciences Department, Universität Hamburg. 44 pp.

Seitzinger, S., Giblin, A.E., 1996. Estimating denitrification in North Atlantic continental shelf sediments. Biogeochemistry 35, 235-260.

Seitzinger, S., Kroeze, C., Bouwman, A.F., Caraco, N., Dentener, F., Styles, R.V., 2002. Global patterns of dissolved inorganic and particulate nitrogen inputs to coastal systems: Recent conditions and future projections. Estuaries 25 (4b), 640-655.

Serna, A. Pätsch, J., Dähnke, K., Wiesner, M.G., Hass, H.C., Zeiler, M., Hebbeln, D., Emeis, K.-C., 2010. History of anthropogenic nitrogen input to the German Bight/SE North Sea as reflected by nitrogen isotopes in surface sediments, sediment, cores and hindcast models. Continental Shelf Research 30, 1626-1638.

Sigman, D.M, Altabet, M., McCorkle, D., Francois, R., Fischer, G., 2000. The $\delta^{15}N$ of nitrate in the Southern Ocean: Nitrogen cycling and circulation in the ocean interior. Journal of Geophysical Research 105, 19599-19614.

Sigman, D.M., Granger, J., DiFiore, P.J., Lehmann, M.M., Cane, G., Ho, R., van Geen, A., 2005. Coupled nitrogen and oxygen isotope measurements of nitrate along the eastern North Pacific margin. Global Biogeochemical Cycles 19, 1-14.

Skogen, M., Søiland, H., 1998. A user's guide to NORWECOM v2.0. The NORWegian ECOlogical Model system. Tech. Rep. Fisken og Havet 18/98. Institute of Marine Research, Pb.1870, N-5024 Bergen. 42 pp.

Skogen, M., Søiland, H., Svendsen, E., 2004. Effects of changing nutrient loads to the North Sea. Journal of Marine Systems 46, 23-38.

Spokes, L., Jickells, T.D., 2005. Is the atmosphere really an important source of reactive nitrogen to coastal waters? Continental Shelf Research 25, 2022-2035.

Struck, U., Emeis, K.-C., Voß, M., Christiansen, C., Kunzendorf, H., 2000. Records of Baltic Sea eutrophication in $\delta^{13}C$ and $\delta^{15}N$ of sedimentary organic matter. Marine Geology 164, 157-171.

Stuiver, M., Reimer, P.J., 1993. Extended ^{14}C database and revised CALIB 3.0 14C age calibration program. Radiocarbon 35, 215-230.

Sugimoto, R., Kasai, A., Miyajima, T., Fujita, K., 2008. Nitrogen isotopic discrimination by water column nitrification in a shallow coastal environment. Journal of Oceanography 64, 39-48.

Sugimoto, R., Kasai, A., Miyajima, T., Fujita, K., 2009. Controlling factors of seasonal variation in the nitrogen isotope ratio of nitrate in a eutrophic coastal environment. Estuarine, Coastal and Shelf Science Volume 85 (2), 231-240.

Teranes, J.L., Bernasconi, S.M., 2005. Factors controlling $\delta^{13}C$ values of sedimentary carbon in hypertrophic Baldeggersee, Switzerland, and implications for interpreting isotope excursions in lake sedimentary records. Limnology and Oceanography 50, 914-922.

Thoms, S., 2006. Parameterization of coagulation processes in the formation of transparent exopolymer particles (TEP). In: International Workshop on Marine Aggregates (IWOMA), 11 and 12 Dec. 2006, MPI Bremen, Germany, [hdl:10013/epic.26137].

Topcu, D., Brockmann, H.U., Claussen, U., 2009. Relationships between eutrophication reference conditions and boundary settings considering OSPAR recommendations and the Water Framework Directive - examples from the German Bight. Hydrobiologia 629, 91-106.

van Bennekom, A.J., Wetsteijn, F.J., 1990. The winter distribution of nutrients in the southern bight of the North Sea (1961-1978) and in the estuaries of the Scheldt and the Rhine/Meuse. Netherlands Journal of Sea Research 25, 75-87.

van Beusekom, J.E.E., 2005. A historic perspective on Wadden Sea eutrophication. Helgoland Marine Research 59, 45-54.

van Beusekom, J.E.E., Brockmann, U. H., Hesse, K. J., Hickel, W., Poremba, K., Tillmann, U., 1999. The importance of sediments in the transformation and turnover of nutrients and organic matter in the Wadden Sea and German Bight. Deutsche Hydrographische Zeitschrift 51(2/3), 245-266.

van Beusekom, J.E.E., de Jonge, V.E., 1998. Retention of phosphorus and nitrogen in the Ems estuary. Estuaries 21, 527-539.

van Beusekom, J.E.E., de Jonge, V.N., 2002. Long-term changes in Wadden Sea nutrients cycles: importance of organic matter import from the North Sea. Hydrobiologia 475/476, 185-194.

van Beusekom, J.E.E., Loebl, M., Martens, P., 2009. Distant riverine nutrient supply and local temperature drive the long-term phytoplankton development in a temperate coastal basin. Journal of Sea Research 61, 26-33.

Vermaat, J.E., McQuatters-Gollop, A., Eleveld, M.A., Gilbert, A.J., 2008. Past, present and future nutrient loads of the North Sea: Causes and consequences. Estuarine, Coastal and Shelf Science 80, 53-59.

Voß, M., Struck, U., 1997. Stable nitrogen and carbon isotopes as indicator of eutrophication of the Oder river (Baltic sea). Marine Chemistry 59, 35-49.

Voß, M., Larsen, B., Leivuori, M., Vallius H., 2000. Stable isotope signals of eutrophication in Baltic Sea sediments. Journal of Marine Systems 25, 287-298.

Voß, M., Deutsch, B., Elmgrenn, R., Humborg, C., Kuuppo, R., Pastusyak, M., Rolff, C., Schulte, U., 2006. River biogeochemistry and source identification of nitrate by means of isotopic tracers in the Baltic Sea catchments. Biogeosciences Discussions 3, 475-511.

Wada, E., Hattori, A., 1978. Nitrogen isotope effects in the assimilation of inorganic nitrogenous compounds sediments: anthropogenic influence on organic matter composition. Marine Chemistry 69, 117-137.

Wakeham, S.G., Hedges, J.I., Lee, C., Pease, T.K., 1993. Effects of poisons and preservatives on the composition of organic matter in a sediment trap experiment. Journal of Marine Research 51, 669-696.

Ward, P.J., Renssen, H., Aerts, J.C.J.H., van Bale, R.T., Vandenberghe, J., 2008. Strong increases in flood frequency and discharge of the River Meuse over the late Holocene: impacts of long-term anthropogenic land use change and climate variability. Hydrology and Earth System Science 12, 159-175.

Waser, N.A.D., Harrison, P.J., Nielsen, B., Calvert, S.E., Turpin, D.H., 1998. Nitrogen isotope fractionation during uptake and assimilation of nitrate, nitrite, ammonium and urea by a marine diatom. Limnology and Oceanography 43 (2), 215-224.

Wiesner, M., Haake, B., Wirth, H., 1990. Organic facies of surface sediments in the North Sea. Organic Geochemistry 15, 419-432.

Wirth, H., Wiesner, M., 1988. Sedimentary facies in the North Sea, in: Kempe S. et al. (Eds.), Biogeochemistry and distribution of suspended matter in the North Sea and implications to fisheries biology. Mitteilungen aus dem Geologisch-Paläontologischen Institut der Universität Hamburg 65, 269-287.

WFD Water Framework Directive, 2000. Richtlinie 2000/60/EG des Europäischen Parlamentes und des Rates vom 23. Oktober 2000 zur Schaffung eines Ordnungsrahmens für Maßnahmen der Gemeinschaft im Bereich der Wasserpolitik. Amtsblatt der Europäischen Gemeinschaften, L327, EC, pp.1-72.

Wu, J., Huang, C., Zeng, H., Schleser, G.H., Battarbee, R., 2007. Sedimentary evidence for recent eutrophication in the northern basin of Lake Taihu, China: human impacts on a large shallow lake. Journal of Paleolimnology 38 (1), 13-23.

Yeatman, S.G., Spokes, L.J., Dennis, P.F., Jickells, T.D., 2001. Comparisons of aerosol nitrogen isotopic composition at two polluted coastal sites. Atmospheric Environment 35, 1307-1320.

York, J.K., Tomasky, G., Valiela, I., Repeta, D.J., 2007. Stable isotopic detection of ammonium and nitrate assimilation by phytoplankton in the Waquoit Bay estuarine system. Limnology and Oceanography 52, 144-155.

Appendix

The isotopic ratios R are expressed in δ-values, which express the $^{15}N/^{14}N$ ratio of a sample in relation to that ratio in atmospheric N_2 as the standard ($\delta^{15}N_{air}$ = 0‰).

(1) $$\delta\,^{15}N = \frac{R_{sample} - R_{standard}}{R_{standard}} \text{ x } 1000\ [‰], \text{ with } R = \frac{^{15}N}{^{14}N}$$

Because the larger model version for the entire shelf area does distinguish between different N-isotopes, the ^{15}N concentrations for the nitrogen state variables (X) were prescribed for the initial values and at the boundaries of the nest (Table 2.2) and calculated the corresponding $^{15}N_X$ concentrations:

(2) $$\left[^{15}N_X\right] = r15_X \cdot [X] \text{ with } r15_X = \frac{1}{1+ra_X} \text{ and } ra_X = \frac{1}{r15_{air} \cdot \left(\frac{\delta^{15}\,N_X}{1000}+1\right)}$$

in which

(3) $$r15_{air} = \frac{1}{272}, \text{ is the } \frac{^{15}N}{^{14}N} \text{ ratio of molecular nitrogen } N_2 \text{ in air.}$$

ECOHAM 4.4 calculates isotope fractionation for all processes in which Nr participates in the model. In the case of a one-way reaction, the fractionation factor α is defined as the ratio of the atomic numbers of the two N-isotopes of the source/substrate compound divided by the corresponding ratio in the product.

(4) $$\alpha(\text{source, product}) = R_{source} / R_{product}$$

The more frequently used ε-value (the enrichment factor of a reaction) is defined as

(5) $$\varepsilon = 1000\ (\alpha\text{-}1)$$

The general temporal deviation of a state variable X reads

(6) $$\frac{\partial X}{\partial t} = \sum_i f(Y_i, X) - \sum_j f(X, Y_j) + tra(X)$$

Where X is the concentration of state variable concerning (N = ^{14}N + ^{15}N), $f(Y_i,X)$ is the flux from state variable Y_i to X (mmol m^{-3} d^{-1}) as a concentration change per day, $f(X,Y_j)$ is the flux

from X to state variable Y_j (mmol m^{-3} d^{-1}) as a concentration change per day, tra(X) is the concentration change per day due to physical transport.

The corresponding equation for ^{15}X reads

(7) $$\frac{\partial^{15}X}{\partial t} = \sum_i {}^{15}f(^{15}Y_i, ^{15}X) - \sum_j {}^{15}f(^{15}X, ^{15}Y_j) + tra(^{15}X)$$

Where ^{15}X is the concentration of state variable concerning ^{15}N, $^{15}f(^{15}Y_i, ^{15}X)$ is the flux from state variable $^{15}Y_i$ to ^{15}X (mmol m^{-3} d^{-1}) as concentration change per day, $^{15}f(^{15}X, ^{15}Y_j)$ is the flux from ^{15}X to state variable $^{15}Y_j$ (mmol m^{-3} d^{-1}) as concentration change per day, tra(^{15}X) is the concentration change per day due to physical transport.

The flux of the ^{15}N variable X to the variable Y_j is defined as

(8) $$^{15}f(^{15}X, ^{15}Y_j) = \alpha(X, Y_j) \cdot \frac{^{15}X}{X} \cdot f(X, Y_j)$$

The flux of the ^{15}N variable Y_i to the variable X is defined as

(9) $$^{15}f(^{15}Y_i, ^{15}X) = \alpha(Y_i, X) \cdot \frac{^{15}i}{i} \cdot f(Y_i, X)$$

Table 2.3 gives all fractionation factors used in ECOHAM 4.4 which differ from zero.

Acknowledgments

I would like to express my gratitude to my advisor Prof. Dr. Kay-Christian Emeis for the guidance that he has given me during the course of my doctorate and for organizing the financial support. His vast experience in research had truly inspired me since I became a student at the University of Hamburg.

I would like to thank my co-advisor, Dr. Johannes Pätsch, who patiently answered all my questions and allowed me to learn much from his enormous knowledge of modeling. I really enjoyed my experience working with him.

I thank my co-authors for their valuable comments during the preparation of the publications which constitute this work. The list includes Dr. Kirstin Dähnke and Dr. H. Christian Hass.

I would like to thank my colleagues from the Institute for Biogeochemistry and Marine Chemistry for the assistance that they gave me the past years. The support of Dr. Birgit Gaye and Dr. Martin Wiesner at the initial level of my research enabled me to develop an understanding of the subject. Dr. Niko Lahajnar encouraged me throughout my study and helped with his discipline to keep my work organized. He also helped with computer technical problems and lab analyses. A special thank to Frauke Langenberg for her technical support in countless analyses. I am indebted to many of my colleagues: Catrin Eickenrodt, Timo Köppen and Marc Metzke, for their help during research expeditions and lab work. All other PhD candidates, including Jürgen Möbius, Berit Schwalger, Astrid Johannsen had inspired me in research and life through our interactions during many days in the institute.

This research was supported by the German Research Foundation. The Institute for Biogeochemistry and Marine Chemistry of the University of Hamburg provided the laboratory facilities and equipment I have needed to complete my thesis.